VOLUME 22 AUGUST, 1934 NUMBER 8

Ray E. Bartos

PROCEEDINGS
of
The Institute of Radio Engineers

Application Blank for Associate Membership on Page XI

Institute of Radio Engineers Forthcoming Meetings

DETROIT SECTION

September 21, 1934

LOS ANGELES SECTION

September 18, 1934

PHILADELPHIA SECTION

October 4, 1934

WASHINGTON SECTION

September 10, 1934

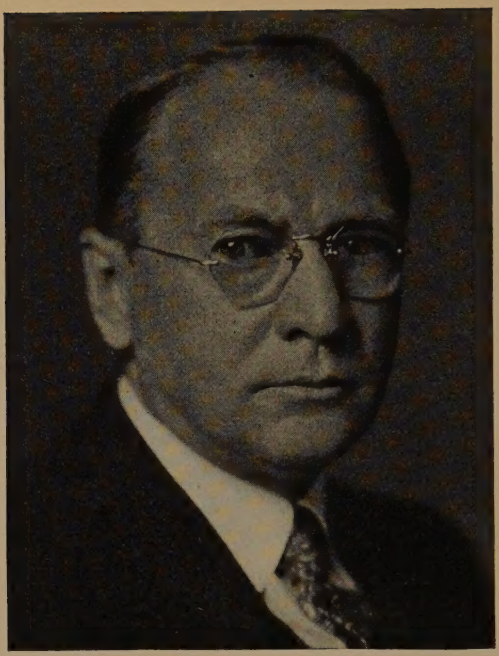

VLADIMIR K. ZWORYKIN

Morris Liebmann Memorial Prize Recipient for 1934

Vladimir K. Zworykin was born in Russia in 1889. He received an electrical engineering degree in 1912 from the Petrograd Institute of Technology where he studied physics under Professor Boris Rosing and first experimented with television. In 1912 he entered the College de France in Paris for X-ray research under Professor P. Langevin. He served in the Russian Army as officer of the radio corps during the World War.

In 1919 he came to the United States and from 1920 to 1929 was a member of the research laboratory of the Westinghouse Electric and Manufacturing Company. A Doctor of Philosophy degree was bestowed upon him by the University of Pittsburgh in 1926. He was transferred in 1929 to the research laboratory of the RCA Victor Company and was made director of the electronic research laboratory in 1934.

He is the author of a number of papers on photo cells, sound recording, facsimile, television, and electron optics as well as being co-author of the book "Photo Cells and Their Applications." He became a Member of the Institute of Radio Engineers in 1930.

Dr. Zworykin was awarded the Morris Liebmann Memorial Prize for 1934 in recognition of his contributions to the development of television.

INSTITUTE NEWS AND RADIO NOTES

Experimental Transmissions for Observing Long Delayed Echoes

Echoes appearing about three seconds after the original transmission from PCJJ in Holland on a frequency of about ninety-six kilocycles were first observed in Norway by J. Hals in 1927. The phenomenon has been verified in a few scattered observations by Dutch, British, and French engineers, echoes being heard from one to thirty seconds after the emitted signal. Signals received after traveling around the world appear as echoes of one-seventh second delay and no single theory as to the reason for the long delays observed has been accepted universally.

C. Stormer of Norway considers that there are streams of electrons in space some hundreds of thousands of miles from the earth's equator converging in a vast toroid upon the magnetic poles of the earth and accounting for the aurora borealis and the reflection of signals to cause these long delayed echoes.

B. van der Pol and E. V. Appleton suggest that these echoes are due to a slowing up and reflection of radio waves by a peculiar distribution of ionization in the ionosphere.

The British Broadcasting Corporation with the aid of Professor Appleton has inaugurated a world-wide endeavor to learn more about these echoes. Special transmissions will be made from GSB, Daventry, England, on 9510 kilocycles with 1000-cycle modulation each Sunday, Tuesday, and Thursday, from 3:25 to 3:55 A.M., Eastern Standard Time. Each transmission consists of a five-minute adjusting period, during which phonograph music will be played, followed by the letters of the alphabet in Morse code spaced one minute apart. During the one-minute intervals between signals the observers listen for echoes and note the elapsed time in seconds using an ordinary watch with a second hand.

Another program of signals will be transmitted from the League of Nations Station, HBL, located in Geneva, Switzerland. These transmissions are on 6675 kilocycles, unmodulated continuous waves each Sunday, Wednesday, and Friday from 6:00 to 6:30 A.M., Eastern Standard Time. During the five-minute adjusting period HBL will transmit its call letters in Morse code and the alphabet will follow at one-minute intervals per letter.

Reports on successful reception in the United States of long delayed

echoes should be forwarded to J. H. Dellinger, Chief, Radio Section, National Bureau of Standards, Washington, D.C. They will be forwarded to the British authorities who are coördinating the investigation for the world as a whole.

Observers should give the identifying letter of the signal observed, the time to the nearest second at which the direct signal was heard, the time to the nearest second at which the echo was heard, an estimate of relative intensities of the direct signal and the echo, a description of the sharpness or apparent shape of the echo, and any pertinent information on interference, fading of signals, or other conditions observed.

Reports of reception of long delayed echoes from other transmissions, especially from high-frequency stations in the United States of America are also valuable although it may be very difficult to obtain accurate observations because of the rate of transmission of the signals.

Summaries of the results of this investigation will be made available later and those desiring to keep in touch with all details of the project, can do so by consulting the weekly issues of "World-Radio" published by Broadcasting House, London, W.C.1, England.

Proceedings Back Copies

The Institute office receives inquiries from those interested in obtaining issues of the PROCEEDINGS which can no longer be supplied from our files and, occasionally, from those who have back issues for which they have no further use. It has been possible in some instances to advise a potential purchaser of the possible sources of these particular issues, and in an endeavor to extend the scope of this service there is listed below those issues which are no longer available from stock. Those having these issues and desiring to dispose of them should forward this information to the secretary estimating the condition of the particular issues and the price asked for them. Where all the issues for a given year are available and they will be sold only as a unit, this should be stated. Anyone desiring the issues listed should bring their requirements to the secretary who will endeavor to put them in contact with a member having these issues available for sale.

Vol. 1 (1913) (Nos. 1 & 2—Jan. & Apr.)
Vol. 2 (1914) (Nos. 1, 3, 4—Mar. Sept. & Dec.)
Vol. 3 (1915) (Nos. 1, 2, 3—Mar. June & Sept.)
Vol. 4 (1916) (Nos. 1, 2, 5, 6—Feb. Apr. Oct. Dec.)
Vol. 5 (1917) (No. 1—Feb.)
Vol. 7 (1919) (No. 3—June)
Vol. 12 (1924) (Nos. 1, 2, 3—Feb. Apr. June)

Vol. 15 (1927) (Nos. 1, 2, 3, 8, 9—Jan. Feb. Mar. Aug. Sept.)
Vol. 16 (1928) (No. 1—Jan.)
Vol. 17 (1929) (Nos. 1, 2, 9, 10—Jan. Feb. Sept. Oct.)

Institute Meeting

Buffalo-Niagara Section

The annual meeting of the Buffalo-Niagara Section was held on June 25 at the University of Buffalo. L. G. Hector, chairman, presided and called for a vote on the election of officers for the next year. As a result, L. E. Hayslett, chief radio engineer for the Rudolph Wurlitzer Manufacturing Company was elected chairman; R. J. Kingsley, chief engineer of Radio Station WBEN was named vice chairman, and E. C. Waud continues as secretary-treasurer.

A paper on "Some Uses of Vacuum Tubes for Other Than Radio Purposes" was presented by L. G. Hector, Professor of Physics at the University of Buffalo. In his paper, Dr. Hector discussed high quality public address systems, photo cells and thyratrons for the automatic recording of time signals, an electrical stethoscope with selective automatic volume control for the reduction of extraneous noises, the demodulation of a broadcast transmission for use as a standard high-frequency source, and the amplifying of very low frequency currents.

After the adjournment of the meeting, those present visited the laboratories where the apparatus described in the paper was examined in operation. Thirty-two members and guests were present.

Chicago Section

A meeting of the Chicago Section was held on January 23 in the auditorium of the Western Society of Engineers. H. S. Knowles, chairman, presided and the attendance totaled 132.

A paper on "Microphonics and Frequency Drift in Short-Wave Receivers" was presented by David Grimes of the RCA License Laboratory. In addition to the subjects indicated by the title of the paper, the author discussed the seriousness of the radiation from many superheterodyne receivers where insufficient provision has been taken to shield the oscillator.

The February meeting of the section was held on the 26th in the main auditorium of the Engineering Building. The attendance was 360 and H. S. Knowles, chairman, presided.

J. A. Chambers, technical supervisor for the Crosley Radio Cor-

poration, presented a paper on "The 500-Kilowatt WLW Transmitter." In it he traced the history of the development in power ratings of radio broadcast transmitters. The problems involved in the planning, securing of equipment, erection, and operating tests of the new 500-kilowatt WLW transmitter were then discussed. It was felt that this does not of necessity mark the final step in broadcast transmitter power.

One hundred and twenty-five members of the Chicago Telephone and Telegraph Section of the American Institute of Electrical Engineers attended as guests.

The March meeting was held on the 30th in the auditorium of the Western Society of Engineers. The attendance totaled twenty-five and H. S. Knowles, chairman, presided.

The first paper of the evening by Guy Wilcox of the Armour Institute of Technology was on "Short-Wave Phenomena." In it Professor Wilcox demonstrated a number of the more interesting and basic principles governing short-wave phenomena.

A paper on "Some Technical Considerations in Short-Wave Design" was then presented by Kendall Clough of the Clough-Brengle Laboratories. The author summarized his paper by drawing up a set of "Do and Don't" rules for engineers confronted with problems in this field.

The May meeting was held in the auditorium of the Western Society of Engineers on the 11th and the attendance totaled eighty-seven. Chairman H. S. Knowles presided.

"Iron-Core Radio-Frequency and Intermediate-Frequency Tuning Systems" was the subject of a paper by Alfred Crossley, consulting engineer. In it he presented data on the performance and economic factors of radio receiver design as affected by the use of iron-core inductors for tuning systems of both radio-frequency and intermediate-frequency types. Curves were shown to indicate the effect of these inductors on both sensitivitiy and selectivity of typical receivers.

Dean Perkins of the Allen Bradley Company then presented a paper on "Auto Radio Installation and Noise Suppression Problems." In it, the problems encountered were viewed from the standpoint of installing automobile radio receivers, the design of such units, and the design of suppression devices for installation in the automobile electric system.

Connecticut Valley Section

A meeting of the Connecticut Valley Section was held on May 25 at the Hotel Garde in Hartford, Conn. It was presided over by K. S. Van Dyke, chairman, and twenty-five members and guests were present.

The first paper on "The Modulator System at WLW" was prepared by J. A. Hutcheson of the Westinghouse Electric and Manufacturing Company and was presented by L. A. Scriven of the same organization due to the unexpected absence of the author. The paper was concerned principally with the presentation of quantitative details of the new modulator system. It was pointed out that the equipment generates ten times as much audio-frequency power as has been developed previously. The nominal output in the fifth and final push-pull stage is 360 kilovolt-amperes with a frequency range of from 30 to 10,000 cycles. This ouput is obtained with an input of $12\frac{1}{2}$ milliwatts representing an amplification of almost 30 million fold. Structural details of the transformers and associated equipment were given.

The second paper of the evening was by Mr. Scriven and covered "Mechanical Design Features of WLW." In it he described the general physical layout of the station. Detailed descriptions were given of the power supply and power amplifier equipment, the system of water cooling, the alternating-current power sources, the antenna transmission line, and the vertical mast antenna. In addition to a general discussion of the papers presented the character of the material now appearing in the PROCEEDINGS was considered.

The June meeting of the section was held on the 18th at Wesleyan University and was presided over by K. S. Van Dyke, chairman.

A. H. Taylor of the Naval Research Laboratory presented a paper on "The Cathode Ray Oscillograph in the Research Laboratory." After describing the characteristics and uses of these devices, Dr. Taylor demonstrated a portable cathode ray oscillograph.

The attendance was about fifty and many of these visited the Physics Laboratory of Wesleyan University at the close of the meeting.

SAN FRANCISCO SECTION

The April 27 meeting of the San Francisco Section was held jointly with the San Francisco Section of the American Institute of Electrical Engineers at Stanford University. A general inspection of the University laboratories was made during the afternoon and the presentation of papers occurred in the evening.

R. W. Sorensen, professor of electrical engineering at the California Institute of Technology and vice president of the American Institute of Electrical Engineers spoke on engineering as a profession. Three short papers were then presented by students from the California Institute of Technology, the University of Santa Clara, and Leland Stanford University. The subjects were "The San Francisco-Oakland

Bay Bridge," "The Magnetic Influence of Sun Spots," and "High Gain, High Efficiency Oscillators."

The attendance was about 200 and W. C. Smith, chairman of the A.I.E.E. section, presided.

The June meeting of the section was held on the 20th at the Bellevue Hotel with G. T. Royden, chairman, presiding. Twenty were present at the informal dinner and sixty attended the meeting.

As this was the annual meeting, election of officers was held with the following results: Chairman, A. H. Brolly, Television Laboratories; Vice Chairman, R. C. Shermund, Heintz and Kaufman; and Secretary-Treasurer, R. D. Kirkland, Mackay Radio and Telegraph Company. A paper on "Activities of the Bell System in the Field of Radio" was presented by A. E. McMahon. This was followed by a demonstration which was held at the Grant Avenue office of the Pacific Telephone and Telegraph Company.

Washington Section

The Washington Section met in the auditorium of the Potomac Electric Power Company on June 11. T. Mc. L. Davis, chairman, presided and eighty-seven were present. Twenty-four attended the informal dinner whicn preceded the meeting.

A paper on "Generation and Utilization of Ultra-Short Waves" was presented by F. A. Kolster of the International Telephone and Telegraph Company. In it he reviewed previous developments in the field of short-wave transmission. Practical considerations underlying the design of suitable oscillatory circuits for use in the generation of power in the region around sixty megacycles were discussed. The design of circuits for this purpose giving careful consideration to the sharpness of resonance and its effect upon oscillator performance was considered. A number of those present participated in the discussion.

Personal Mention

Formerly in consulting practice, I. J. Saxl has become director of research development for the Waypoyset Manufacturing Company, Pawtucket, R.I.

F. V. Schultz is now a seismograph operator for Gulf Research and Development Corporation of Pittsburgh having previously been with Globe Radio Manufacturing Company.

B. A. Schwarz formerly with DeForest Radio Corporation of Canada is now in charge of automobile radio engineering development for the Zenith Radio Corporation of Chicago.

Previously with the Westinghouse Electric and Manufacturing Company, E. E. Schwarzenbach has become a radio engineer in the export division of the United American Bosch Corporation, Springfield, Mass.

W. K. Sherman, Lieutenant, U.S.N., has been transferred from Pearl Harbor, T.H., to the USS Blakeley with base at Washington, D.C.

S. B. Slavin formerly with the Radio Corporation of America has become a receiving engineering for RCA Communications at Inverness, Calif.

G. H. Sparhawk, Lieutenant, U.S.A., has left Yale University for a station at Wheeler Field, Oahu, T.H.

Previously with J. P. Burns Research Laboratories, J. R. Stimps has become chief engineer of Television Research Corporation, Havre, Mont.

A. R. Taylor, Lieutenant, U.S.N., has been transferred from Boston Navy Yard to the USS Augusta basing at Seattle, Wash.

Formerly with Centralized Sound Apparatus Laboratories, W. H. Troutbeck has become chief engineer for Electro-Acoustic Engineering Company, London, England.

Previously with Boeing Air Transport, A. F. Trumbull is now in charge of aircraft radio service for United Air Lines, Chicago, Ill.

H. J. Tyzzer has left Pilot Radio and Tube Corporation to join the staff of Crosley Radio Corporation at Cincinnati.

Previously at Massachusetts Institute of Technology, H. M. Wagner has joined the electrical Research division of RCA Radiotron Company, Harrison, N.J.

T. B. White, Lieutenant, U.S. Marine Corps, has been transferred from Harvard University to Marine Barracks at Quantico, Va.

F. G. Allen, Lieutenant, U.S. Army Air Corps, has been transferred from Chanute Field to the Signal School at Fort Monmouth, N.J.

R. M. Blair formerly with Zenith Radio Corporation has become chief engineer for the Eastern Division of the Meissner Manufacturing Company, New York City.

W. P. Cogswell, Lieutenant, U.S.N., has been transferred from the USS Saratoga to the Bureau of Engineering, Washington, D.C.

L. R. Daspit, Lieutenant, U.S.N., has been transferred from the USS-S20 to Postgraduate School, U.S. Naval Academy, Annapolis, Md.

J. H. Foley, Lieutenant, U.S.N., is now at the Boston Navy Yard having previously been on the USS Arizona.

S. L. Leonard formerly with Higgs, Ltd., has joined the Research Department of Burndept's Ltd., Erith, England.

Formerly with Hygrade Sylvania Corporation, F. C. Hinderson has joined the engineering staff of Raytheon Production Corporation, Newton, Mass.

Previously with Standard Telephones and Cables, A. D. Hodgson has joined the aircraft radio department of the Plessey Company, Ilford, England.

C. M. Kimball, Jr., has joined the development engineering department of the National Union Radio Corporation, Newark, N.J., having recently obtained a doctorate in science from Harvard University.

Previously chief engineer for Rudolph Wurlitzer Company, V. C. McNabb has joined the staff of the Atwater Kent Manufacturing Company in Philadelphia.

T. D. Meola of RCA Communications has been transferred from Rocky Point to Norco, La.

J. W. Million, Jr., has left Utah Radio Products Company to become vice president of Audiola Radio Company, Chicago.

H. G. Moran, Lieutenant, U.S.N., has been transferred from the Brooklyn Navy Yard to the Naval Air Station at Lakehurst, N.J.

Previously with Yoshimura and Company, Katsumi Moriwaki has become designer of radio apparatus for Oki Electric Company, Tokyo.

G. A. Norton recently at Harvard Engineering School has joined the staff of Arthur D. Little, Inc., of Cambridge, Mass.

Previously on the USS Concord, L. W. Nuesse, Lieutenant, U.S.N., has been transferred to the Philadelphia Navy Yard.

R. T. Palmer has left Duell, Dunn, and Anderson to establish a patent law practice of his own in Boston, Mass.

Having left the deForest-Crosley Radio Corporation, F.H.R. Pounsett is now with the Stewart-Warner-Alemite Corporation at Bellevue, Ontario, Canada.

R. L. Snyder formerly with the Bell Telephone Company of Pennsylvania has established a consulting practice for sound, telephone, and electrical problems at Glassboro, N.J.

Previously with the RCA Victor Company, J. D. Stacy has become capacitor design engineer for the General Electric Company at Pittsfield, Mass.

Eugene Wesselman formerly with Rudolph Wurlitzer Manufacturing Company has joined the engineering department of the Colonial Radio Corporation at Buffalo, N.Y.

Previously with the Hazeltine Service Corporation, M. L. Thompson has joined the staff of the Philco Radio and Television Corporation in Philadelphia.

Proceedings of the Institute of Radio Engineers
Volume 22, Number 8 *August, 1934*

TECHNICAL PAPERS

PHASE ANGLE OF VACUUM TUBE TRANSCONDUCTANCE AT VERY HIGH FREQUENCIES*

By

F. B. Llewellyn

(Bell Telephone Laboratories, Inc., New York City)

Summary—*Theoretical considerations indicate that the transconductance of a vacuum tube exhibits a phase angle when the transit time of electrons from cathode to anode becomes an appreciable fraction of the high-frequency period. Measurements show that such a phase angle actually occurs and that its behavior is in general agreement with the theoretical predictions.*

A RECENT paper[1] gives a theoretical development leading to an equivalent circuit for vacuum tubes at frequencies so high that electrons take an appreciable part of a high-frequency cycle to cross from cathode to plate of the tube. This development shows that even at these high frequencies the internal cathode-plate path of the tube may be represented by a fictitious generator acting in series with an impedance. The generator has an effective electromotive force of μe_g where, however, μ is complex instead of real and thus introduces a phase angle into the driving electromotive force of the plate circuit. Likewise, the internal plate impedance of the tube is no longer a pure resistance, but is a general impedance z_p containing both real and imaginary components corresponding, respectively, to resistance and reactance. This introduces a phase angle into the resultant current.

The ratio μ/z_p is called the transconductance and this term will be retained temporarily even when μ and z_p are complex. The phase of this quantity as calculated by the methods described in the paper referred to is plotted in Fig. 1, where the abscissas are expressed in terms of transit angle of the electron. The transit angle denotes the angular phase through which the current changes while the electron is crossing from cathode to plate of the vacuum tube. For example, if an electron takes a whole cycle to cross, then its transit angle is 2π radians.

* Decimal classification: R130. Original manuscript received by the Institute, February 27, 1934. Presented before the U.R.S.I. and Institute of Radio Engineers, April, 1934, Washington, D. C.

[1] F. B. Llewellyn, "Vacuum tube electronics at ultra-high frequencies," Proc. I.R.E., vol. 21, p. 1532; November, (1933).

The experiments which form the basis of the present paper were designed to measure the phase angle of the transconductance and to compare the measured results with the calculated ones. The method of

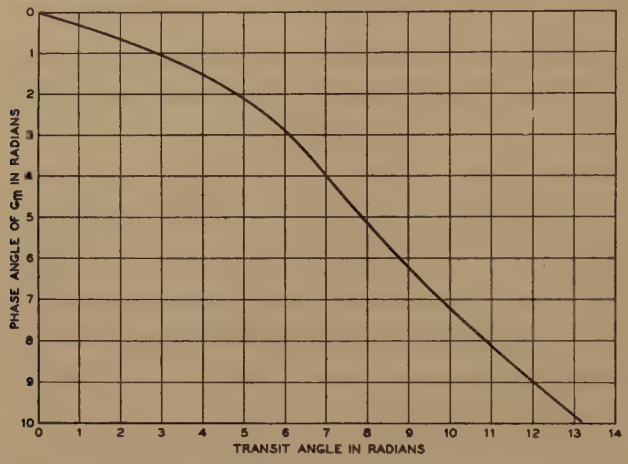

Fig. 1—Calculated phase of transconductance.

measurement is based on a simple circuit property which may be derived from the schematic diagram shown in Fig. 2(a). This sketch shows a vacuum tube having an impedance Z_1 connected between its

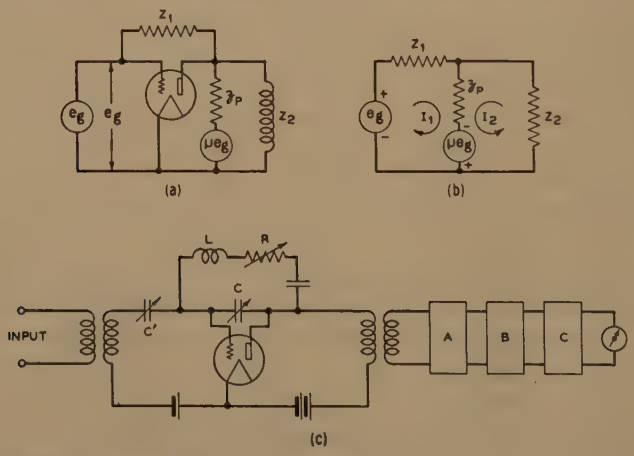

Fig. 2—Experimental circuit for measuring phase of transconductance.

grid and plate terminals. The vacuum tube works into an output impedance Z_2 which is connected between the plate and cathode terminals. It is assumed that e_g is a high-frequency electromotive force applied between the grid and cathode terminals.

The internal action of the tube is represented by a general impedance z_p which replaces the low-frequency resistance r_p and a fictitious generator μe_g where a complex μ replaces the real μ of low-frequency application.

Fig. 2 (b) shows the equivalent network which corresponds to the schematic drawing (a) and is prepared for the writing of circuit equations. These equations yield the result,

$$I_2 = \frac{e_g(\mu Z_1 - z_p)}{Z_1 Z_2 + Z_1 z_p + Z_2 z_p}.$$

From this expression it is seen that if Z_1 is adjusted to make the numerator zero, that is, so that

$$\mu Z_1 = z_p$$

then the current I_2 which flows through the output impedance Z_2 becomes zero.

The general method of experiment is to introduce a high-frequency electromotive force on the grid side of the vacuum tube and then adjust the value of Z_1 until the output current is zero. When this has been done

$$Z_1 = \frac{z_p}{\mu} = \frac{1}{g_m}$$

and the phase of the transconductance g_m is given by the phase of the impedance Z_1.

The problem is therefore reduced to finding the phase of Z_1 when it is adjusted to make the output zero.

The physical set-up of the experimental circuit is shown in Fig. 2 (c). The impedance Z_1 consists of the tunable circuit LCR in which both C and R are variable. The condenser in series with L and R is merely a stopping condenser of low reactance which is used to prevent the direct-current plate potential from reaching the grid. The condenser C must be connected as directly to the grid and plate electrodes of the tube as possible. Because of this a tube of special construction was employed. Moreover, C should be large compared with the internal grid to plate capacity of the tube. The reason for this is to minimize the effect of small capacity changes resulting from changes of space charge within the vacuum tube. The resistance R consisted of a length of pencil lead about 1-1/2 inches long. Its value was varied by changing the position of two clip connections which held it in place.

The condenser C' was used for the purpose of series resonating the input and output circuits; thus to adjust C', the heating current for the filament of the tube was turned off and the B battery potential reduced to zero. The impediance Z_1 was then short-circuited. When this

had been done, the high-frequency input electromotive force was introduced and C' was adjusted for maximum output current. With this adjustment the removal of the short circuit from the impedance Z_1 produced a current in Z_2, whose magnitude is very nearly equal to the input electromotive force divided by the magnitude of the impedance Z_1.

In the experimental procedure, the first step was to adjust C' as described above. The short circuit was then removed from Z_1 and the direct-current potentials applied to the vacuum tube. Next the value of Z_1 was adjusted by means of R and C until the output current was zero. When this has been done the phase angle of the impedance Z_1 is equal to the phase angle of the transconductance g_m. Hence, the next step is to measure the phase angle of Z_1.

For this measurement the vacuum tube filament current is turned off and the value of the output current is recorded. Call this value I_a. Next the tuning of Z_1 is adjusted to give minimum current when the filament current is kept turned off. Under this condition Z_1 is tuned to antiresonance. Call the resulting current value I_b.

From these two current readings the phase angle of the mutual conductance may be calculated from the formula

$$\cos \theta = \frac{I_b}{I_a}.$$

(The derivation of this formula is given in the Appendix.)

The experimental technique thus involves the measurement of two currents. It will be recognized that the current I_b which flows when Z_1 is tuned to antiresonance is very small. Its measurement, therefore, requires the use of a high gain amplifier in order that readable deflections may be obtained. To eliminate the necessity for amplifying at the high frequencies involved, the radio-frequency input in Fig. 2 (c) was modulated by a 1000-cycle note. Then a detector was placed at A. With this arrangement an audio-frequency amplifier B could be used instead of the radio-frequency amplifier which would otherwise be necessary. The audio-frequency current to be amplified is proportional to the square of the radio-frequency current. A calibrated vacuum tube voltmeter was used at C for reading the 1000-cycle output.

The vacuum tube on which data were taken was of special construction designed for high-frequency work. The modification consisted in bringing out short direct leads at the top of the glass bulb from the grid and plate electrodes of the tube. These leads allow the condenser C in Fig. 2 (c) to be connected between the grid and plate with a minimum length of lead. The supporting wires for the grid and plate were insulated from the tube elements themselves by fused quartz

beads so that extraneous wires within the glass bulb were of negligible length. The cathode terminals were brought out through a press at the base of the bulb.

Under normal conditions this tube would be operated with a plate potential of about 750 volts. In these phase angle measurements a somewhat lower potential was employed so that the transit time of the electrons would be lengthened and hence larger phase angles produced. This allows the data to be taken at a somewhat lower frequency than would otherwise be necessary.

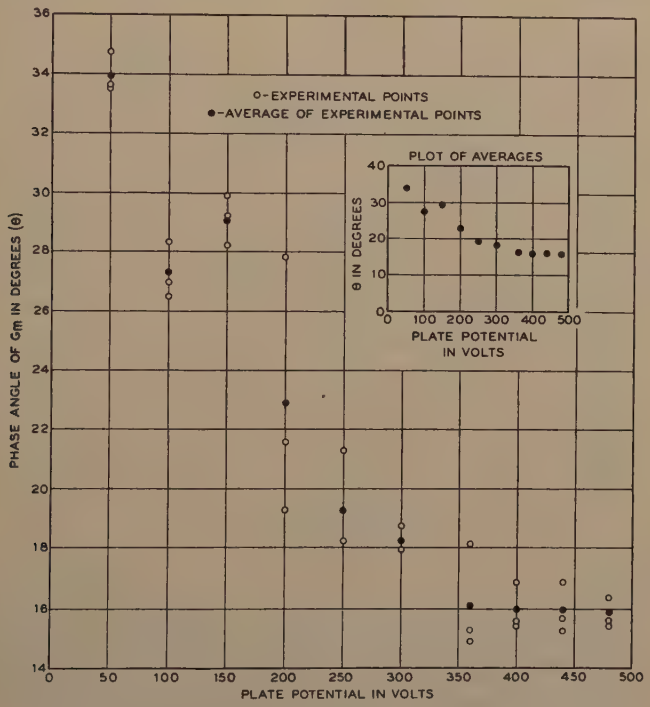

Fig. 3—Phase of transconductance versus plate potential
$\lambda = 7$ meters
$V_g = -5$ volts
$I_f = 3.2$ amperes

Results of the measurements are shown on the accompanying graphs Figs. 3 to 7. On account of the experimental difficulties in obtaining accurate measurements several readings were taken for each adjustment. These are plotted on the graphs where hollow circles are used to indicate the data points. The average of the experimental values is shown in each case by a solid circle. On each sketch, a graph showing the solid circles only is drawn in a small box. The data in

all cases except Fig. 7 were taken at a wavelength of 7 meters. This was low enough to produce appreciable transit angles, but was large enough to allow reliable circuit adjustments to be made.

Fig. 3 shows the phase of the transconductance as a function of the plate potential when all other adjustments are held fixed. The grid bias was -5 volts. The graph shows that a decrease in plate potential produced an increase in the phase angle. This is in agreement with the prediction that an increase in transit time produces an increase in phase angle.

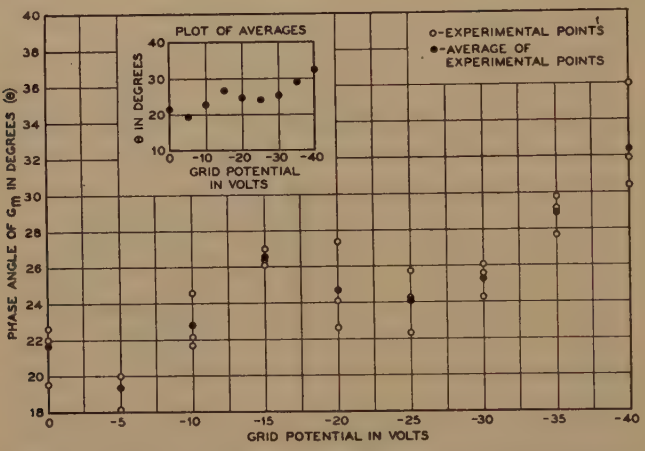

Fig. 4—Phase of transconductance versus grid potential
$\lambda = 7$ meters
$V_p = 250$ volts
$I_f = 3.2$ amperes

The next figure shows the angle as a function of the grid potential. The result here is an increasing angle for an increasing negative grid potential. This also agrees with the prediction that the phase angle increases when the transit time increases, since the more negative grid causes the electrons to take a longer time for their crossing.

Fig. 5 shows what happens to the phase angle when both grid and plate potentials are varied simultaneously in such a way as to keep the plate current constant. The result shows practically no change in the phase angle for a wide range of plate and grid potentials. This has an interesting significance as tending to show that the grid potential has approximately μ times as much effect on the transit time as does the plate potential.

Fig. 6 shows the effect of space charge on the phase angle. Data for this graph were obtained by varying the filament temperature. The re-

sult is somewhat inconclusive, although following predictions fairly well. The space current is plotted on the sketch. For values of filament

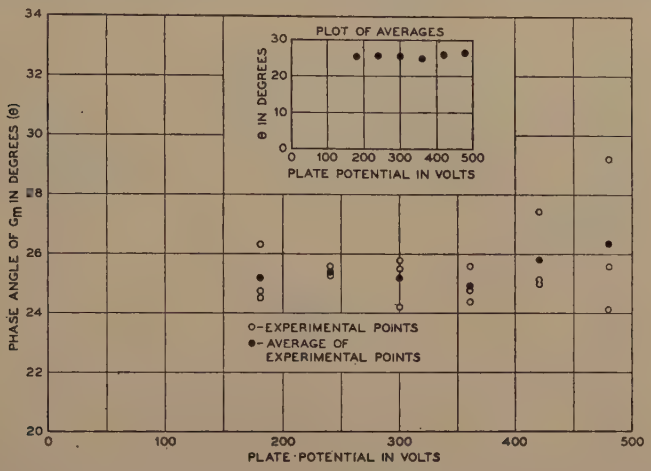

Fig. 5—Phase of transconductance versus plate potential for constant plate current

$\lambda = 7$ meters
$I_p = 10$ mils
$I_f = 3.2$ amperes

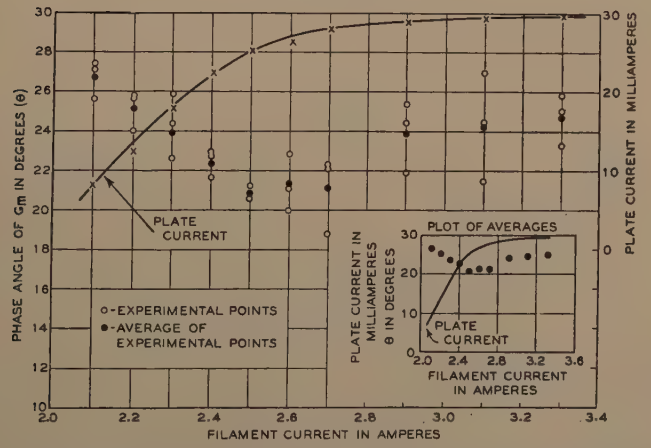

Fig. 6—Phase of transconductance versus filament current

$\lambda = 7$ meters
$V_g = -5$ volts
$V_p = 250$ volts

current just below 2.8 amperes, the space current begins to fall. This means that the space charge begins to decrease and consequently that

the electrons travel somewhat faster. A corresponding decrease in phase angle appears in the graph. At still lower values of filament current, for example below 2.4 amperes, the equivalent μe_g generator convention begins to fall down, since changing grid potentials have little effect on the plate current when the filament is not operating under space charge conditions. When this happens, the tube behavior approaches that of a condenser which should have a phase angle in the neighborhood of 90 degrees. Thus it is to be expected that the phase angle should increase at the smaller values of filament heating current, and this tendency is illustrated in the graph.

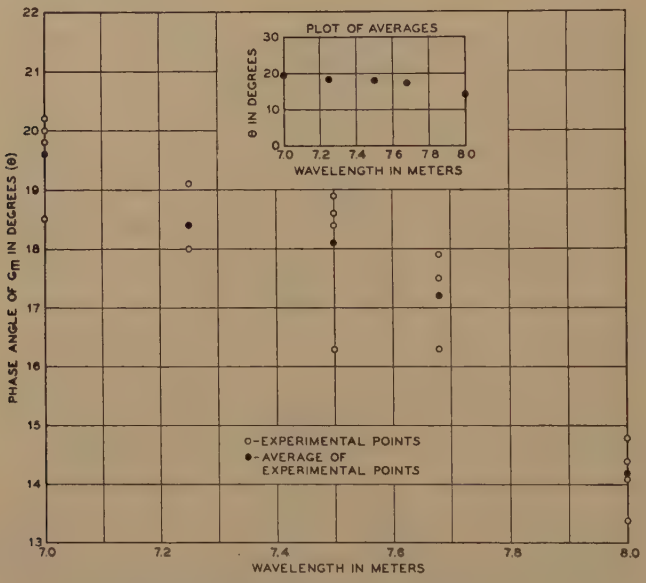

Fig. 7—Phase of transconductance versus wavelength
$V_p = 250$ volts
$V_g = -5$ volts
$I_f = 3.2$ amperes

A comparison of the measured values of phase angle with the computed values shown in Fig. 1 is of some interest. Fig. 5 shows measured values of about 25 degrees corresponding to 0.437 radian. From the theoretical curve, this yields a value of transit angle of 1.3 radians or nearly 75 degrees. This indicates that the electron crosses from filament to plate of the tube in roughly one fifth of the time of a high-frequency cycle. It is not thought advisable to attempt definite calculations of the transit time because the effect of the grid is not adaptable to exact calculation.

The final curve, Fig. 7, shows the effect of the frequency on the phase angle. This curve has a general trend which would be expected, since the phase angle increases with increase of frequency, that is, decrease of wavelength.

The foregoing data and graphs give a description of the cathode-plate internal path of the vacuum tube. It must be emphasized that the data give no information concerning the cathode-grid path which plays an important part in the determination of ultra-high-frequency oscillation conditions.

In general the data verify the qualitative predictions of the theory. Quantitative results depend on the calculation of transit angles and as has been stated no accurate way of computing these for the triode has been found. From general considerations and comparison with conditions existing in diodes, the transit angle which fits the experiments and theory together appears to be of the right order of magnitude.

One result of this work is the indication that phase modulation may always be expected to accompany the amplitude modulation of an ultra-high-frequency amplifier working in the state where transit times are appreciable.

Acknowledgment

A large part of the experimental portion of this investigation was conducted by Mr. W. E. Kirkpatrick of the Bell Telephone Laboratories.

Appendix

Proof that $\cos\theta = I_b/I_a$

The impedance of Z_1 is in general

$$Z_1 = \frac{(R + i\omega L)\,\dfrac{1}{i\omega C}}{R + i\left(\omega L - \dfrac{1}{\omega C}\right)} = \frac{L}{CR}\,\frac{1 - i\dfrac{R}{\omega L}}{1 + i\left(\dfrac{\omega L - \dfrac{1}{\omega C}}{R}\right)}.$$

Let $\tan\phi = -R/\omega L$ and

$$\tan\theta = \frac{\omega L - \dfrac{1}{\omega C}}{R}.$$

Then we may write

$$Z_1 = \frac{L}{CR}\,\frac{\cos\theta}{\cos\phi}\,e^{i(\phi-\theta)}$$

so that $(\phi-\theta)$ is the phase angle of Z_1 and is the angle sought.

In general when the vacuum tube is dead and C' is tuned, the output current is given by $I = V/Z_1$, where V is the input electromotive force. This relation holds because the impedance of other parts of the circuit is negligible in comparison with Z_1 as provided for by the series tuning of condenser C'. Thus the current I_a has the magnitude

$$|I_a| = \frac{V}{\dfrac{L}{CR}\,\dfrac{\cos\theta}{\cos\phi}}.$$

The minimum current I_b occurs when θ is approximately zero so that $\cos\theta$ is unity. Thus,

$$|I_b| = \frac{V}{\dfrac{L}{CR}\,\dfrac{1}{\cos\phi}}.$$

Therefore,

$$\left|\frac{I_b}{I_a}\right| = \cos\theta.$$

It will be recognized that the phase angle θ is the one found whereas the angle sought is $(\phi-\theta)$. However, as seen by its definition, $\tan\phi = -R/\omega L$ so that ϕ is a small angle and moreover will vary only slightly, since the per cent variations in the resistance R are not large. Hence θ gives a very good approximation to the angle of the transconductance of the tube and an even better approximation to its variations.

Proceedings of the Institute of Radio Engineers
Volume 22, Number 8 *August, 1934*

THE ANALYSIS OF AIR CONDENSER LOSS RESISTANCE*

By

W. Jackson
(Engineering Laboratory, Oxford, England)

Summary—*This paper gives the results of an analysis of the variation over the wavelength range from 35 to 63.5 meters of the loss resistance of a specially constructed variable air condenser. The condenser and the method of measurement are described. It is shown that the losses at any capacitance value and frequency may be represented by a fixed resistance plus an effective resistance arising from a constant power factor in the insulating material supporting the movable plate. The expression for the condenser loss resistance is compared with similar expressions for variable air condensers obtained by previous authors.*

I. Introduction

IN THE course of some precision measurements of dielectric loss, in the frequency range $5-10\times10^6$ cycles per second, it became necessary to determine the inherent power factor of a continuously variable air condenser constructed to hold the dielectrics being tested. Two methods have been devised for measuring the power factor of condensers at radio frequencies, due, respectively, to D. W. Dye and E. B. Moullin. Dye's method[1] makes use of a specially designed air condenser consisting of two capacitance portions in parallel; one an imperfect portion containing the insulating supports for the main capacitance, and the other this main capacitance, which is a pure air condenser and is presumed to have no loss. This perfect portion is removable and is replaced by the equal capacitance of the condenser to be tested. The total circuit resistance is measured by a resonance method before and after the substitution, and the difference of value ascribed to the loss in the test condenser. Moullin's method[2] possesses the great advantage that it does not require a special condenser, and is therefore more generally applicable. It requires only a set of inductances, appropriate in value to the frequency of measurement, which are identical in every respect save in the material used for the wire. If each of these coils is connected in turn to the condenser to be tested, and the circuit resistance or power factor measured either by the insertion at resonance of additional resistance or from the width of the resonance curve, delineated by making suitable changes in the fre-

* Decimal classification: R 241. Original manuscript received by the Institute, January 19, 1934.
[1] *Proc. Phys. Soc.*, vol. 40, p. 285, (1928).
[2] *Proc. Royal Soc.*, A, vol. 137, p. 116, (1932).

quency of the injected electromotive force, any losses which are not located in the wire itself will remain unchanged by the substitution so that the resistance inherent in the test condenser at the frequency employed can be separated. For measurements at the same capacitance value, but at some other frequency, a new set of coils of appropriate inductance must be provided.

Previous analysis[1,2,3] of the effective series resistance of variable air condensers have shown that it can usually be expressed by the relation,

$$R_s = r + \frac{\phi C_1}{pC^2} \text{ where } p = 2\pi \times \text{frequency}.$$

The first conponent, r, is believed to be due to contact resistances between neighboring plates of the same bank, and is apparently constant

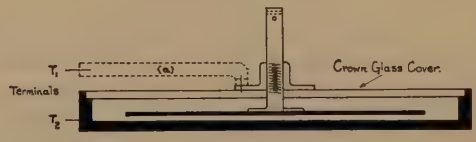

Fig. 1

and independent of the capacitance and frequency values. The second term results from dielectric loss in the insulation supporting one set of plates. The capacitance C of such condensers may be regarded as composed of a fixed and imperfect portion C_1 due to the supporting insulation, in parallel with a variable air portion devoid of energy loss. The power factor ϕ of the portion C_1 seems usually to be substantially constant over a wide range of frequency.

The measurements described in the paper were made to determine the intrinsic power factor and resistance of the aforementioned air condenser over the range of wavelength 35 to 63.5 meters. Moullin's method was adopted. When the condenser resistance had been measured it was found to comply with the equation for R_S given above.

Details of the Condenser

The general details of the condenser are shown in Fig. 1. It consists of a thick circular brass disk mounted inside a shallow cylindrical brass container. The disk is provided with a spindle threaded at its lower end, on which it is supported in a metal bush located at the center of a

[3] R. M. Wilmotte, *Jour. Sci. Instr.*, vol. 5, p. 369, (1928).

thick circular crown glass plate which rests on the rim of the container. At the upper end of the spindle holes are drilled into which a long ebonite rod can be inserted for the purpose of rotating the disk and varying its distance from the bottom of the container. In this way any capacitance value between 200 and 1400 micromicrofarads is obtainable with a 9-inch diameter movable plate. Electrical connection to this plate was made, for the purpose of the present measurements, through a half-inch diameter copper rod (shown dotted in Fig. 1) and the central supporting bush, the weight of the plate serving to ensure an efficient contact at the thread.

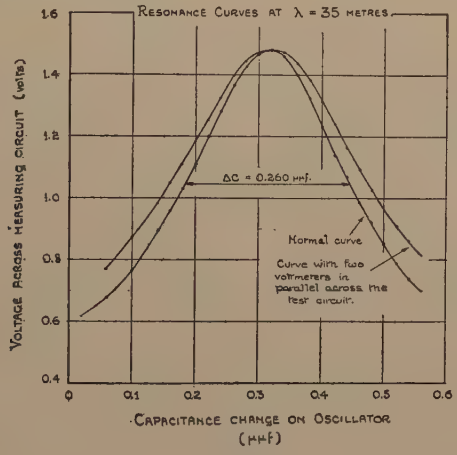

Fig. 2

Details of the Coils

The coils employed were some of those used by Moullin and described by him.[2] They consisted of long narrow rectangles in which the spacing D between the wires was twenty times the diameter d of the wire, and of length about six times their breadth. For coils of this form, in which D/d is constant, Moullin has shown that the conductor resistance at frequency f cycles per second varies as $\sqrt{R_0 l}$, where R_0 is the steady current resistance and l the perimeter of the rectangle. In view of this the coils did not need necessarily to be made of wire of the same diameter, and those used consisted of three copper rectangles having wire diameters of 0.96, 0.642, and 0.22 centimeter, respectively, and one of brass conductor of 0.642 centimeter diameter.

Details of the Measurements

These coils were connected in turn between the terminals T_1 and T_2, Fig. 1, and the power factor of the whole circuit deduced by meas-

uring the fractional width of the resonance curve at $1/\sqrt{2}$ of its height. The frequency of the source of electromotive force was varied continuously over the requisite range by means of a fine adjustment condenser on the generator. The differences in reading of this condenser could be converted to frequency changes from a calibration performed by a double beat process.

A thermionic voltmeter, connected across the test condenser, was used as the indicator. Since the voltmeter itself introduced some energy

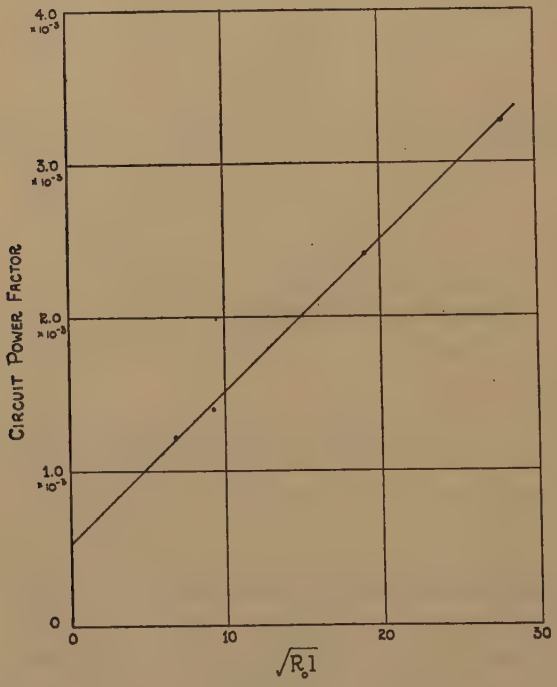

Fig. 3

loss it was necessary to determine this amount for otherwise it would have been credited to the condenser. Resonance curves were plotted, therefore, first with one, and then with two voltmeters in parallel, connected across the circuit. The increase in circuit power factor which resulted on connection of the second voltmeter gave the required correction since tests showed that both voltmeters introduced the same additional power factor. Fig. 2 shows specimen resonance curves taken at a wavelength of 35 meters, and will explain the method of allowing for the voltmeter loss.

Results of the Measurements

Fig. 3 shows the circuit power factor, as measured at a wavelength of 45 meters, plotted against $\sqrt{R_0 l}$ for the four rectangular coils described. (In this figure the power factor due to the voltmeter has been subtracted from the measured circuit values.) As in Moullin's measurements the result is a straight line which does not pass through the origin. The intercept on the axis of power factor indicates that the circuit has a residual power factor of 5.4×10^{-4}. The radiation resistance of the circuit is shown later to be negligibly small, so that this residual is due to the condenser (and the common connecting bar (*a*), Fig. 1) and gives its power factor at this wavelength and the capacitance value of 562 micromicrofarads.

Having ascertained that the results conformed to those obtained by Moullin, the use of several coils of equal inductance at each of the testing frequencies was not adhered to, and the variation of the condenser resistance with frequency was studied by employing the copper rectangle of wire diameter 0.96 centimeter throughout. This called for appropriate adjustment of the test condenser value at each of the several frequencies. The resistance of the condenser was then determined from the difference between the circuit resistance, as deduced from the measured circuit power factor, and the calculated resistance of the rectangular coil.

For the above coil, $D/d = 20$, the resistance per unit length of conductor is increased by the presence of the return conductor by less than 0.125 per cent,[2] so that the "proximity effect" can be ignored and the resistance calculated from the formula for skin effect in an isolated wire. This gives the resistance R_f at frequency $f = p/2\pi$, for the rectangle of perimeter l, in terms of its direct-current resistance R_0, in the form

$$\frac{R_f}{R_0} = \frac{\sqrt{2}Z + 1}{4} \quad \text{where} \quad Z^2 = \frac{\pi p d^2}{\rho} \quad \text{and} \quad R_0 = \frac{4\rho}{\pi d^2} \cdot l.$$

There is a correction term for self-capacitance which cannot be calculated accurately but which can be estimated approximately. It is such that it could not increase the coil resistance by more than 3 per cent at a wavelength of 35 meters. As this correction will be proportional to the square of the frequency, it is only 1 per cent at 63.5 meters. In addition, the rectangle has a radiation resistance which can be calculated from the equation

$$R_r = 320\pi^4 \frac{S^2}{\lambda^4} \text{ ohms}$$

where S is the area of the rectangle in square meters. The value of this is only 0.0002 ohm at 35 meters, and decreases rapidly with increase in wavelength.

The results of the measurements at several wavelengths between 35 and 63.5 meters are tabulated below.

TABLE I

Wavelength (meters)	35.0	40.0	42.5	45.0	50.0	56.0	63.5
Capacitance ($\mu\mu$f)	338	440	503	562	688	865	1110
Circuit power factor	1.280×10^{-3}	1.235×10^{-3}	1.220×10^{-3}	1.215×10^{-3}	1.200×10^{-3}	1.190×10^{-3}	1.185×10^{-3}
Circuit resistance (ohms)	0.0705	0.0595	0.0545	0.0520	0.0465	0.0410	0.0360
Coil + connection bar resistance	0.0375	0.0350	0.0335	0.0330	0.0315	0.0295	0.0265
Condenser resistance	0.0330	0.0245	0.0210	0.0190	0.0150	0.0115	0.0095
$10^6/fC^2$	1.015	0.690	0.560	0.475	0.355	0.250	0.170

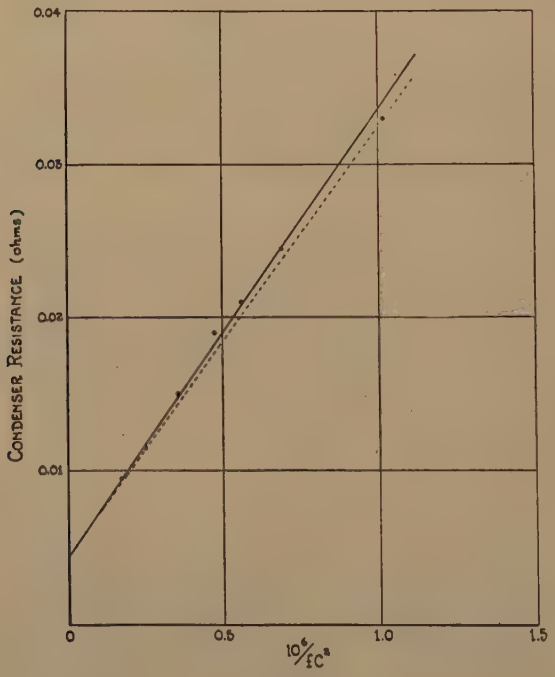

Fig. 4

The derived values of the condenser resistance, without allowance for the small self-capacitance correction and the radiation resistance of the circuit, are represented as a function of $10^6/fC^2$ in the full curve of

Fig. 4, from which it is seen that the effective resistance of the condenser can be expressed by the equation[4]

$$R_S = 0.0045 + 0.028 \cdot \frac{10^6}{fC^2} \text{ ohm}$$

where C is in micromicrofarads and f is in megacycles per second. The dotted line in the same figure has been drawn after subtracting self-capacitance and radiation resistance corrections for the rectangle based on the values already stated for them at 35 meters.

On connecting the spindle and bush of the test condenser by a short thick copper strap, the circuit resistance at 61 meters was reduced by rather more than 0.001 ohm. This suggests that the constant term, 0.0045 ohm, arises largely from contact resistance on the thread. The linear form of the curve of Fig. 4 suggests further that the power factor of the crown glass cover was substantially constant over the frequency range considered. The capacitance C_1 across the crown glass cover is probably about 5 micromicrofarads, so that the power factor of the glass must be of the order of 3×10^{-2}.

The results recorded in the above table give the power factor of the condenser (plus that due to the common connecting bar (*a*) Fig. 1) at 45 meters as 5.1×10^{-4}, which compares favorably with the value of 5.4×10^{-4}, obtained from the curve of Fig. 3.

Acknowledgment

The author is indebted to Mr. E. B. Moullin for his interest in the measurements, which were made in the Engineering Laboratory of Oxford University.

[4] The corresponding expressions obtained by previous authors for the variable air condensers treated by them, with C and f in micromicrofarads and megacycles respectively throughout, are as follows:

Dye[1] $R_S = 0.007 + 0.012\ (10^5/fC^2) + (10/f^2C^2)$ ohms.
Moullin[2] $R_S = 0.05 + 0.091\ (10^6/fC^2)$ ohms.
Wilmotte[3] $R_S = 0.02 + 0.022\ (10^3/fC^2)$ ohms.

Proceedings of the Institute of Radio Engineers
Volume 22, Number 8 *August, 1934*

CONTRIBUTION TO THE THEORY OF NONLINEAR CIRCUITS WITH LARGE APPLIED VOLTAGES*

By

W. L. Barrow

(Round Hill Research Division, Department of Electrical Engineering, Massachusetts Institute of Technology, Cambridge, Mass.)

Introduction

IN MANY instances problems arise in which the resistance does not have a constant value but varies in some way with the current. Such an element is usually referred to as "nonlinear." Rectification, amplification, modulation, and demodulation are but several of the processes inseparably connected with a nonlinear circuit element. The large and rapidly growing number of practical applications of nonlinear elements makes the calculation of the performance of this type of circuit a problem of fundamental importance.

While the present paper deals particularly with the nonlinear properties of a vacuum tube, there are many other cases of practical interest to which the analysis is directly applicable. For example, a microphone, telephone, loud speaker or similar device employing a diaphragm displays a nonlinear relation between the magnitude of the acoustic pressure wave and the displacement of the diaphragm because of hydrodynamic friction and radiation. That type of nonlinearity characterized by hysteresis, as found in inductors with iron cores, certain gaseous tubes, etc., will not be considered. Concisely stated, only those devices will be treated which have *a single valued current-voltage characteristic of arbitrary shape.* Thus, the following analysis deals with nonlinear resistance elements.

Historically, the first analytical attack seems to be that of J. R. Carson[1] in 1919. The power series method given there forms the basis of our present conventional vacuum tube theory for small amplitudes of applied voltage, and this method has been further developed and extended in a large number of subsequent papers. However, for large amplitudes, this method becomes quite cumbersome, and consequently in recent years effort has been made to secure a less involved mode of attack. By far the most fruitful of the several proposed schemes seems to be that in which the current-voltage characteristic is represented by a trigonometric series, rather than a power series. The

* Decimal classification: R140. Original manuscript received by the Institute, March 1, 1934.

[1] Numbers refer to bibliography.

first application of this idea to vacuum tube circuit theory appears to have been made by E. Peterson and C. R. Keith[2] in 1928. Their treatment was confined to a single special case and brought out neither its general nature nor its great advantage over power series and graphical methods. More recently (1933) a paper by W. R. Bennett[3] has developed the Fourier series method into a more general tool, but seems to be clothed in a mathematical complexity far beyond that warranted by the nature of the problem. Since completing this work a discussion of rectification by a similar method has been given by Strutt[7]; some of his results are of interest here.

It is thought that the present treatment, which is based on a trigonometric polynomial representation of the current-voltage characteristic obtained by schedule analysis, allows computation to be made with much less labor than preceding methods and at the same time possesses all of their generality. This advantage is secured by the artifice of extending the characteristic beyond its actual curve so as to make the trigonometric polynomial representation converge very rapidly, (in the sense that successive terms of the polynomial become smaller than the preceding), and by dealing with a small number of terms instead of with infinite series of integrals. Three different types of impressed voltage are dealt with, namely, a direct voltage bias plus a sine wave alternating voltage (representing the process of amplification), a bias plus two different frequency sine waves (modulation), and a bias plus an amplitude modulated wave (demodulation).

Representation of the Current-Voltage Characteristic by a Trigonometric Polynomial

A three-electrode vacuum tube has a grid-voltage—plate-current characteristic of the general form shown by the heavy curve *abd* in Fig. 1; this is the so-called dynamic characteristic and includes the effect of the resistance load in the external plate circuit. Such an experimentally obtained curve forms the basis of all further analysis (note that the differential parameters μ, r_p, etc., do not appear here).

By means of one of several available schemes for harmonic analysis,[4] an approximate representation for the curve of Fig. 1 can be obtained in about an hour.* The representation is periodic by nature and so does not represent the actual characteristic outside of the interval $a<e<c$, which is no limitation, since this interval may be made sufficiently large at the outset to include all desired voltage fluctuations. A 24-ordinate analysis has been made and the resulting approxi-

* The stencils of Terebesi (see reference 4) for 24-point analysis have been found particularly convenient and rapid.

mation curve plotted as a dotted line over the curve of Fig. 1. It is obvious that the approximation curve passes through the 24 selected points of the original curve, as it must, but is nevertheless a poor approximation, although given by a 12-term polynomial. The explanation is simply that the sharp jump required of the approximation curve at the ends of the interval a, c demands a very large number of terms before the original curve is closely approximated, and near the ends the agreement will even then be poor because of the Gibb's phenomenon.† This same undesirable occurrence is also fundamental to the treatment wherein a Fourier series is secured from an analytical expression

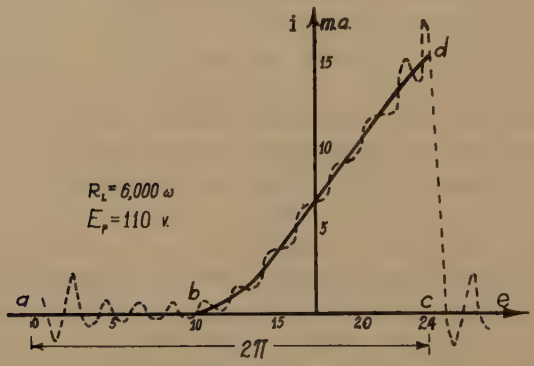

Fig. 1—Nonlinear current-voltage curve (heavy curve *abd*) and the approximation curve (dotted) obtained by taking *ac* as the fundamental period for a 24-point schedule analysis.

for the curve (for example, as has been done in the case of a linear rectifier).[2] Since the discontinuous character of the above type of curve is responsible for the large number of terms required, or better expressed, for the rate of convergence of the terms, the obvious thing to do is to remove this discontinuity. This may be done with remarkable improvement in results by artificially extending the characteristic as shown in Fig. 2. The interval *ak* is now made equal to 2π and a 24-ordinate schedule analysis again carried out; plotting the approximation curve so obtained over the original curve gives such a close agreement of the two curves that the deviation is not discernible on the scale used in the figure. Besides this, the fact that the approximation secured in this way is very excellent has the additional advantage that of the twelve terms in the polynomial only the first six are of consequential magnitude (terms are considered negligible only when their magnitude is less than 0.01 of the largest term present). It may be

† *See*, for example, Carslaw, "Fourier Series and Integrals," Chap. IX.

easily recognized that the above procedure leads to material reductions in the amount of computation necessary to secure accurate results. Clearly, the reason for the excellency of the approximation obtained by the method of Fig. 2 is that the curve which is to be represented is already very similar to a sinusoid and thus only small corrections are necessary. In fact, the last statement forms the general rule to be observed in extending any actual curve. This is usually best done by giving the segment d, e' odd symmetry to the segment d, b, etc. A further simplification is effected by making f the point of even symmetry and choosing f as the origin for the harmonic analysis, whereupon only

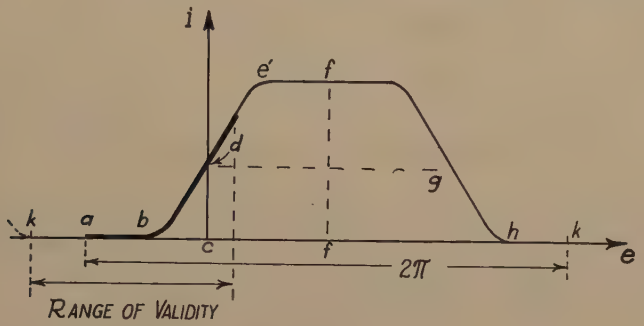

Fig. 2—Showing artificial extension (e' f g h k) of the actual characteristic (a b d e') to secure better convergence of the trigonometric polynomial approximation.

cosine terms appear in the results (the angle corresponding to cf is then added as a constant so that all voltages are measured from the real point of zero grid voltage).

With the above in mind, it will be assumed that a trigonometric polynomial representation has been obtained for the given current-voltage characteristic. If i represents the current and e the voltage, this representation will have the form,

$$i = a_0 + \sum_{n=1}^{\nu} a_n \cos\left(\frac{n\pi}{e_0} e + \theta_n\right) \tag{1}$$

where a_n, θ_n are the coefficients and phase angles calculated from the harmonic analysis, e_0 is half the distance a, k is measured in volts, e is the arbitrary impressed electromotive force, i is the current produced in the tube, and ν is the number of cosine terms of nonnegligible magnitude in the trigonometric polynomial. Since the effect of the external load resistance has been included in the dynamic current-voltage curves, the schematic diagram of the circuit under consideration is

that of Fig. 3, where R' represents a nonlinear resistance having the characteristic defined by $i=f(e)$ and given specifically by (1).

The problem is now to determine the magnitudes of all components of current flowing in the plate circuit for the three types of voltages previously mentioned.

Calculation of Amplification Products

When a sinusoidal voltage is applied to a circuit having the characteristic represented by (1) the current flowing in the plate circuit

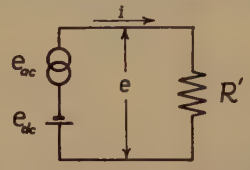

Fig. 3—Schematic diagram of the nonlinear circuit.

will depend upon the magnitude of this voltage and upon the operating point. If the voltage is given by $E \sin pt$ and the bias by E_0, the total impressed electromotive force is then

$$e = E_0 + E \sin pt, \tag{2}$$

which substituted into the expression (1) for the current gives

$$i = a_0 + \sum_{n=1}^{\nu} a_n \cos (u_n + v_n \sin pt)$$

where, for convenience,

$$u_n = \frac{n\pi}{e_0} E_0 + \theta_n \tag{3}$$

and,

$$v_n = \frac{n\pi}{e_0} E$$

has been written. After replacing $\cos (u_n + v_n \sin pt)$ by its equivalent expression in terms of single angles, (3) may be written:

$$i = a_0 + \sum_{n=1}^{\nu} a_n [\cos u_n \cdot \cos (v_n \sin pt) - \sin u_n \cdot \sin (v_n \sin pt)]. \tag{4}$$

Making use of the expansions due to Jacobi*

* *See*, for example, Whittaker and Watson, "Modern Analysis, p. 379.

$$\cos(x \sin\phi) = J_0(x) + 2\sum_{k=1}^{\infty} J_{2k}(x) \cos 2k\phi$$
$$\sin(x \sin\phi) = 2\sum_{k=1}^{\infty} J_{2k-1}(x) \sin(2k-1)\phi \tag{5}$$

in which $J_n(x)$ is a Bessel function of the first kind of order n and modulus x, (4) becomes

$$i = a_0 + \sum_{n=1}^{\nu} a_n \Big[\cos u_n \Big\{ J_0(v_n) + 2\sum_{k=1}^{\infty} J_{2k}(v_n) \cos 2kpt \Big\} - \sin u_n \Big\{ 2\sum_{k=1}^{\infty} J_{2k-1}(v_n) \sin(2k-1)pt \Big\} \Big]. \tag{6}$$

Inverting the order of summation in the two repeated summations* and rearranging gives

$$i = a_0 + \Big\{ \sum_{n=1}^{\nu} a_n J_0(v_n) \cos u_n \Big\} + \sum_{k=1}^{\infty} \Big\{ 2\sum_{n=1}^{\nu} a_n J_{2k}(v_n) \cos u_n \Big\} \cos 2kpt - \sum_{k=1}^{\infty} \Big\{ 2\sum_{n=1}^{\nu} a_n J_{2k-1}(v_n) \sin u_n \Big\} \sin(2k-1)pt. \tag{7}$$

The expressions within the brackets of (7) give the amplitudes of the various components of current flowing in the plate circuit. The first bracket represents the direct components due to the bias and rectification; the rectified current alone may be easily seen to be given by

$$i_{\text{rect}} = \sum_{n=1}^{\nu} [J_0(v_n) - 1] a_n \cos u_n. \tag{8}$$

From the behavior of $J_0(v_n)$ as v_n approaches zero, it may be seen that for small values of applied alternating voltage E the rectified component of current is independent of E and practically zero. The fundamental and harmonic current amplitudes are given by one or the other of the last two bracketed expressions, which may be expressed by the single equation

$$|i_m| = \left| 2\sum_{n=1}^{\nu} a_n \cdot J_m(v_n) \cdot \cos\left(u_n + \frac{m\pi}{2}\right) \right| \tag{9}$$

* This step can be justified by proving the absolute convergence of the expansions (5). Another proof has been offered by W. R. Bennett, (reference 3).

where m represents the order of the harmonic; thus, i_1 is the fundamental, i_2 is the second harmonic, and so on.

Equation (9) is the desired result. It allows the amplitude of fundamental and any harmonic current to be calculated with very little effort. For example, in most of the practical cases it has been found that six terms gave an adequate accuracy for engineering purposes; ν is then equal to six and the amplitude of any specified component of current is obtained by adding six numbers, each consisting of the product of three easily found quantities, viz., the coefficient a_n previously discussed, a sine or cosine value, and the value of a Bessel function. The latter presents no greater difficulty here than does the sine or cosine, as tables of values for $J_0(x)$, $J_1(x)$, . . . are quite generally available.[5]

Calculation of Modulation Products

Upon impressing two sinusoidal voltages of different frequencies on the nonlinear characteristic a current having sum, difference, double, etc., frequency components will be established. If $E_c \sin ct$ represent one of the alternating voltages, which may be taken to be the carrier, and $E_p \sin pt$ represent the other alternating voltage, considered to be the modulating voltage, the usual interest from the distortion point of view is in the series of components having frequencies equal to $c \pm mp$, where $m = 0, 1, 2, 3, \ldots$. Therefore, of all the components appearing in the plate circuit, only this series will be specifically calculated, although the results will allow the amplitude of *any* existing component of current to be readily secured. For a given characteristic, represented analytically by (1), the amplitudes depend upon the values of E_c, E_p, and the direct bias voltage E_0; thus the total impressed electromotive force is given by

$$e = E_0 + E_p \sin pt + E_c \sin ct. \tag{10}$$

Substituting this value of e into (1) gives the following expression for the current

$$i = a_0 + \sum_{n=1}^{\nu} a_n \cos (u_n + v_n \sin pt + w_n \sin ct) \tag{11}$$

where,

$$u_n = \frac{n\pi}{e_0} E_0 + \theta_n, \qquad v_n = \frac{n\pi}{e_0} E_p, \qquad w_n = \frac{n\pi}{e_0} E_c.$$

The remaining calculation is quite like that done in obtaining the amplification products. Equation (11) may be written in the equivalent form

$$i = a_0 + \sum_{m=1}^{\nu} a_n \{\cos u_n [\cos (v_n \sin pt) \cdot \cos (w_n \sin ct) - \sin (v_n \sin pt) \cdot \cos (w_n \sin ct)] - \sin u_n [\sin (v_n \sin pt) \cdot \cos (w_n \sin ct) + \cos (v_n \sin pt) \cdot \sin (w_n \sin ct)]\}$$

which may, with the aid of (5) and a rearrangement of terms, be transformed into

$$\begin{aligned} i = a_0 + \sum_{n=1}^{\nu} a_n \Bigg\{ & \cos u_n \Bigg[J_0(v_n) + 2 \sum_{l=1}^{\infty} J_{2l}(v_n) \cos 2lpt \Bigg] \\ & \cdot \Bigg[J_0(w_n) + 2 \sum_{k=1}^{\infty} J_{2k}(w_n) \cos 2kct \Bigg] \\ & - \cos u_n \Bigg[2 \sum_{l=1}^{\infty} J_{2l-1}(v_n) \sin (2l-1)pt \Bigg] \\ & \Bigg[2 \sum_{k=1}^{\infty} J_{2k-1}(v_n) \sin (2k-1)ct \Bigg] \\ & - \sin u_n \Bigg[2 \sum_{l=1}^{\infty} J_{2l-1}(v_n) \sin (2l-1)pt \Bigg] \\ & \Bigg[J_0(w_n) + 2 \sum_{k=1}^{\infty} J_{2k}(w_n) \cos 2kct \Bigg] \\ & - \sin u_n \Bigg[J_0(v_n) + 2 \sum_{l=1}^{\infty} J_{2l}(v_n) \cos 2lpt \Bigg] \\ & \Bigg[2 \sum_{k=1}^{\infty} J_{2k-1}(w_n) \sin (2k-1)ct \Bigg] \Bigg\}. \end{aligned} \tag{12}$$

The amplitudes of all component currents may be obtained directly from (12) by performing the indicated multiplications and then selecting the terms having the desired frequency. As previously stated, only the fundamental carrier and its upper and lower side bands of different orders will be explicitly evaluated. An inspection of (12) shows that the carrier is given by the last term alone for $k = 1$ and is

$$i_{\text{carrier}} = \left\{ -2 \sum_{n=1}^{\nu} a_n \cdot J_0(v_n) \cdot J_1(w_n) \cdot \sin u_n \right\} \sin ct.$$

Similarly, the side bands may be found to be given by the expression

$$i_{\text{side bands}} = \sum_{l=1}^{\infty}\left\{2\sum_{n=1}^{\nu} a_n J_{2l-1}(v_n)J_1(w_n)\cos u_n\right\}\begin{Bmatrix}-\cos[(2l-1)p-c]t\\+\cos[(2l-1)p+c]t\end{Bmatrix}$$

$$+\sum_{l=1}^{\infty}\left\{2\sum_{n=1}^{\nu} a_n J_{2l}(v_n)J_1(w_n)\sin u_n\right\}\begin{Bmatrix}-\sin[2lp+c]t\\+\sin[2lp-c]t\end{Bmatrix}.$$

Examining the expression above for the carrier and side bands shows readily that if m represents the order of the side band, i.e., $m=0$ gives the carrier, $m=1$ gives the first side band, $m=2$ gives the second side band, etc., one expression will suffice to give the magnitude of any component of current present. This expression may be found to be

$$|i_m| = \left|2\sum_{n=1}^{\nu} a_n \cdot J_m(v_n)\cdot J_1(w_n)\cdot\sin\left(u_n+\frac{m\pi}{2}\right)\right|. \qquad (13)$$

Expression (13) corresponds to (9) already obtained for the fundamental and distortion products in amplification, and is very similarly constituted. From (13) the amplitude of carrier, first side band and all distortion side bands may be computed with practically the same ease as could the amplification products. In both cases there are ν additive terms, the only difference being that for the modulation products there are four factors to each term instead of three, which represents an almost trivial increase in labor.

Calculation of Demodulation Products

A knowledge of the production of audio frequencies other than the modulation frequency $p/2\pi$ in the demodulation of an amplitude modulated voltage is of fundamental importance in a large number of practical problems. If the modulated voltage be taken in the customary form, the total voltage to be impressed on the nonlinear current voltage characteristic represented by (1) is given by

$$e = E_0 + E(1 + f\cos pt)\sin ct \qquad (14)$$

where E_0 is the direct-current bias, E the amplitude of the carrier in unmodulated state, and $0 \leqq f \leqq 1$ the per cent modulation. The expression for the current may be written as

$$i = a_0 + \sum_{n=1}^{\nu} a_n \cos[u_n + v_n \sin ct + w_n \sin(c+p)t + w_n \sin(c-p)t] \qquad (15)$$

where,

$$u_n = \frac{n\pi}{e_0} E_0 + \theta_n, \qquad v_n = \frac{n\pi}{e_0} E, \qquad w_n = \frac{n\pi}{e_0} \frac{f}{2} E = \frac{f}{2} v_n.$$

The manipulations leading to the amplitudes of the several components of current follow the same lines as those already used in the cases of amplification and modulation, but are considerably longer and more involved. As nothing new is added thereby, this calculation will be omitted; anyone interested may carry through the calculation by following the same line of argument, expansions, etc., as previously employed. Accordingly, the expressions for the amplitude of fundamental and first two harmonic currents will be given without proof. If $m=1$ denotes the fundamental frequency p, $m=2$ the second harmonic frequency $2p$, etc., the amplitude of the mth harmonic current is given by

$$| i_m | = \left| 4 \sum_{r=1}^{\infty} \sum_{n=1}^{\nu} a_n \cdot G_n \cdot \cos u_n \right| \tag{16}$$

where,

$$\begin{aligned}
G_1 &= J_1(v_n)J_0(w_n)J_1(w_n) + J_{4r-1}(v_n)J_{2r-1}(w_n)J_{2r}(w_n) \\
&\quad + J_{4r+1}(v_n)J_{2r+1}(w_n)J_{2r}(W_n) \\
G_2 &= J_2(v_n)J_0(w_n)J_2(w_n) + J_{4r+2}(v_n)J_{2r+2}(w_n)J_{2r}(w_n) \\
&\quad - J_{4r}(v_n)J_{2r+1}(w_n)J_{2r-1}(w_n) - \tfrac{1}{2}J_0(v_n)J_1^2(w_n) \\
G_3 &= J_3(v_n)J_0(w_n)J_3(w_n) + J_1(v_n)J_1(w_n)J_2(w_n) \\
&\quad + J_{4r+1}(v_n)J_{2r-1}(w_n)J_{2r+2}(w_n) \\
&\quad + J_{4r+3}(v_n)J_{2r+3}(w_n)J_{2r}(w_n).
\end{aligned}$$

It is obvious that the computation of demodulation products is many times longer than that for amplification or for modulation, which is in accord with the greater physical complexity of the process (an impressed electromotive force of bias and three sinusoidal voltages having interrelated frequencies and amplitudes, etc.). While longer,* the computation still involves only multiplication and addition of numbers to be located in available tables.

* That this method nevertheless possesses an advantage over the power series solution may be seen by comparing (16) with the expressions used by Woods (reference 6). When the difficulty attached to the evaluation of the power series coefficients is remembered, this advantage becomes even more apparent.

Illustration of the Method. Calculation of Distortion in Amplification*

In order to give an idea of the actual use of the trigonometric polynomial method of calculating the performance of nonlinear resistance circuits some results obtained for the case of a single sinusoidal electromotive force impressed on a Western Electric type 101-D vacuum tube for the three values of external load resistance R_L of 1000, 6000, and 10,000 ohms, respectively, will be presented. For com-

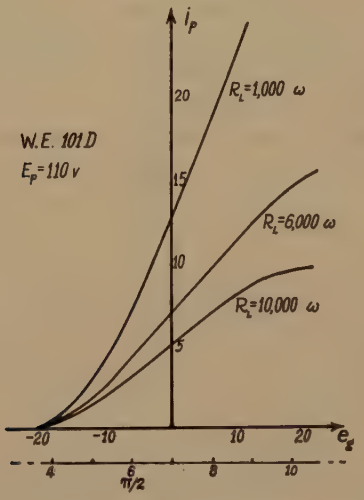

Fig. 4—Grid voltage—plate current (milliamperes) curves of Western Electric 101D for three different values of external plate resistance R_L. Lower abscissa scale refers to the 24-point schedule analysis. With a range of validity of $-60 < e_g < +12$ volts, the following representations were found:

$R_L = 1{,}000$ ohms: $i = 11.4 - 15.9 \cos \omega x + 3.88 \cos 2\omega x + 1.41 \cos 3\omega x - 0.91 \cos 4\omega x + 0.26 \cos 5\omega x - 0.28 \cos 6\omega x$

$R_L = 6{,}000$ ohms: $i = 6.05 - 8.31 \cos \omega x + 2.02 \cos 2\omega x + 0.45 \cos 3\omega x - 0.14 \cos 4\omega x - 0.14 \cos 6\omega x$

$R_L = 10{,}000$ ohms: $i = 4.09 - 5.37 \cos \omega x + 0.94 \cos 2\omega x + 0.58 \cos 3\omega x - 0.18 \cos 4\omega x$

where,

$$\omega = \frac{2\pi}{24}, x = \frac{e_g - k}{6 \cdot \frac{2\pi}{24}}$$

e_g being the total applied voltage (alternating voltage + bias), k = a constant (equal to *cf*, Fig. 2) displacing the zero axis, used in calculating the coefficients, to the true axis of zero grid voltage, and $6 \cdot (2\pi/24)$ = number of grid volts per radian.

* The author is greatly indebted to Mr. R. S. Morse for the use of the material presented in this section, which forms part of his bachelor's thesis at M.I.T., June, 1933, entitled, "A Mathematical Study of Distortion in Non-linear Circuits."

parison purposes the corresponding e_g, i_p curves are reproduced in Fig. 4. It may be easily seen that if a straight line approximation to the

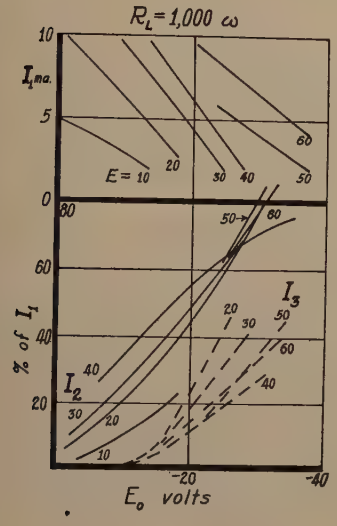

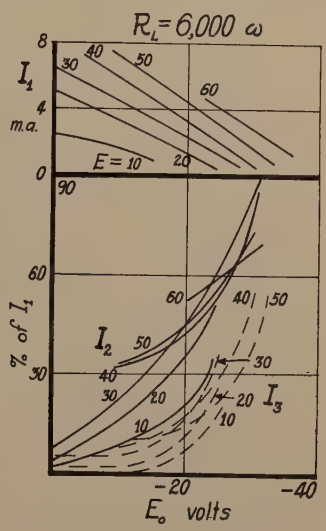

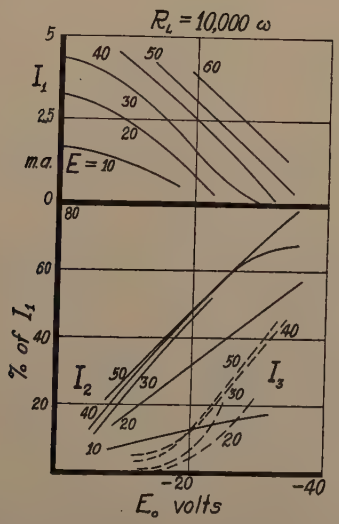

Figs. 5, 6, 7. Curves of fundamental current I_1 (milliamperes) and 2nd and 3rd harmonics I_2 and I_3 (as per cent of fundamental) vs. grid bias E_0 for various values of applied peak alternating voltage $\frac{1}{2}E$ (E = total grid swing) and external resistance R_L. Computation from characteristics shown in Fig. 4.

actual curve were to be used, as is sometimes done in discussing linear rectifiers, etc., it would leave much to be desired. However, by artificially extending the curves according to the general principles laid down in the first part of this paper very good approximations were obtained (the deviations of the approximation curves from the originals were barely noticeable when plotted to the scale used in Fig. 4) with only four terms for $R_L = 10{,}000$ ohms and only six terms for $R_L = 6000$ and 1000 ohms, respectively. Values of grid bias equal to one of the selected values used in the harmonic analysis were used in computing, as the work is then somewhat shortened.

Families of curves showing the magnitude of fundamental and per cent second and third harmonic (compared to the fundamental) currents were computed and are reproduced in Figs. 5 to 10. In Figs. 5, 6, and 7, the grid bias has been used as the independent variable, while in Figs. 8, 9 and 10 the load resistance was used. Consequently, there is a fundamental difference in the physical problem represented in these two cases, namely, the first set of three curves represents the changes in currents *in a given circuit* for different applied voltages, while the second set represents the currents produced *in different circuits* by given voltages (because the shape and magnitude of the current-voltage curve changes with R_L).

An examination of the curves of distortion vs. grid bias shows the following general features:

(a) The fundamental amplitude increases almost linearly with increasing negative bias.

(b) The per cent second harmonic is always larger than the per cent third harmonic, but both vary in about the same way with the bias.

(c) Distortion increases rapidly with decreasing bias. From a distortion point of view, there is nothing to distinguish so-called "class B" from "class C" operation.

A similar examination of the curves of distortion vs. load resistance brings out the additional features:

(d) The fundamental current slowly becomes smaller with decreasing external resistance.

(e) The per cent second harmonic is always larger than the per cent third harmonic, but both vary with the external resistance in about the same way.

(f) Almost no change in distortion occurs with changing external resistance when the bias is small. For large values of negative

bias the per cent distortion may decrease, increase, or go through a maximum with increasing external resistance, which indicates that the somewhat prevalent idea, that a reduction of har-

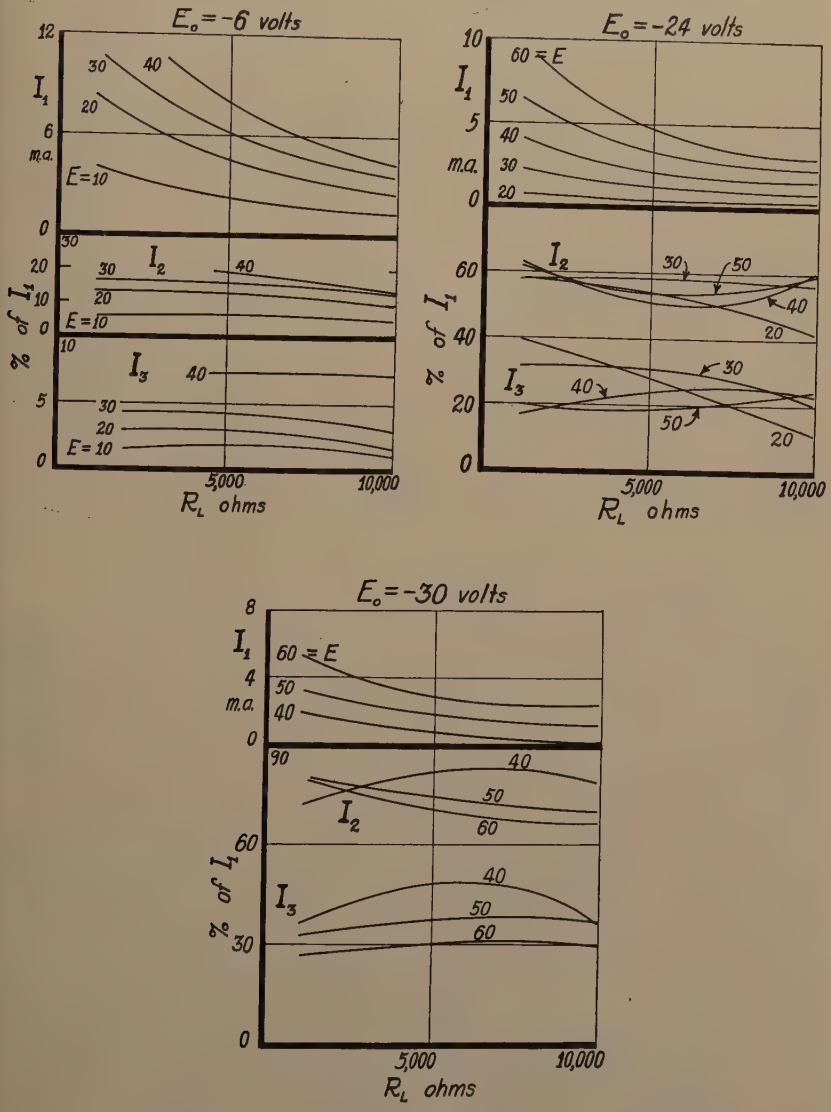

Figs. 8, 9, 10. Curves of fundamental current I_1 (milliamperes), second harmonic I_2 and third harmonic I_3 (as per cent of fundamental) vs. external resistance R_L for various grid bias values E_0 and various values of applied alternating peak voltage $\frac{1}{2}E$ (E = total grid swing).

monics is a necessary consequence of increasing the external resistance, does not possess unqualified validity.

Quite complete curves of distortion vs. alternating-current magnitude for different external loads and different bias values were also computed, but are too voluminous to present here. It is felt that the practical usefulness and advantage of the trigonometric polynomial method for large impressed voltages has been well demonstrated. The fact that thorough studies of the performance of an actual nonlinear resistance device may be made with relative rapidity, and without the use of idealizing approximations should make this method worth while in many instances.

One point, perhaps worthy of mention, is the possibility of using one expression to represent the whole family of characteristic e_g- i_p curves obtained for different values of plate voltage. Changing the plate voltage shifts the e_g- i_p curve to the right or left without material change in shape (this is only approximately so), so that this effect may be given analytical expression in the formulas developed here by adding a constant voltage to E_0 of proper magnitude to shift the zero by the required amount, and thus also the curve. Only u_n in the final results is altered thereby.

Approximation for Parallel Resonant Circuit Load

When the external impedance in series with the nonlinear element, which may again be considered to be a vacuum tube, is a parallel resonant circuit, an exact analysis is beyond the reach of the present analysis. An approximation can nevertheless be obtained for certain practically important cases.

The parallel resonant circuit may be thought replaced by an impedance having a definite value other than zero for a given frequency f and zero for all other frequencies; also, the impedance is to be considered to be a pure resistance R_f at the frequency f. An approximation to the performance of this idealized circuit may be obtained by using the nonlinear characteristic previously found for the combination of vacuum tube and external resistance, taking the magnitude of the external resistance equal to that of the tuned circuit at the frequency f. When f coincides with the frequency of one of the components of current i_f calculated as before, the total effective electromotive forces across the tuned circuit may be taken as $e_f = R_f \cdot i_f$. Naturally, actual computation need only be carried out for the single component i_f, a very simple task indeed. This formulation of the problem includes in

its range of application considerations of class B and C amplifiers, modulated amplifiers, and other important devices.

Modulated Amplifier

The case of a modulated amplifier operated class B or C may be studied from the calculations based on a single sinusoidal voltage plus a bias of form given by (2) without recourse to the more involved expressions dealing with an electromotive force of form (10). The frequency f of the tuned circuit is taken to coincide with the fundamental alternating-current component of current (the carrier), so that the 2nd, 3rd, . . . harmonics of the carrier are eliminated. A bias considerably past cut-off is usual, but other ranges may be included with ease. The steady valued alternating current thus produced is modulated by imposing a sinusoidal variation (the signal) on the bias voltage E_0. Therefore, if the magnitude of the fundamental current is calculated by the method given in this paper and plotted against E_0, the performance of the modulator may be easily estimated. In particular, if this curve is a straight line there will be no distortion produced during the modulation process. Deviation from a straight line will produce distortional components of double, triple, etc., voice frequency and these components can be evaluated by resolution of the graphically determined wave envelope into its harmonics constituents. A study of the curves of Figs. 5, 6, and 7 will serve to illustrate this point. The fact that I_1 vs. E_0 is invariably a straight line when the bias is past cut-off and only becomes curved, indicating distortion, when operated "class A" is in agreement with the known behavior of modulated amplifiers.

Conclusion

The trigonometric polynomial method of calculating the performance of nonlinear resistance circuits under impressed voltages of the forms usually of interest in communication is believed to possess definite advantages over power series, graphical and other methods. Of particular merit are its ability to give results with a minimum expenditure of time and labor, an accuracy well within that required by the nature of the problem, and its applicability to arbitrarily shaped current-voltage characteristics.

Due to its limitation to a resistance circuit, there is need for a suitable extension to include a nonlinear resistance with inductive, capacitive, or other more general external impedance. If this can be accomplished, the method might presumably be developed as a standard one for large amplitude nonlinear vacuum tube circuit

theory and the conventional r_p, g_m, etc., abandoned in favor of the more easily managed trigonometric coefficients in cases of class B and C amplifiers, oscillators, modulators, detectors, etc. A general method for this large class of problems is a real need in present-day circuit theory.

Bibliography

(1) J. R. Carson, Proc. I.R.E., vol. 7, p. 187; April, (1919).
(2) E. Peterson and C. R. Keith, *Bell Sys. Tech. Jour.*, vol. 17, p. 106, (1928).
(3) W. R. Bennett, *Bell Sys. Tech. Jour.*, vol. 12, p. 228, (1933).
(4) Terebesi, "Rechenschablonen fuer harmonische Analyse und Synthese," Springer, Berlin, (1930); J. Lipka, "Graphical and Mechanical Computation"; Whittaker and Robinson, "The Calculus of Observations."
(5) Jahncke-Emde, "Funktionen Tafeln mit Kurven"; Gray and Mathews, "Treatise on Bessel Functions."
(6) J. P. Woods, *Physics*, vol. 2, no. 4, p. 225; April (1932).
(7) M. J. O. Strutt, *Hochfrequenztechnik und Elektroakustik*, vol. 42, no. 6, pp. 206–208; December, (1933).

Proceedings of the Institute of Radio Engineers
Volume 22, Number 8 *August, 1934*

ON CONVERSION DETECTORS*

By

M. J. O. Strutt

(Natuurkundig Laboratorium der N. V. Philips' Gloeilampenfabrieken, Eindhoven, Holland)

Summary—*Conversion detectors for superheterodyne sets are classified in two groups, containing two types each. These types are illustrated in Figs. 1(a), 1(b), 2(a), 2(b), 2(c), 2(d), and 2(e). It has been found possible to represent measured static characteristics (current versus applied voltage) of all types of detectors considered accurately by an equation of the type*

$$i = \sum A_n e^{anV}$$

By using this expression for the static characteristics, conversion gain, distortion effects (modulation rise, modulation distortion, cross-modulation), and harmonics (causing whistling notes) could be calculated for all types of conversion detectors. An apparatus is described, permitting of easy measurements of conversion gain and harmonics. Measured and calculated data check as well as could be expected. Conversion gains of more than 400 were found with modern valve conversion detectors. It is pointed out that distortion may be determined by measuring the harmonics.

Introduction

MANY possibilities have been proposed hitherto for the use as a first detector (modulator) in superheterodyne sets. The object of this paper is to treat the more common systems theoretically and experimentally with a view of comparing their relative merits. Before starting this, it might be worth while to give a brief description of these systems.

Two main groups of first detectors are considered, indicated by I and II. With the detectors of group I, input signal voltage E_i and local oscillator voltage E_h are put on one single electrode. With group II they are put on different and separate electrodes. As examples of group I we have:

I(a) Diode Detectors.

The simplest form hereof is contained in Fig. 1(a). The two voltages E_h and E_i, issuing from a common tapped coil of small impedance are acting on the diode D in series with an impedance z. Let ω_h be the angular frequency ($2\pi \times$cycles per second) of the voltage E_h and ω_i of the voltage E_i, then the impedance z is designed to have an appreciable value only for alternating current of the angular frequency $\omega_0 = |\omega_h - \omega_i|$. For ω_0 we have $z = R$, at all other frequencies including

* Decimal classification: R134. Original manuscript received by the Institute, January 18, 1934.

direct current $z=0$. Another form of diode detection is shown in Fig. 1(b), where the grid-cathode circuit forms the diode, grid bias being such as to cause grid current flow and the voltage is amplified by the triode. The impedance is now in the anode circuit.

I(b) Variable Slope Detectors.

Here also, the circuit of Fig. 1(b) illustrates the principle, grid bias being this time such that no grid currents flow. Tetrodes and pentodes may replace the triode of Fig. 1(b). Detection is caused by the variable slope of the (direct current) anode-current—grid-tension characteristic. Internal resistance is high.

Numerous representatives of group II have appeared recently; some of the more common ones are here dealt with.

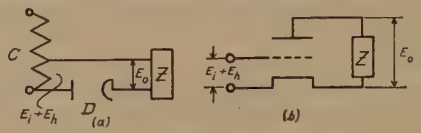

Fig. 1

(a) *Diode detector.* Two voltages in series (peak values E_i and E_h) coming off a tapped coil transformer C act on the diode D and on the impedance Z, which is in series with the diode. This impedance Z has a zero value for the frequencies of E_i and of E_h but it has a very large value (e.g., one megohm) for a frequency which is the difference of these frequencies, this difference being the frequency of E_0.
(b) *Triode detector.* Symbols similar to Fig. 1(a).

II(a) Double Grid Detectors.

The principle is shown in Fig. 2(a). Grid bias is such that no grid currents flow in the input circuit. More recent forms of this principle are shown in Figs. 2(b), 2(c), 2(d), and 2(e). These embody the essential parts of the valves 2A7 (RCA); E448 (Philips Co., Ltd.), the octode (of Philips), and the "emission valve" of the Hazeltine Corporation, respectively.[1] The underlying idea of these constructions resides in controlling the slope (anode-current—signal-grid voltage) by a second grid, upon which the local oscillator voltage E_h is put. By shielding the two grids electrostatically the voltage E_h can be prevented from getting on the antenna and radiating thence. Electron coupling of the grids is, however, not prevented by the shield. Moreover the valves of the groups I(b) and II(a) permit dispensing with an extra oscillator valve, as they can generate the voltage E_h by themselves.

II(b) Grid-Anode Detectors.

This type is different from II(a) in as much as the anode is used instead of a second grid (see Fig. 2(e)). By suitably choosing the anode tension, detection in the anode bends is made possible.

It is emphasized here, that *detector* properties only of the valves, just given as examples, will be contemplated in this article. Generation of local voltage is an essential claim of some of them. These oscillator properties should therefore be considered also, before forming a complete view on their relative merits as detector-oscillator valves. However, as will be shown, detector properties alone already involve such complex considerations, that one is justified in putting aside at first the oscillator properties.

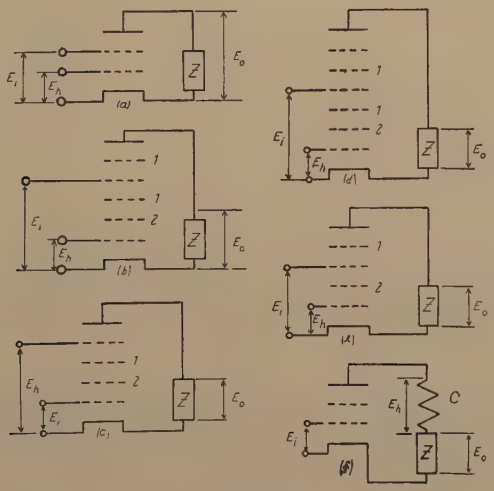

Fig. 2

(a) *Double-grid detector.* (Principle.) Symbols similar to Fig. 1(a).
(b) *Oscillator-modulator valve RCA 2A7.* Grids Nr. 1 are screens, grid 2 is the anode for the oscillator, grid nearest to cathode is the oscillator grid, acting at the same time as the one grid of the modulator. Other symbols as in Fig. 1(a).
(c) *Oscillator-modulator valve Philips E 448.* Grids Nrs. 1 and 2 are oscillator anode and screen, respectively. Other symbols as in Fig. 1(a).
(d) *Philips Octode.* This valve is similar to Fig. 2(b), with the addition of a suppressor grid, in order to obtain an increased interior resistance. Symbols as above.
(e) *Emission valve.* (Hazeltine Corporation.) Grids 1 and 2 are screen and oscillator anode, respectively. Other symbols as in Fig. 1(a).
(f) *Gride-anode conversion detector.* Local oscillator voltage is induced in coil *C*. Other symbols as in Fig. 1 (a).

Mathematical Formulation of Valve Characteristics.

As is well known, some mathematical relation between anode current and grid voltage must be assumed in order to calculate the performance of valves. After several trials, a special formulation of this relation was found, permitting of sufficiently close approximation of actual valve characteristics on one side and of relatively easy calcula-

[1] H. A. Wheeler, *Electronics*, p. 76, March, (1933).

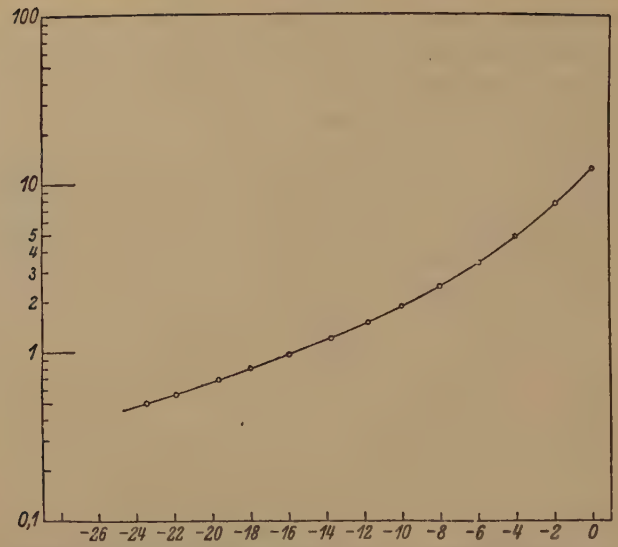

Fig. 3—Horizontal axis: grid tension V (Volts); vertical axis: anode current i (milliamperes). Valve RCA 58. Curve calculated from $i = 3.3\ e^{0.080V} + 8.7\ e^{0.318V}$. Points measured.

tion on the other. Dealing, first, with valves of group I, the current i (diode current with type I(a) or anode current with type I(b)) is related to the input voltage V (both direct current) by

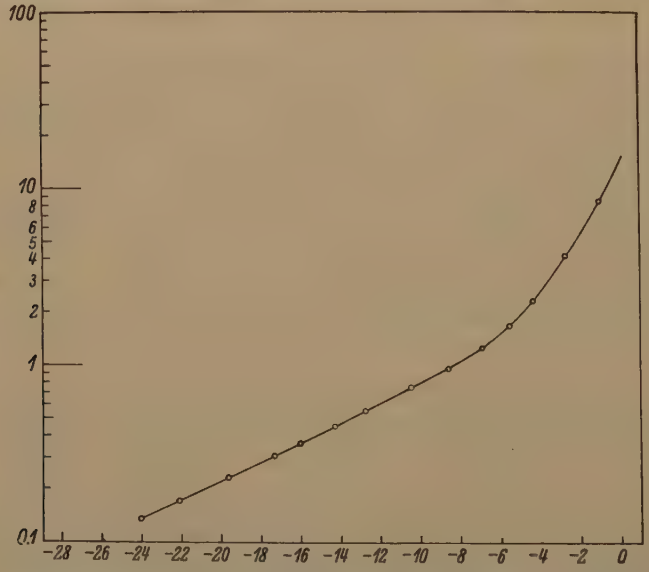

Fig. 4—Coördinates as in Fig. 3. Curve calculated from $i = 2.60\ e^{0.122V} + 11.6\ e^{0.613V}$. Points measured. Valve Philips E447.

$$i = \sum A_n e^{a_n V}. \qquad (1)$$

Here, practically, a finite sum, consisting, e.g., of two or three terms, is meant, n being 1, 2, 3 and so on. Theoretically, it may be shown, that *any* curve *in any interval* of V may be approximated by a series (1) as closely as is desired, if the number of terms is taken sufficiently great. In order to show the *practical* value of the approximation (1), some examples are given in Figs. 3, 4, 5, 6, and 7. Not more than three

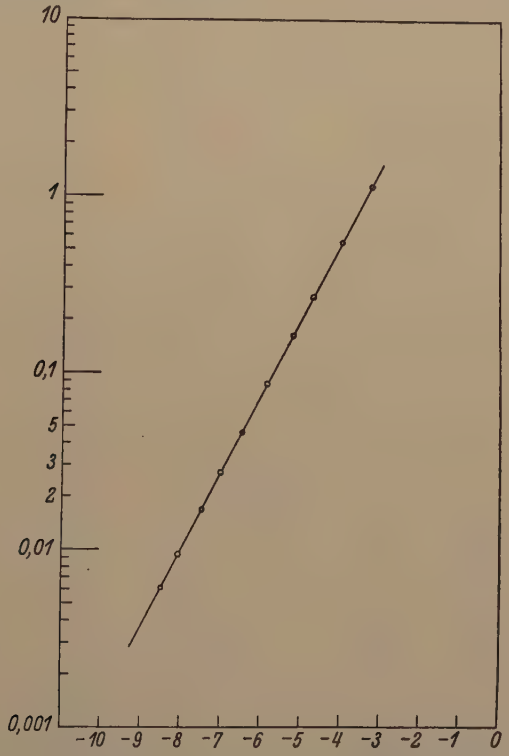

Fig. 5—Coördinates as in Fig. 3. Curve calculated from $i = 28.7\ e^{0.995V}$. Points measured. Valve Philips E452T.

terms are considered in any of these examples, already giving a close approximation to the experimental curve.

Coming to valves of the group II, two separate input voltages are to be considered, named V_a and V_b respectively. The dependence of the anode (direct) current on these voltages is expressed by

$$i = \sum C_n e^{a_n V_a + b_n V_b}. \qquad (2)$$

Here again, any experimental function of V_a and V_b in any interval of these voltages may be approximated as closely as desired by a series,

like (2), if a sufficiently great number of terms is taken. Practically, some two or three will suffice, as is shown by the example, given in Fig. 8.

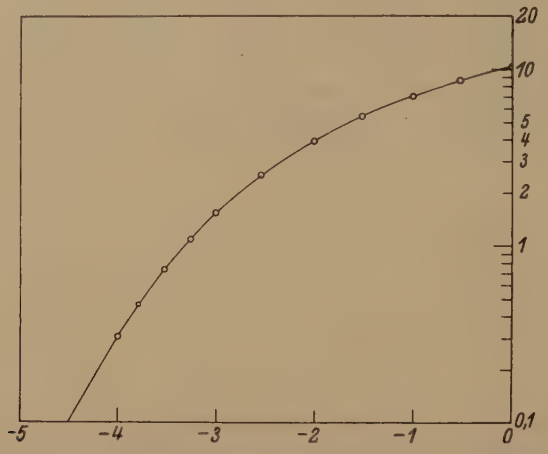

Fig. 6—Coördinates as in Fig. 3. Curve calculated from $i = 11.5\ e^{0.28V} - 1.2\ e^{0.377V} + 0.18\ e^{-4.10(V+3.5)}$. Points measured. Valve Philips E446.

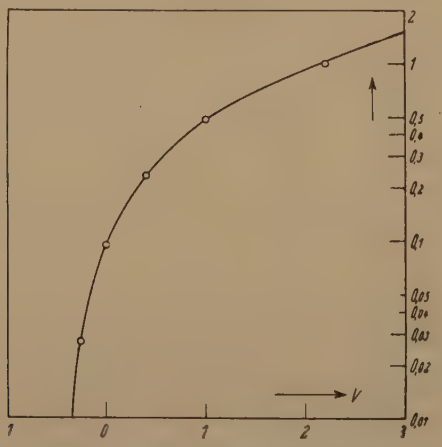

Fig. 7—Coördinates as in Fig. 3. In this case anode was diode part of valve Philips E444. Curve calculated from $i = 0.365\ e^{0.546V} - 0.271\ e^{0.551V}$. Points measured.

Thus we have found two functional expressions, (1) and (2), permitting to approximate experimental curves very closely. The advantage of these expressions will be shown to be twofold. In the first place, they enable one, to calculate accurately the complete detector performance, if the direct-current characteristic of a detector is known.

Second, they permit of general deductions, independent of any particular detector characteristics. Examples hereof are given below.

Calculated Conversion Gain of Type I(a) *Detectors.*

Considering the scheme of Fig. 1(a), a voltage of frequency

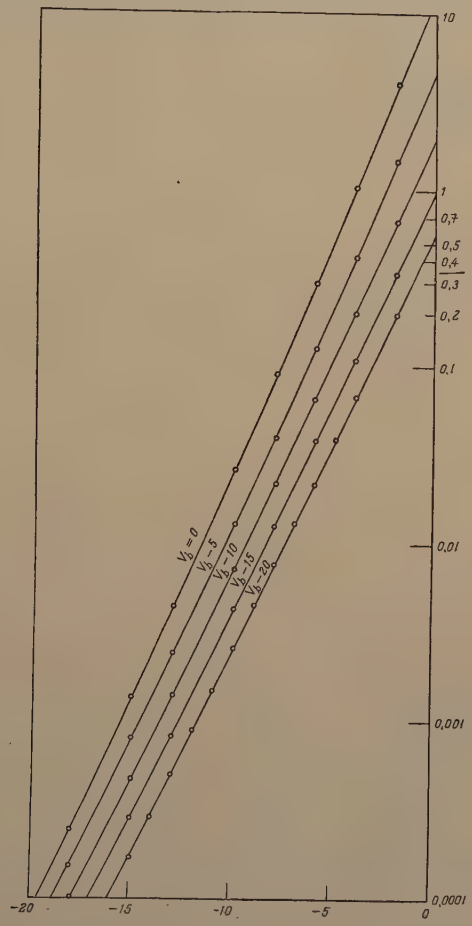

Fig. 8—Coördinates as in Fig. 3. This is a double-grid modulator, the anode current depending on the tensions of two grids. The tension of one grid is taken as horizontal axis, while the tension of the other grid is taken as parameter. Curves calculated from: $i=9.8\ e^{0.72V_a+0.3V_b}+4.1\ e^{0.54V_a+0.1V_b}$. Points measured. Experimental valve of this laboratory.

$\omega_0=|\omega_i-\omega_h|$ will be developed across the impedance $z=R$. Hence, the total voltage, acting on the diode, assuming an additional direct bias tension V_0, is

$$V = V_0 + E_i \sin \omega_i t + E_h \sin \omega_h t - E_0 \cos \omega_0 t. \tag{3}$$

This voltage (3) has to be substituted in (1), in order to get the current i through the detector. This total current i consists of a direct-current part and alternating-current parts of angular frequencies ω_i, $2\omega_i$, $3\omega_i \cdots$; ω_h, $2\omega_h$, $3\omega_h \cdots$ and sums and differences of these quantities. Of this total current i only one component is of interest here; i.e., $i_0 \cos \omega_0 t$, as this component gives rise to the voltage $E_0 \cos \omega_0 t = Ri_0 \cos \omega_0 t$ across the impedance R. *The conversion gain of the detector with very small input voltages is defined as*

$$g_1 = \frac{E_0}{E_i}. \tag{4}$$

Assuming, that the input signal voltage E_i is small, such that the relations $a_n E_i \ll 1$ are satisfied (see (1)), this conversion gain may easily be calculated and is found to be (see appendix A)

$$g_1 = \frac{\sum \frac{1}{j} A_n I_1(j a_n E_h) a_n e^{a_n V_0}}{\frac{1}{R} + \sum A_n I_0(j a_n E_h) a_n e^{a_n V_0}}. \tag{5}$$

Here I_0 is Bessel's function of the first kind, of order zero and with the argument $j a_n E_h$, where $j = +\sqrt{-1}$. Similarly I_1, is Bessel's function of order one. Tables of I_0 and I_1 are available. Hence, if the direct-current detector characteristic is known and has been approximated by (1), the gain is also known by (5), with given value R of the impedance z at the angular frequency ω_0.

Some important general conclusions may be drawn from (5). We assume $1/R$ to be small, compared with the sum in the denominator. This means, that the value R of the impedance z at the angular frequency ω_0 is large, compared with the "internal resistance" of the detector. The latter term is somewhat vague, of course, if the detector characteristic is not a straight line. Furthermore, the local oscillator voltage E_h is assumed to be large, such that $a_n E_h \gg 1$. Then we have

$$\frac{1}{j} I_1(j a_n E_h) = I_0(j a_n E_h)$$

and hence by (5)

$$g = 1. \tag{5a}$$

Thus, in this case of maximum output voltage E_0, the conversion gain is unity. As it often appears that all terms in the numerator and in the denominator of (5) are positive in actual calculations (see Figs. 3, 4, and 5), the conversion gain decreases, if E_h decreases and also if R decreases. The special value (5a) of (5) may also be deduced in a more

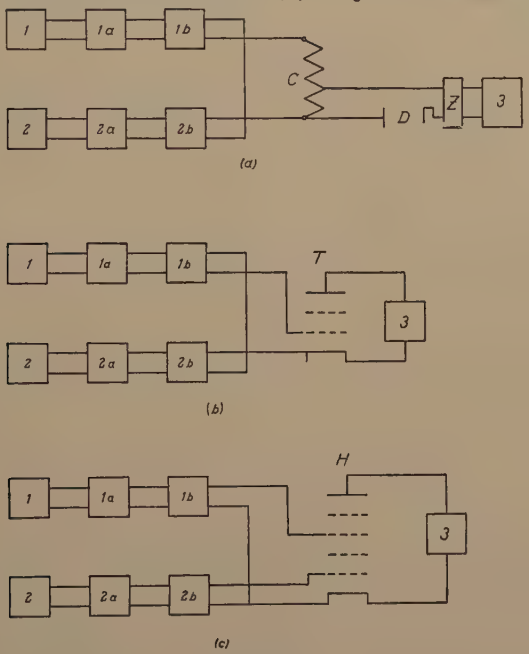

Fig. 9

(a) Measuring arrangement for determining the conversion conductance and the conversion gain of conversion detectors, as used for type 1*a* detectors. The meaning of the number and letter symbols is as follows: 1 = generator of frequency ω_i; 2 = generator of frequency ω_h; 1*a* = band-pass filter for the frequency ω_i; 2*a* = band-pass filter for the frequency ω_h; 1*b* = voltmeter for the frequency ω_i; 2*b* = voltmeter for the frequency ω_h; C = autotransformer coil; D = diode under investigation; Z = impedance having a very high value (e.g., one megohm for the frequency $\omega_i - \omega_h = \omega_0$) and a small value for all other frequencies including direct current; 3 = milliammeter tuned to the frequency ω_0 and having a very small impedance (e.g., vibration galvanometer). A suitable amplifier was used between Z and 3 in Fig. 9(a).

(b) Arrangement of Fig. 9(a) set up for the measurement of type 1(b) detectors. Meaning of symbols as in Fig. 9(a). T = valve under investigation.

(c) Arrangement of Fig. 9(a) set up for measuring type 2 detectors. H = valve under consideration. Symbols as in Fig. 9(a).

elementary way, e.g., using the heterodyne envelope of the two alternating voltages[2] E_i and E_h. In combinations with tetrodes and pentodes, conversion gains of 500 and more are possible. From (5) and (5a), one can easily see the influence of the bias voltage V_0 on the con-

[2] F. M. Colebrook, Wireless Eng., vol. 9, pp. 195–201, (1932).

version gain. With given local oscillator voltage E_h, the expressions $a_n E_h$ are greater, if the values of a_n are greater. If $a_n E_h$ decrease, g_s decreases also. Hence, if V_0 is adjusted, so as to move to parts of the direct-current detector characteristic, where a_n is smaller, the conversion gain is decreased, other things being equal, and inversely.

A different arrangement of conversion detector is obtained, if the impedance z, instead of being only appreciable for the angular frequency ω_0, is made a pure and very large resistance. This case was considered for a straight line and for a square-law static detector characteristic[3] and for such bias, as to result in half-wave detection. It was shown, that conversion gain amounts to about 0.3. Hence, this arrangement is inferior to the one considered above.

Measured Conversion Gain of Type I(a) Detectors

A measuring arrangement, with which detectors of any type can be investigated, was set up. Its essential parts are contained in Fig. 9(a). In Fig. 9(b) the arrangement is set up for use with type I(b) detectors. Obviously, the same arrangement may be used for measuring the gain of group II detectors, by disconnecting the outputs of the oscillators and connecting them separately to the two detector electrodes, as shown in Fig. 9(c). Several tests were applied to the measuring apparatus, before actually measuring conversion gains. It is noteworthy, that the resistance R of the impedance z (Fig. 9(a)) at the frequency ω_0 was of the order of 10^6 ohms. Furthermore $\omega_i/2\pi$ and $\omega_h/2\pi$ were both about 20 kilocycles, while $\omega_0/2\pi$ was of the order of 1000 cycles. In all tables, given below, E_i and E_h, as is clear from (3) are *amplitude* values, i.e., $\sqrt{2}$ times the *effective* voltages. We secured the following data for a special detector (diode part of valve Philips E444)

E_i (volts)	0.1	0.1
E_h (volts)	3	4
g_1 (meas.)	0.94	0.98
g_1 (calc.)	0.93	0.97

The coincidence between observed and calculated values (by the aid of (5)) is as good as could be expected.

Calculated and Measured Conversion Gain of Type I(b) Detectors.

With type I(b) detectors, it will be assumed throughout, that internal resistance of the valves (being tetrodes or pentodes) is large and hence conversion gain principally dependent on exterior (anode) impedance. It is more convenient, therefore, to consider primarily the conversion conductance S_c instead of the conversion gain g_1. This con-

[3] W. R. Bennett, Bell Laboratories reprint No. 724.

version conductance S_c is defined as follows: The anode current i has one component $i_0 \cos \omega_0 t$. And one can write,

$$i_0 = S_c E_i. \tag{6}$$

Taking,

$$V = V_0 + E_i \sin \omega_i t + E_h \sin \omega_h t \tag{7}$$

in (1), the conversion conductance S_c can easily be calculated and is found to be (see appendix B)

$$S_c = \frac{2}{E_i} \sum A_n e^{a_n V_0} \frac{1}{j} I_1(j a_n E_h) \cdot \frac{1}{j} I_1(j a_n E_i). \tag{8}$$

This equation holds good for any values of E_i and E_h. It simplifies, if E_i is small, such that $a_n E_i \ll 1$. We have then

$$S_c = \sum A_n e^{a_n V_0} a_n \frac{1}{j} I_1(j a_n E_h). \tag{8a}$$

If E_h is also small, such that $a_n E_h \ll 1$, one obtains

$$S_c = \frac{1}{2} E_h \sum A_n e^{a_n V_0} a_n^2. \tag{8b}$$

Hence, with small local oscillator voltage E_h, the conversion conductance is proportional to E_h. By (1), we see that the conversion conductance may in this case be expressed as

$$S_c = \frac{1}{2} E_h \left(\frac{d^2 i}{dV^2} \right)_{V=V_0}$$

i.e., by the second differential quotient of the direct current i with respect to the grid voltage V, as is well known. In some practical cases, the bias voltage V_0, in order to prevent grid current, is taken such, that, e.g., $V_0 + E_h = -1$ or -2 volts. Taking moreover E_i small ($a_n E_i \ll 1$) and E_h large ($a_n E_h \gg 1$), (8a) reduces to

$$S_c = \frac{1}{\sqrt{2\pi E_h}} \sum A_n \frac{a_n}{\sqrt{a_n}} e^{a_n (V_0 + E_h)}. \tag{8c}$$

If $V_0 + E_h$ is constant, S_c must decrease with increasing E_h. As S_c increases with increasing E_h, for small values of E_h, by (8b), the conversion conductance must have a maximum value.[4]

It is interesting, to compare the conversion conductance S_c with

[4] J. F. Herd, *Wireless Engineer*, vol. 7, pp. 493–499, (1930).

the common mutual conductance S of the same valve, if used as a high-frequency amplifier. The value of S, by inserting $V = V_0 + E_i \sin \omega_i t$ in (1), is found to be

$$S = \frac{\partial i}{\partial V}. \tag{9}$$

By (1), (9) yields

$$S = \sum A_n e^{a_n V_0} a_n. \tag{9a}$$

Comparing this with (8b) and bearing in mind, that with the latter equation $a_n E_h \ll 1$, one concludes, that S_c is always much smaller

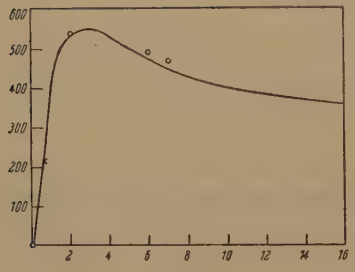

(a)

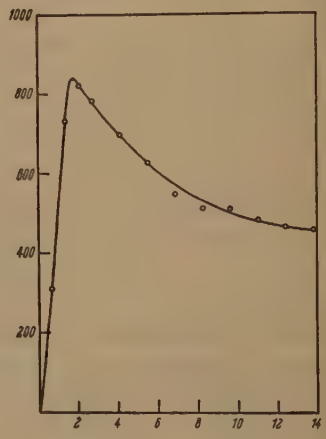

(b)

Fig. 10

(a) Vertical axis: conversion conductance expressed in microamperes/volts; horizontal axis: local oscillator tension volts peak value. Grid bias was such that grid current did not flow. Points measured. Curve calculated from static valve characteristic by (8a). Valve Philips E447.

(b) Coördinates as in Fig. 10(a). Valve Philips E446.

than S in this case. But, comparing (9a) with (8c) and remembering that $a_n E_h \gg 1$ in the latter equation, it is seen, that S may be of the same order as S_c. *It is possible, to make S_c more than one half times S theoretically.* This was checked by experiments (see below).

In measuring conversion gains, the apparatus of Fig. 9(b) was used. Some measured and calculated conversions are shown in Figs. 10(a), 10(b), and 10(c). It is noteworthy, that, e.g., in the case of Fig. 10(b) the actual effective interior resistance of the valve at the maximum conversion conductance was of the order of $2 \cdot 10^6$ ohms. Hence, with an exterior impedance z in the anode circuit, which amounts to a value

$z = R = 0.5 \cdot 10^6$ ohms at the angular frequency ω_0, conversion gain will be something like 400. It is emphasized, that this gain is not merely a theoretical value, but was actually measured in experiments, conducted by the author in this laboratory.

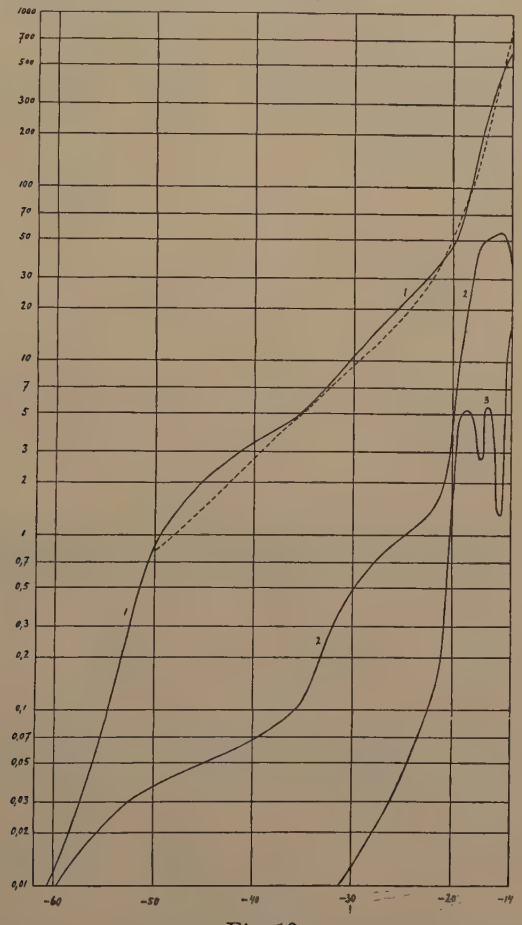

Fig. 10

(c) Full curve numbered 1: Vertical axis as in Fig. 10(a). Horizontal axis bias volts of grid for volume control, while local oscillator voltage was 13 volts peak value. Dotted curve calculated from (8a); full curve measured. Curve numbered 2 gives measured values of second harmonic; vertical axis for this curve is microamperes/volts squared. Curve numbered 3 gives measured values of third harmonic. Vertical axis for this curve is microamperes/cube of input volts. Valve E447.

Conversion Gain of Group II Detectors.

We shall start with a discussion of type II(b) detectors. An essential condition with these detectors is, that the anode current de-

pends markedly on the anode voltage, as is seen by (2). Hence, valves used as type II(b) detectors cannot have a very great interior resistance. This low interior resistance results in a poor conversion gain, though conversion conductance may be not so bad. This general conclusion has been borne out by experiments.[5] Obtained conversion gains with a screen-grid valve and, e.g., 10^5 ohms in the anode were about 0. 6. If compared with the gains, obtained with type I(a) and type I(b) detectors, this value appears so small, that no further time should be spent on type II(b) detectors.

Coming now to type II(a) detectors, interior resistance will be assumed large, as compared with exterior impedance in the anode circuit

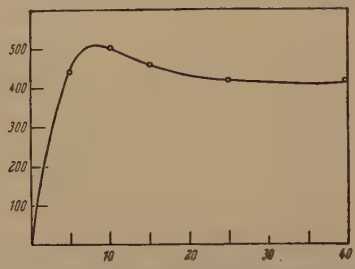

Fig. 11—Coördinates as in Fig. 10(a). Experimental type of Philips octode valve. Curve calculated by (11). Points are measured values. Publication data of these octodes now show $S_c = 600$.

at the angular frequency ω_0. Hence, conversion conductance is first considered, instead of conversion gain. Inserting

$$\begin{aligned} V_a &= V_{a0} + E_i \sin \omega_i t; \\ V_b &= V_{b0} + E_h \sin \omega_h t, \end{aligned} \tag{10}$$

in (2), one obtains (see appendix C)

$$S_c = \frac{2}{E_i} \sum C_n e^{a_n V_{a0} + b_n V_{b0}} \frac{1}{j} I_1(j a_n E_i) \cdot \frac{1}{j} I_1(j b_n E_h). \tag{11}$$

Here, S_c is quite similarly defined as with type I(b) detectors (see (6)). Considering the case, that E_i and E_h are both small ($a_n E_i \ll 1$; $b_n E_h \ll 1$), (11) yields

$$S_c = \frac{1}{2} E_h \sum C_n e^{a_n V_{a0} + b_n V_{b0}} a_n b_n. \tag{11a}$$

Here again, as was already found with type I(b) detectors, S_c is proportional to E_h in this case. If E_i is small, as taken above, but E_h is large, such that $b_n E_h \gg 1$, one obtains from (11)

[5] E. L. C. White, *Wireless Engineer*, vol. 9, pp. 618–621, (1932).

$$S_c = \frac{2}{\sqrt{2\pi E_h}} \sum C_n e^{a_n V_{a0} + b_n V_{b0} + b_n E_h} \frac{a_n}{\sqrt{b_n}}. \tag{11b}$$

Hence, if $V_{b0}+E_h$ is constant, S_c decreases with increasing E_h in this region. Just as was already shown with type I(b) detectors, conversion conductance has a maximum value as a function of E_h, by (11(a)) and (11(b)). Calculated and observed values of S_c are compared in Fig. 11. Conversion gains of more than 200 are obtained with commercial type II(a) detectors These gains do not compare too unfavorably with those of type I(b) detectors. They are, however, often lower than the gains of type I(b) detectors.

Modulation Rise, Distortion, and Cross-Modulation.

Though a very important item in the comparison of conversion detectors, gain is not the only important factor. The several distortion effects, connected with not straight tube characteristics, should be taken into consideration. They are the same ones, as occur with high-frequency amplifiers.[6] If E_i is no longer very small, we have

$$E_0 = g_1 E_i + g_3 E_i^3 + \cdots \tag{12}$$

(even powers of E_i do not occur; see appendix D). The following values are obtained for the distortion effects

$$\frac{M_1' - M}{M} = \frac{g_3}{g_1} e^2 (2 - \frac{3}{4} M^2). \tag{13}$$

Here $E_i = e(1+M \cos pt)$. Furthermore M_1' is the modulation depth of E_0 with the angular frequency p. Hence (13) expresses the modulation rise. Besides a modulation of angular frequency p, the output voltage E_0 has also a modulation M_2' with the angular frequency $2p$ (see appendix D).

$$\frac{M_2'}{M} = \frac{g_3}{g_1} \cdot \frac{3}{2} e^2 M. \tag{14}$$

This is obviously a measure for the distortion of modulation. Taking an input signal $e \sin \omega_i t + E_k(1+M_k \cos pt) \sin \omega_k t$, where the latter term is a crossing signal, the modulation depth M_0 of the output signal voltage E_0 with the modulation of the crossing signal is (see appendix D)

$$M_0 = 4E^2{}_k M_k \frac{g_3}{g_1}. \tag{15}$$

[6] R. O. Carter, *Wireless Engineer*, vol. 9, pp. 429–438, (1932).

This is cross modulation. Expressions (13), (14), and (15) only hold good for small input voltages E_i, such that $a_n E_i \ll 1$. Otherwise more terms of the development (12) have to be taken into account.[5] From (13), (14), and (15) it is clear that the modulation rise and the distortion are known, as soon as expressions for g_1 and g_3 are available. Now g_1 has already been given for group I and for group II detectors. Here expressions for g_3 are set forth.

With type I(a) detectors we obtain (see appendix E) if $V_0 = 0$.

$$g_3 \left\{ \frac{1}{R} + \sum A_n I_0(j a_n E_h) a_n \right\}^{-1} = \left(-\frac{1}{4} g_1 - \frac{1}{8} g_1^3\right) \sum A_n I_0(j a_n E_h) a_n^3$$

$$+ \left(\frac{1}{8} + \frac{1}{4} g_1^2\right) \sum A_n \frac{1}{j} I_1(j a_n E_h) a_n^3 + \frac{1}{8} g_1 \sum A_n I_2(j a_n E_h) a_n^3. \quad (16)$$

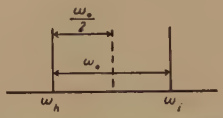

Fig. 12—Illustrating generation of detector whistles, especially as caused by the second detector harmonic.

With type I(b) detectors, $g_1 = RS_1$ and $g_3 = RS_3$, where $i_0 = S_1 E_i + S_3 E_i^3 + \cdots$. The following value was obtained for S_3 (see appendix E)

$$S_3 = \frac{1}{8} \sum A_n e^{a_n V_0} \frac{1}{j} I_1(j a_n E_h) a_n^3. \quad (17)$$

Finally, with type II(a) detectors, again $g_1 = RS_1$ and $g_3 = RS_3$, where $i_0 = S_1 E_i + S_3 E_i^3 + \cdots$. Here

$$S_3 = \frac{1}{8} \sum C_n e^{a_n V_{a_0} + b_n V_{b_0}} \frac{1}{j} I_1(j b_n E_h) a_n^3. \quad (18)$$

By the aid of (16), (17), and (18), modulation rise, distortion, and cross-modulation can easily be calculated for all types of detectors under consideration. These effects may be determined by measuring harmonics (see below).

Generation of Harmonics.

The harmonics generated by conversion detectors give rise to the well-known whistling tones in superheterodyne sets. It may be worth while to consider these whistling notes more closely, in order to get a view of some of their causes. Considering Fig. 12, the angular frequency

of the incoming signal is assumed to be ω_i, the fundamental angular frequency of the local oscillator ω_h. The band-pass filter behind the first detector only passes the angular frequency $\omega_0 = |\omega_i - \omega_h|$. But the modulator, if not perfect, will also produce angular frequencies $2\omega_0$, $3\omega_0$, etc., even if the local oscillator and incoming signal are ideal, i.e., purely sinusoidal. Hence, if an incoming signal ω_i' occurs (see Fig. 12), such that $|\omega_i' - \omega_h| = \frac{1}{2}\omega_0$, the second harmonic, generated by the detector, will be $2 \times \frac{1}{2}\omega_0 = \omega_0$, i.e., will be passed by the filter. This is then heard as a whistling note, while adjusting the local oscillator so as to receive the signal ω_i. Similarly, a signal ω_i'', such as $|\omega_i'' - \omega_h| = \frac{1}{3}\omega_0$ will produce a whistle by the third harmonic, generated by the detector, i.e., $3 \times \frac{1}{3}\omega_0 = \omega_0$, and so on. These whistles are present even with perfect local oscillators and incoming signals; they will be designated as *detector whistles*. A second group of whistling notes is found, if the detector is considered as perfect, i.e., generating not one single harmonic of ω_0, if ω_i and ω_h were purely sinusoidal. Consider a local oscillator, producing the angular frequencies $2\omega_h$, $3\omega_h$, $4\omega_h$, etc., besides the wanted ω_h. Then, if $|2\omega_h - \omega_i'| = \omega_0$, a whistle is heard, and similarly for the higher harmonics. These whistles may be diminished by choosing a low ω_0 frequency, such that the signal of angular frequency ω_i' is already much attenuated by the selective circuit before the first detector. If the incoming signals are not purely sinusoidal, their harmonics will result in whistles, while adjusting the local oscillator so as to receive a different signal. This effect is generally small. All the whistles, just considered, are called *input whistles*, as they are caused by the input not being purely sinusoidal. A third group of whistling notes is caused by the detector producing harmonics of the input frequencies. Thus, with a local oscillator ω_h, if a frequency $2\omega_h$ is formed *in the output circuit*, this can combine with a not wanted signal ω_i', such that $|\omega_i' - 2\omega_h| = \omega_0$ and causes a whistle. For the prevention of the *mixed whistles*, just considered, a choice of low ω_0 may be favorable, for then no appreciable signal ω_i' will be passed by the selective circuit before the first detector. If the impedance z, being equal to R at the frequency ω_0, is sufficiently selective and the other impedances in the input circuit sufficiently small, no considerable voltage of frequency $2\omega_h$ can be formed in the input circuit. Of course, a serious whistle may be produced by the so-called *mirror effect*, the local oscillator causing a passed ω_0 frequency *on both sides* of the oscillator ω_h. For the prevention of this mirror effect a high ω_0 is favorable.

In what follows, *detector whistles* will be considered quantitatively.

Considering, first, type I(a) detectors, the voltage $E_2 \cos 2\omega_0 t$, where $\omega_0 = |\omega_h - \omega_i|$ and $z = R$ for $2\omega_0$ is found to be (see appendix F)

$$E_2 = \frac{1}{2}\cdot\frac{1}{\underline{|2}}\cdot E_i^2 \frac{\sum A_n a_n^2 I_2(j a_n E_h)}{\frac{1}{R} + \sum A_n a_n I_0(j a_n E_h)} \Bigg\} e^{a_n V_0}. \tag{19}$$

Similarly,

$$E_3 = \frac{1}{2^2}\cdot\frac{1}{\underline{|3}}\cdot E_i^3 \frac{\sum A_n a_n^3 \frac{1}{j} I_3(j a_n E_h)}{\frac{1}{R} + \sum A_n a_n I_0(j a_n E_h)} \Bigg\} e^{a_n V_0}. \tag{20}$$

From these equations, some important conclusions on the whistling tones may be drawn. It is seen that the second whistle (19) is proportional to the second power of whistling signal input voltage, the third whistle (20) proportional to the third power, etc. Furthermore, if the local oscillator voltage E_h is small, the second whistle (19) is proportional to E_h^2, the third whistle (20) to E_h^3, etc. It is interesting to know the ratio of the whistling voltages E_2, E_3, etc., to the conversion voltage E_0. Of course, one should remember, that E_i means the wanted input signal voltage in (5) for the conversion voltage and means the unwanted (whistling) input signal voltage in (19) and (20). If we regard E_2/E_0, E_3/E_0, etc., as a function of E_h only, it is seen from the aforesaid equations that these ratios start with zero and increase to be finally constant, if E_h increases from zero upwards. Finally, from (13), (14), (15), (16), and (20) it may be deduced that if $a_n E_h \gg 1$ the distortion effects may be determined by measuring the third whistle (20). In fact, they are proportional to (20) (see appendix G).

Coming to type I(b) detectors the voltages E_2, E_3, etc., are given by the equations (see appendix F)

$$E_2 = i_2 R = \frac{1}{4} R E_i^2 \sum A_n e^{a_n V_0} I_2(j a_n E_h) a_n^2; \tag{21}$$

$$E_3 = i_3 R = \frac{1}{24} R E_i^3 \sum A_n e^{a_n V_0} \frac{1}{j} I_3(j a_n E_h) a_n^3, \text{ etc.} \tag{22}$$

From (21) and (22) similar conclusions may be drawn, as stated above for type I(a) detectors. Moreover, it is seen from (17), (18), (21), and (22), that for small values of E_h: $a_n E_h \ll 1$, S_3/S_1 is proportional to E_2/E_0 and for large values of $E_h (a_n E_h \gg 1)$, S_3/S_1 is proportional to E_3/E_0 (see appendix G). This remark includes an easy way of measuring distortion effects with type I(b) detectors by simply measuring their harmonics.

Finally, with type II(a) detectors, we have

$$E_2 = i_2R = \frac{1}{4} RE_i^2 \sum C_n e^{a_nV_{a0}+b_nV_{b0}} I_2(jb_nE_h)a_n^2; \quad (23)$$

$$E_3 = i_3R = \frac{1}{24} RE_i^3 \sum C_n e^{a_nV_{a0}+b_nV_{b0}} \frac{1}{j} I_3(jb_nE_h)a_n^3, \text{ etc.} \quad (24)$$

With regard to the proportionality of S_3/S_1 (i.e., of the distortion effects) to the ratios E_2/E_0 and E_3/E_0, quite the same remarks hold, as were brought forward above in connection with type I(b) detectors.

Measurements of Harmonics.

The measuring apparatus of Figs. 9(a), 9(b), and 9(c) was utilized for the present purpose. The oscillator frequency ω_i was so adjusted, that $|\omega_i - \omega_h| = \omega_0/2$ for measuring the second harmonic. It was so adjusted, that $|\omega_i - \omega_h| = \omega_o/3$ for the third harmonic, etc. Measurements were further carried out in quite the same way, as was described formerly for the conversion gain g_1.

The following table shows the comparison of measurements and calculations for the second harmonic etc., of a type I(b) detector, in this case a Philips E447 valve.

TABLE I

Grid bias volts	−14	−16	−17	−20	−22	−23
Second harm. calc.		51		40	1.4	1.2
Second harm. obs.		46		44	1.5	1.0
Third harm. calc.	15	5	2.8		0.12	0.078
Third harm. obs.	16	5	2.8		0.13	0.075

Second harmonic expressed in microamperes/input volts squared. Third harmonic: microamperes/cube of input volts.

In general, the ratios E_2/E_0, E_3/E_0, etc., were found to be some per cents at most, for commercial detector valves. It is noticeable, that type I(a) detectors are in general *not* inferior to type I(b) and type II(a) detectors, as regards harmonics and distortion effects.

Acknowledgment

The author takes pleasure in expressing his appreciation of the assistance given by Mr. N. S. Markus and by Mr. C. P. Fritzius in the experiments and measurements described in this paper.

Appendix A

In order to derive the expression for the conversion gain of a diode, use is made of the series expansion[7]

[7] G. N. Watson, "Bessel Functions," p. 369, eq. (3).

$$e^{a \sin \omega t} = I_0(ja) + 2 \sum_{m=1}^{\infty} I_{2m}(ja) \cos 2m\omega t + \frac{2}{j} \sum_{m=0}^{\infty} I_{2m+1}(ja) \sin (2m+1)\omega t.$$

Here $I_m(ja)$ is Bessel's function of the first kind, of order m and with the argument ja, where $j = +\sqrt{-1}$. Two properties of Bessel's functions are used in the course of these calculations:

$$\lim_{x \to 0} | I_m(jx) | = \left(\frac{x}{2}\right)^m \cdot \frac{1}{\lfloor m}; \quad \lfloor m = m(m-1) \cdots 2.1;$$

$$\lim_{x \to \infty} | I_m(jx) | = \frac{e^x}{\sqrt{2\pi x}},$$

giving respectively the values of Bessel's functions for small and for large arguments. Tables of the functions I_0, I_1 are available.[7] The voltage V, to be inserted into the equation of the static diode characteristic

$$i = \sum A_n e^{a_n V}$$

is

$$V = V_0 + E_h \sin \omega_h t + E_i \sin \omega_i t - E_0 \cos \omega_0 t.$$

Assuming E_i and E_0 to be so small, that $a_n E_i \ll 1$ and $a_n E_0 \ll 1$, one obtains

$$i = \sum A_n F_n \tag{1}$$

where,

$$F_n = e^{a_n V_0} \left\{ I_0(ja_n E_h) + 2 \sum_{m=1}^{\infty} I_{2m}(ja_n E_h) \cos 2m\omega_h t + \frac{2}{j} \sum_{m=0}^{\infty} I_{2m+1}(ja_n E_h) \sin (2m+1)\omega_h t \right\} (1 + a_n E_i \sin \omega_i t)(1 - a_n E_0 \cos \omega_0 t).$$

Picking out the component of F_n, proportional to $\cos \omega_0 t$, this equation yields

$$F_{0n} = \left[- I_0(ja_n E_h) a_n E_0 + \frac{1}{j} I_1(ja_n E_h) a_n E_i \right] e^{a_n V_0} \cos \omega_0 t. \tag{2}$$

Now the left side of (1) also contains a component $i_0 \cos \omega_0 t$, proportional to $\cos \omega_0 t$. Equating these components on both sides of (1), using (2), yields

$$i_0 = \frac{E_0}{R} = \sum A_n F_{0n}$$

or,

$$\frac{E_0}{E_i} = g_1 = \frac{\sum A_n e^{a_n V_0} a_n \frac{1}{j} I_1(j a_n E_h)}{\frac{1}{R} + \sum A_n I_0(j a_n E_h) a_n e^{a_n V_0}},$$

which is (5) of the text.

Appendix B

With type I(b) detectors we have

$$i = \sum A_n e^{a_n V}$$

and,

$$V = V_0 + E_i \sin \omega_i t + E_h \sin \omega_h t.$$

Using the same series expansions as in the preceding appendix A, one obtains for the current $i_0 \cos \omega_0 t$, where $\omega_0 = |\omega_h - \omega_i|$, the expression

$$\frac{i_0}{E_i} = S_c = \frac{2}{E_i} \sum A_n e^{a_n V_0} \frac{1}{j} I_1(j a_n E_h) \frac{1}{j} I_1(j a_n E_i).$$

Moreover, the current components $i_2 \cos 2\omega_0 t$, $i_3 \cos 3\omega_0 t$, $i_4 \cos 4\omega_0 t$, etc., are easily found to be

$$i_2 = 2 \sum A_n e^{a_n V_0} I_2(j a_n E_h) I_2(j a_n E_i);$$

$$i_3 = 2 \sum A_n e^{a_n V_0} \frac{1}{j} I_3(j a_n E_h) \cdot \frac{1}{j} I_3(j a_n E_i), \text{ etc.}$$

Appendix C

Type II(a) detectors have an anode current i, depending on the grid tensions V_a and V_b by

$$i = \sum C_n e^{a_n V_a + b_n V_b}.$$

Inserting

$$V_a = V_{a0} + E_i \sin \omega_i t \quad \text{and} \quad V_b = V_{b0} + E_h \sin \omega_h t$$

and using the series expansion, given in Appendix A, one finds for the current component $i_0 \cos \omega_0 t$, where $\omega_0 = |\omega_h - \omega_i|$ the expression,

$$\frac{i_0}{E_i} = \frac{2}{E_i} \sum C_n e^{a_n V_{a0} + b_n V_{b0}} \frac{1}{j} I_1(j a_n E_i) \frac{1}{j} I_1(j b_n) E_h).$$

It is a simple matter to pick out the harmonic current components $i_2 \cos 2\omega_0 t$, $i_3 \cos 3\omega_0 t$, etc. One obtains

$$i_2 = 2 \sum C_n e^{a_n V_{a0} + b_n V_{b0}} I_2(j a_n E_i) I_2(j b_n E_h);$$

$$i_3 = 2 \sum C_n e^{a_n V_{a0} + b_n V_{b0}} \frac{1}{j} I_3(j a_n E_i) \frac{1}{j} I_3(j b_n E_h), \text{ etc.}$$

Appendix D

Considering first type I(a) detectors, one can show, that the voltage E_0 contains only odd powers of E_i. The even powers of E_i in the expansion

$$e^{E_i \sin \omega_i t} = 1 + E_i \sin \omega_i t + \frac{E_i^2}{\lfloor 2} \sin^2 \omega_i t + \frac{E_i^3}{\lfloor 3} \sin^3 \omega_i t + \cdots$$

cannot give rise to terms, containing the angular frequency $\omega_0 = |\omega_h - \omega_i|$. Similar remarks hold for type I(b) and for type II(a) detectors. This may be seen, for the former type, from the expression:

$$E_0 = R \cdot 2 \sum A_n e^{a_n V_0} \frac{1}{j} I_1(j a_n E_i) \frac{1}{j} I_1(j a_n E_h),$$

where $1/j \cdot I_1(j a_n E_i)$, by the well-known series expansion,[7] contains only odd powers of E_i. Quite the same reasoning holds for type II(a) detectors. Taking,

$$E_0 = g_1 E_i + g_3 E_i^3 + \cdots$$

and,

$$E_i = e(1 + M \cos pt),$$

one obtains

$$E_0 = g_1 e(1 + M \cos pt) + g_3 e^3 \left(1 + 3M \cos pt + \frac{3}{2} M^2 \cos 2pt + \frac{3}{2} M^2 + \frac{1}{4} M^3 \cos 3pt + \frac{3}{4} M^3 \cos pt \right) + \cdots$$

[7] *Loc. cit.*, p. 15.

or,

$$E_0 = g_1 e + g_3 e^3\left(1 + \frac{3}{2}M^2\right) + \left(g_1 eM + 3g_3 e^3 M + \frac{3}{4}g_3 e^3 M^3\right)$$

$$\cos pt + \left(g_3 e^3 \frac{3}{2}M^2\right)\cos 2pt + \frac{1}{4}g_3 e^3 M^3 \cos 3pt + \cdots.$$

Hence the modulation depth M_1' of E_0 with the angular frequency p is given by (13) of the text. Similarly, from the above expansion, the expressions for M_2', being the modulation depth of E_0 with the angular frequency $2p$, and M_3', being the modulation depth of E_0 with the angular frequency $3p$, are easily found (see (14) of the text).

In order to calculate the cross-modulation coefficient M_0, take $E_i = e + E_k(1 + M_k \cos pt)$ in the development $E_0 = g_1, E_i + g_3 E_i^3 + \cdots$. The modulation depth of E_0 will be found as in (15) of the text.

Appendix E

The calculation of g_3 for type I(a) detectors may be performed as follows: The voltage

$$V = -E_0 \cos \omega_0 t + E_i \sin \omega_i t + E_k \sin \omega_k t$$

is put into the equation of the static characteristic, while $V_0 = 0$

$$i = \sum A_n e^{a_n V}.$$

Picking out the component $i_0 \cos \omega_0 t$, by using the series development formulas of Appendix A, and remembering, that $i_0 = E_0/R$ one obtains

$$\frac{E_0}{R} = \frac{1}{R}(g_1 E_i + g_3 E_i^3) = -\sum A_n\left(a_n g_1 E_i + a_n g_3 E_i^3 + \frac{1}{8}a_n^3 g_1^3 E_i^3\right.$$

$$\left. + \frac{1}{4}g_1 a_n^3 E_i^3\right) I_0(j a_n E_k) + \sum A_n\left(a_n E_i + \frac{1}{4}a_n^3 g_1^2 E_i^3\right.$$

$$\left. + \frac{1}{8}a_n^3 E_i^3\right)\frac{1}{j} I_1(j a_n E_k) + \sum A_n\left(\frac{1}{8}a_n^3 g_1 E_i^3\right) I_2(j a_n E_k).$$

From this equation one finds for g_1 the value of Appendix A and (5). For g_3 one obtains (16) of the text.

The expression (17) for S_3 is found by inserting $V = V_0 + E_i \sin \omega_i t + E_k \sin \omega_k t$ into the equations of the static characteristic:

$$i = \sum A_n e^{a_n V}.$$

Picking out the terms of frequency ω_0, one obtains

$$\frac{i_0}{E_i} = \sum A_n e^{a_n V_0} \frac{1}{j} I_1(j a_n E_h) a_n + E_i^2 \sum \frac{1}{8} A_n e^{a_n V_0} \frac{1}{j} I_1(j a_n E_h) a_n^3$$
$$= S_1 + S_3 E_i^2.$$

whereby (17) of the text results. Similarly (18) is obtained.

Appendix F

Equation (19) results, if $V = -E_2 \cos 2\omega_0 t + E_i \sin \omega_i t + E_h \sin \omega_h t$ is put into the static characteristic equation, where $i_2 = E_2/R$. In order to obtain (20), V should be taken to equal $-E_3 \cos 3\omega_0 t + E_i \sin \omega_i t + E_h \sin \omega_h t$. Equations (21) and (22) may immediately be written down from the last two equations of Appendix B, remembering, that for small values of $E_i(a_n E_i \ll 1)$, we have

$$I_2(j a_n E_i) = \frac{a_n^2 E_i^2}{2^2} \cdot \frac{1}{2};$$

$$\frac{1}{j} I_3(j a_n E_i) = \frac{a_n^3 E_i^3}{2^3} \cdot \frac{1}{6}.$$

Similarly, (23) and (24) are simple deductions from the last two equations of Appendix C.

Appendix G

With type I(a) detectors, for large values of E_h: $(a_n E_h \gg 1)$ we have by (20) and (5) (assuming $V_0 = 0$, though this condition is *not* essential),

$$\frac{E_3}{E_0} = \frac{1}{24} E_i^2 \frac{\sum A_n a_n^3 e^{a_n E_h} \frac{1}{\sqrt{2\pi a_n E_h}}}{\sum A_n a_n e^{a_n E_h} \frac{1}{\sqrt{2\pi a_n E_h}}}.$$

Under the same condition for E_h one obtains

$$\frac{g_3}{g_1} = \frac{\left(\frac{1}{8} - \frac{1}{8} g_1 + \frac{1}{4} g_1^2 - \frac{1}{8} g_1^3\right) \sum A_n a_n^3 e^{a_n E_h} \frac{1}{\sqrt{2\pi a_n E_h}}}{\sum A_n a_n e^{a_n E_h} \frac{1}{\sqrt{2\pi a_n E_h}}}.$$

Hence,

$$\frac{E_3}{E_0} = \frac{1}{24} E_i^2 \left(\frac{1}{8} - \frac{1}{8} g_1 + \frac{1}{4} g_1^2 - \frac{1}{8} g_1^3\right)^{-1} \frac{g_3}{g_1}.$$

With type I(b) detectors, the case of small $E_h(a_nE_h \ll 1)$ will be considered first. We obtain from (21) and (8)

$$\frac{E_2}{E_0} = \frac{1}{16} E_i E_h \frac{\sum A_n e^{a_n V_0} a_n^4}{\sum A_n e^{a_n V_0} a_n^2},$$

whereas $g_3/g_1 = S_3/S_1$ is, by (17) and (8b),

$$\frac{g_3}{g_1} = \frac{1}{8} \frac{\sum A_n e^{a_n V_0} a_n^4}{\sum A_n e^{a_n V_0} a_n^2}.$$

Hence, if $a_nE_h \ll 1$ we have with type I(b) detectors,

$$\frac{E_2}{E_0} = \frac{1}{2} E_i E_h \frac{g_3}{g_1}.$$

If $a_nE_h \gg 1$, i.e., for large values of E_h, (22) and (8c) yield,

$$\frac{E_3}{E_0} = \frac{1}{24} E_i^2 \frac{\sum A_n e^{a_n V_0 + a_n E_h} a_n^3 \dfrac{1}{\sqrt{2\pi a_n E_h}}}{\sum A_n e^{a_n V_0 + a_n E_h} a_n \dfrac{1}{\sqrt{2\pi a_n E_h}}}.$$

Under this condition, it is found by (17) and (8c),

$$\frac{S_3}{S_1} = \frac{g_3}{g_1} = \frac{1}{8} \frac{\sum A_n e^{a_n V_0 + a_n E_h} a_n^3 \dfrac{1}{\sqrt{2\pi a_n E_h}}}{\sum A_n e^{a_n V_0 + a_n E_h} a_n \dfrac{1}{\sqrt{2\pi a_n E_h}}}.$$

Thus, if $a_nE_h \gg 1$, one obtains with type I(b) detectors,

$$\frac{E_3}{E_0} = \frac{1}{3} E_i^2 \frac{g_3}{g_1}.$$

Similar relations, as were derived for type I(b) detectors, are easily found for type II(a) detectors.

Bibliography

Completeness for the period from January, 1930, to January, 1934, was aimed at, while some of the previous papers were included. Reference is made to the bibliography in these PROCEEDINGS, vol. 19, pp. 1034–1089; June, (1931).

(1) C. B. Aiken, "Further notes on the detection of two modulated waves which differ slightly in carrier frequency," PROC. I.R.E., vol. 20, pp. 569–578; March, (1932).
(2) C. B. Aiken, "Theory of detection of two modulated waves by a linear rectifier," PROC. I.R.E., vol. 21, pp. 601–629; April, (1933).

(3) E. V. Appleton, "Thermionic Vacuum Tubes," Methuen and Co., (1932).
(4) E. V. Appleton and D. Boohariwalla, "The mutual interference of wireless signals in simultaneous detection," *Wireless Eng.*, vol. 9, pp. 136–139, (1932).
(5) H. Ataka, "On the modulation of an ultra-short wave by a modulated medium wave and its detection," *Jour. I. E.E.* (Japan), vol. 53, no. 540, pp. 54–55, (1933).
(6) S. Ballantine, "Detection at high signal voltages," Proc. I.R.E., vol. 17, pp. 1153–1177; July, (1929).
(7) A. C. Bartlett, "The calculation of modulation products," *Phil. Mag.*, vol. 16, pp. 845–847, (1933).
(8) W. R. Bennett, "New results in the calculation of modulation products," *Bell Sys. Tech. Jour.* vol. 12, pp. 228–243, (1933).
(9) E. A. Biedermann, "Some notes on the use of a diode as a cumulative grid rectifier," *Wireless Eng.*, vol. 10, pp. 123–133, (1933).
(10) H. A. Brown and C. T. Knipp, "Power detection characteristics of pentode tubes," *Electronics*, pp. 126–127; April, (1932).
(11) H. A. Brown, G. W. Pickels, and C. T. Knipp, "Detector distortion at low input signals," *Radio Eng.*, vol. 12, pp. 21–23, (1932).
(12) C. S. Bull, "Non-linear valve characteristics. A brief discussion of their use," *Wireless Eng.*, vol. 10, pp. 83–88, (1933).
(13) M. V. Callendar, "A note on demodulation under practical conditions," *Wireless Eng.*, vol. 10, pp. 480–483, (1933).
(14) E. L. Chaffee, "Theory of Thermionic Vacuum Tubes," McGraw Hill Co., (1933).
(15) W. T. Cocking, "Comparing detector valves," *Wireless World*, vol. 28, pp. 427–429, (1931).
(16) R. de Cola, "An analysis of power detection," Proc. I.R.E., vol. 21, pp. 984–989; July, (1933).
(17) F. M. Colebrook, "The theory of the straight line rectifier," *Wireless Eng.*, vol. 7, pp. 595–603, (1930).
(18) F. M. Colebrook, "The frequency analysis of the heterodyne envelope," *Wireless Eng.*, vol. 9, pp. 195–201, (1932).
(19) E. J. C. Dixon, "The heptode a novel thermionic valve," *P. O. Elec. Eng. Jour.*, vol. 24, pp. 299–302, (1932).
(20) C. Fayard, "Elementary theory of a system of multiple modulation of an r. f. oscillation," *l'Onde Électrique*, vol. 12, pp. 295–325, (1933).
(21) C. B. Fisher, "S. g. valve as superhet detector," *Wireless Eng.*, vol. 10, pp. 541–542, (1933).
(22) W. F. Floyd, "A note on interference tones in superheterodyne receivers," *Proc. Phys. Soc.*, vol. 45, pp. 610–616, (1933).
(23) Y. Fukuta and E. Kido, "Graphical determination of the detection characteristics of a triode," *Rep. Radio Res.* (Japan), vol. 13, pp. 8–9, (1933).
(24) W. Ch. van Geel, "On rectifiers," *Zeit. für Physik*, vol. 69, p. 765, (1931).
(25) W. Ch. van Geel, "Stopping layer of rectifiers," *Nature*, vol. 132, p. 711, (1933).
(26) W. Ch. van Geel and H. Emmens, "On rectifiers," *Zeit. für Physik*, vol. 87, p. 220, (1933).
(27) W. Greenwood and S. J. Preston, "Quality detectors. A survey of rectification," *Wireless Eng.*, vol. 8, pp. 648–658, (1931).
(28) Y. B. F. J. Groeneveld, B. van der Pol, and K. Posthumus, "Grid detection," *Zeit. für Hochfrequenz.*, vol. 29, p. 139, (1927).
(29) C. D. Hall, "The estimation of the sensitivity of the grid rectifier for large inputs," *Wireless Eng.*, vol. 7, pp. 668–670, (1930).
(30) S. Harris, "Cross modulation in r-f amplifiers," Proc. I.R.E., vol. 18, pp. 350–354; February, (1930).
(31) J. F. Herd, "Some measurements on optimum heterodyne," *Wireless Eng.*, vol. 7, pp. 493–499, (1930).
(32) H. E. Hollmann, "Push-pull brake field audion as a receiver for decimeter waves," *Zeit. für Hochfrequenz.*, vol. 42, pp. 185–190, (1933).
(33) H. E. Hollmann, "Brake field audion controlled without power expenditure," *Elek. Nach. Tech.*, vol. 11, pp. 3–15, (1934).
(34) W. Jackson, "Modulation and the heterodyne," *Wireless Eng.*, vol. 8, pp. 425–426, (1931).

(35) L. B. W. Jolley, "Alternating-Current Rectification and Allied Problems," Chapman and Hall, London, (1926).
(36) J. Kammerloher, "The h.f. s.g. valve as an anode bend detector," *Elek. Nach. Tech.*, vol. 10, pp. 345–352, (1933).
(37) W. Kautter, "Double anode valves for anode bend detection and retroaction," *Telefunken Zeitung*, vol. 14, no. 65, pp. 46–51; November, (1933).
(38) C. E. Kilgour and J. M. Glessner, "Diode detection analysis," Proc. I. R. E., vol. 21, pp. 930–943; July, (1933).
(39) K. Kotschubey, "Mercury arc power rectifiers for wireless stations," *Wireless Eng.*, vol. 11, pp. 130–133, (1934).
(40) M. Lambrey and S. Krauthamer, "Two grid valves as frequency changers," *Comptes Rendus*, vol. 198, pp. 156–158, (1934).
(41) W. B. Lewis, "The detector," *Wireless Eng.*, vol. 9, pp. 487–499, (1932).
(42) H. W. Lord, "A life test power supply using Thyratron rectifiers," Proc. I. R. E., vol. 21, pp. 1097–1102; August, (1933).
(43) G. S. C. Lucas, "Distortion in valve characteristics," *Wireless Eng.*, vol. 8, pp. 595–598; pp. 660–661, (1931).
(44) G. S. C. Lucas, "The graphical solution of detector problems," *Wireless Eng.*, vol. 9, pp. 202–207; pp. 253–258, (1932).
(45) C. L. Lyons, "The pentagrid converter," *Wireless World*, vol. 32, pp. 347–348, (1933).
(46) E. D. McArthur, "Electronics and electron tubes," *Gen. Elec. Rev.*, vol. 36, pp. 136–138; pp. 177–181, (1933).
(47) D. McDonald, "The design of power rectifier circuits," *Wireless Eng.*, vol. 8, pp. 522–531, (1931).
(48) E. Mallett, "Apparent demodulation," *Wireless Eng.*, vol. 9, pp. 248–252, (1932).
(49) E. B. Moullin, "The detection by a straight-line rectifier of modulated and heterodyne signals," *Wireless Eng.*, vol. 9, pp. 378–383, (1932).
(50) J. A. Moyer and J. F. Wostrel, "Radio Receiving Tubes," McGraw Hill Co., (1931).
(51) W. Mulder, Dissertation, Delft, (1934).
(52) J. R. Nelson, "Notes on grid circuit detection," Proc. I.R.E., vol. 17, pp. 551–561; March, (1929).
(53) J. R. Nelson, "Grid circuit power rectification," Proc. I.R.E., vol. 19, pp. 489–500; March, (1931).
(54) J. R. Nelson, "Grid circuit linear detection," *Radio Eng.*, vol. 11, pp. 32–34, (1931).
(55) J. R. Nelson, "Some notes on grid circuit and diode rectification,", Proc. I.R.E., vol. 20, pp. 989–1003; June, (1932); pp. 1971–1974; December, (1932).
(56) J. R. Nelson, "Considerations on detector output tube systems," *Electronics*, vol. 6, pp. 94–95 and 98, (1933).
(57) E. Peterson and C. R. Keith, "Grid current modulation," *Bell Sys. Tech. Jour.* vol. 7, pp. 106–139, (1928).
(58) H. Pitsch, "Retroaction coupling with binodes," *Funktech. Monatshefte*, no. 12, pp. 487–488, (1933).
(59) R. C. A., "Use of 1A6 tube," *Radio Eng.* vol. 13, no. 10, p. 26; October, (1933).
(60) E. Y. Robinson, "Pentode as detector amplifier," *Wireless World*, vol. 27, pp. 238–240, (1930).
(61) G. D. Robinson, "Test procedure for detectors with resistance coupled output," Proc. I. R. E., vol. 19, pp. 806–811; May, (1931).
(62) Y. Rocard, "Two grid valves as frequency changers," *Comptes Rendus*, vol. 198, pp. 554–556, (1934).
(63) H. Roder, "Some notes on demodulation," Proc. I.R.E., vol. 20, pp. 1946–1961; December, (1932).
(64) H. Roder, "Superposition of two modulated radio frequencies," Proc. I.R.E., vol. 20, pp. 1962–1970; December, (1932).
(65) H. O. Roosenstein, "Demodulation which is little affected by fading," *Zeit. für Hochfrequenz.*, vol. 42, pp. 85–89, (1933).
(66) H. Rudolph, "Maximum aperiodic amplification and anode bend detection," *Archiv Elektrotech.*, vol. 24, pp. 1–3, (1930).

(67) R. Ruedy, "Rectifier characteristics and detection diagrams," *Phys. Rev.*, vol. 35, p. 129, (1930).
(68) I. Runge and H. Beckenbach, "Ein Beitrag zur Berechnung des Parallelwechselrichters," *Zeit. Tech. Physik*, vol. 14, pp. 377–384, (1933).
(69) E. Severini, "Equivalent entrance resistance of grid leak triode detector," *Alta Frequenza*, vol. 2, pp. 537–547; October, (1933).
(70) C. N. Smyth and J. Stewart, "The double diode triode," *Wireless World*, vol. 32, pp. 355–356, (1933).
(71) A. L. M. Sowerby, "The penthode as an anode rectifier," *Wireless World*, vol. 25, pp. 391–394, (1929).
(72) K. Steimel, "Mixing and fading hexodes," *Telefunken Zeit.*, vol. 14, no. 65, pp. 33–46, November, (1933).
(73) M. J. O. Strutt, "Rectification analysis," *Zeit. für Hochfrequenz.*, vol. 42, pp. 206–208, (1933).
(74) M. J. O. Strutt, "Radio receiving tubes of large interior resistance. B. modulator (detector) tubes," *Zeit. für Hochfrequenz.*, vol. 43, pp. 18–22, (1934).
(75) T. Tanasescu, "The performance of a thermionic tube as a rectifier." *Wireless Eng.*, vol. 11, p. 68–71, (1934).
(76) Telefunken Co., "Hexodes, a new type of receiving valve," *Elek. Zeit.*, vol. 54, p. 611, (1933).
(77) F. E. Terman and B. Dystart, "Detection characteristics of screen-grid and space-charge grid tubes," Proc. I.R.E., vol. 17, pp. 830–833; May, (1929).
(78) F. E. Terman and Thomas M. Coogin, "Detection characteristics of three-element vacuum tubes," Proc. I.R.E., vol. 17, pp. 149–160; January, (1929).
(79) F. E. Terman, "Notes on the Wunderlich tube (for grid leak power detection)," *Electronics*, p. 148, April, (1932).
(80) P. K. Turner, "A new valve characteristic," *Wireless Eng.*, vol. 9, pp. 384–387, (1932).
(81) A. G. Tynan, "Modulation products in a power law modulator," Proc. I.R.E., vol. 21, pp. 1203–1209; August, (1933).
(82) R. Urtel, "The mode of action of diode detection," *Telef. Zeit.* vol. 14, no. 64, pp. 30–45, (1933).
(83) G. Varret, "Detection of modulated waves," *l'Onde Électrique*, vol. 11, pp. 315–328, (1932).
(84) N. Vermes, "General analysis of amplification and detection by thermionic valves," *Annalen der Physik*, vol. 4, pp. 943–969, (1930).
(85) J. C. Warner, E. W. Ritter, and D. F. Schmit, "Recent trends in receiving tube design." Proc. I.R.E., vol. 20, pp. 1247–1262; August, (1932).
(86) Westinghouse Brake and Shaxby Signal Co., "The Westector," *Wireless World*, vol. 32, pp. 173–174, (1933).
(87) H. A. Wheeler, "The hexode vacuum tube," *Radio Eng.*, vol. 13, no. 4, pp. 12–14, (1933).
(88) E. L. C. White, "The s.g. valve as a frequency changer in the superhet," *Wireless Eng.*, vol. 9, pp. 618–621, (1932).
(89) J. P. Woods, "The calculation of detection performance for large signals," *Physics*, vol. 2, pp. 225–241, (1932).

Proceedings of the Institute of Radio Engineers
Volume 22, Number 8 *August, 1934*

THE DETERMINATION OF DIELECTRIC PROPERTIES AT VERY HIGH FREQUENCIES*

By

J. G. Chaffee
(Bell Telephone Laboratories, Inc., New York City)

Summary—*A simple method of determining the dielectric constant and power factor of solid dielectrics at frequencies as high as 20 megacycles, with an accuracy which is sufficient for most purposes, is described. The major sources of error are discussed in detail, and several precautions which should be observed are pointed out.*

Measurements of the dielectric properties at 18 megacycles of a number of commonly used materials has shown that in general the power factor and dielectric constant are not widely different from those which obtain at frequencies of the order of one megacycle.

In addition, the results of an investigation of the input impedance of vacuum tube voltmeters at high frequencies are described as an illustration of the further application of this method of measurement.

Introduction

THE quantitative determination of the losses in solid dielectrics at frequencies much higher than 10^6 cycles per second is a subject concerning which very little information is available in the literature. At lower frequencies bridge methods of measurement are capable of yielding a high order of accuracy, but at present their use is limited to moderately high frequencies. A very simple method, capable of yielding useful results at frequencies at least as high as 2×10^7 cycles, has been found very useful for testing dielectric materials, and while the absolute accuracy of the results may properly be questioned on several grounds, it is thought to be of sufficient simplicity to be of interest to others. While based upon familiar principles the successful application at very high frequencies has required an extensive examination of the sources of error before it was felt that reliance could be placed upon the results.

Method of Measurement

In general, a suitable tuned circuit is set up and its equivalent series resistance measured by appropriate means. Then a parallel plate condenser having as its dielectric a slab of the material to be tested, is connected in parallel with the condenser in the tuned circuit. Reso-

* Decimal classification: R281. Original manuscript received by the Institute, January 22, 1934.

nance is then reëstablished and the resistance of the circuit is measured a second time. The amount by which the main tuning condenser is altered is equal to the total capacity of the attached sample, and the increase in the resistance of the tuned circuit is a measure of the losses in the sample.

Let,

X_c = reactance of main tuning condenser
X_c' = reactance of sample condenser
R = effective shunt resistance of sample condenser
r = equivalent series resistance of sample condenser
Δr = increase in resistance of tuned circuit.

It is easily shown that when the sample condenser is connected

$$\Delta r = \frac{RX_c^2}{R^2 + X_c^2}. \tag{1}$$

In most cases it may be safely assumed that $R^2 \gg X_c^2$, so that

$$R = \frac{X_c^2}{\Delta r}. \tag{2}$$

The equivalent series resistance of the sample may then be written, assuming $R^2 \gg X_c'^2$

$$r = \frac{X_c'^2}{R}. \tag{3}$$

Analogous to the usual factor $Q = \omega L/r$ as applied to a coil, we may write

$$Q_c = \frac{X_c'}{r} = R\omega C \tag{4}$$

where C is the capacity of the sample. The reciprocal of Q_c is closely equal to the power factor of the sample condenser provided that the losses are low. The dielectric constant may be calculated from the measured capacity and the geometry of the sample.

The resistance of the tuned circuit may, of course, be measured by any desired method, but it has been found very convenient to use the resistance variation method. A study of this method has shown that reliable results may be obtained even at frequencies as high as 20 megacycles if proper precautions are taken. It is essential to employ a resistance unit for introduction into the tuned circuit which has negligible inductance and a resistance which does not vary appreciably

with frequency. It would be very difficult to meet these requirements in a continuously variable resistance unit, but a fixed unit of a value roughly equal to the resistance of the circuit to be measured can be employed. If N is the ratio of currents in a resonant circuit before and after introducing a resistance r', then the resistance of the circuit itself will be

$$r = \frac{r'}{N - 1}. \tag{5}$$

A resistance unit suitable for this purpose has been constructed from a short length of No. 40 Advance wire arranged in bifilar form (see Fig. 1). This is soldered to two lugs fastened to a pair of large brass blocks which are separated by a small gap. A tapered hole drilled

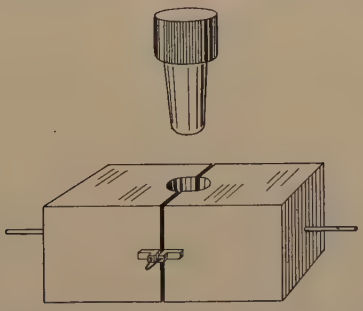

Fig. 1—Construction of resistance unit for use in connection with the resistance variation method of determining circuit resistance.

between the blocks and a plug permit the resistance unit to be short-circuited in the manner frequently employed in laboratory resistance boxes. The lugs to which the ends of the wire are soldered are very close together and the loop formed by the wire is made as small as possible in order to reduce the inductance to a minimum.

Calculation of the skin effect of a straight length of No. 40 Advance wire at 20 megacycles shows that the increase in resistance is about 0.1 per cent. Since the wire is in bifilar form the skin effect will be greater. Comparison of the resistance of a bifilar length of this wire at 60 cycles and at 20 megacycles was made in a specially constructed calorimeter, and while the accuracy obtainable was open to some question the results indicated an increase in resistance of the order of about 1 per cent.

While the reactance of these units is quite small it is still appreciable since it is necessary to retune very slightly when a unit is inserted

in the circuit. Calculating the magnitude of this reactance by noting the extent of retuning necessary showed that for a unit having a direct-current resistance of 0.92 ohm the reactance was $+j0.7$ ohm at 18 megacycles. In cases where the current in the tuned circuit is noted by measuring the voltage across the coil by means of a vacuum tube voltmeter, as was done in the present instance, the second reading of voltage will be high by an amount depending upon the relative reactances of the coil and resistance unit. Since coils having a reactance of the order of 200 ohms are usually employed, the error in this case is of the order of 0.5 per cent. In fact the errors due to skin effect and inductance in the resistance unit are of opposite sign, so that the differential error is usually neglected in view of other small errors which are not so readily evaluated.

Observation of the current in the circuit is preferably made by means of a vacuum tube voltmeter connected across the coil. This device can in general be made to introduce less resistance into the tuned circuit than the introduction of a thermoelement for observing the current directly. The losses in the tube voltmeter need not be known for the present purpose since they can be assumed constant at a given frequency, but in the interest of accuracy in measuring dielectric losses they should be reduced to a minimum. For the measurement of the losses of coils the voltmeter losses must, of course, be known.

Two checks of the accuracy of this method of measuring circuit resistance were made. The resistance of a circuit was measured by both the resistance and the reactance variation methods, the same set-up being used for both. As an example of the agreement between the two methods, the following figures were obtained on a certain circuit:

	Resistance	*Reactance*
f	*Variation*	*Variation*
13.5 mc	0.806 ohm	0.814 ohm
18 mc	1.18 ohms	1.19 ohms

The greatest discrepancy which was noted in a number of different cases was 2 per cent.

A second check was made by arranging two resistance units in a circuit. The circuit resistance alone was measured at 18 megacycles by means of one of the units. Then the second unit having a resistance of 2.0 ohms (direct current) was inserted and the combination remeasured. The resistance of the circuit alone was found to be 2.85 ohms while the value observed after adding the two-ohm unit was 4.88 ohms, a discrepancy of but 1.5 per cent.

As a result of these tests it was felt that the results of the resistance variation method could be depended upon to an accuracy of about 2

per cent. As compared with the reactance variation method, the latter, involving the accurate determination of capacity changes of the order of a fraction of a micromicrofarad and being critically dependent upon the accuracy with which the reactance of the coil is known, is more subject to error and requires greater skill in manipulation to obtain consistent results. Therefore, it is considered of value mainly as a check on the accuracy of the simpler and more direct method.

The complete circuit for the determination of dielectric losses is shown in Fig. 2. The sample condensers consist of rectangular slabs of the dielectric material coated on opposite faces with metal foil which is held in place with the minimum amount of very thin shellac. The application of both heat and pressure is necessary to insure intimate con-

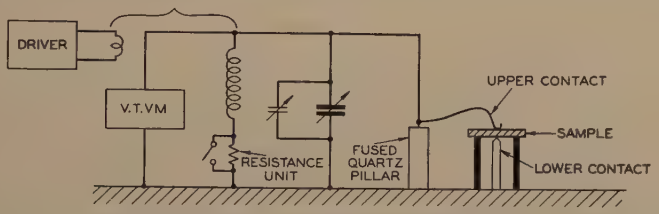

Fig. 2—Circuit for determining properties of dielectric at high frequencies.

tact between the foil and the dielectric material. After the resistance of the circuit alone has been measured the sample is placed in the holder shown in the figure. This consists of a central brass pillar for making contact with the lower electrode and two very thin hard rubber pillars forming additional supports for the sample, the three supports being arranged so as to form a triangle. The sample is raised a considerable distance from the ground plane in order to reduce the capacity between the upper electrode and ground. Contact is made to the upper electrode by means of a length of spring brass wire as shown.

With the sample in position the circuit is retuned to resonance and its resistance again measured. From the observed values of increase in circuit resistance, change in tuning capacity, and the geometry of the sample, the dielectric properties of the material can be calculated.

It should be noted that in determining the reactance of the tuning condenser account should be taken of the effective capacity of the coil to ground. Assuming a linear distribution of voltage along the coil, the effective capacity across its terminals is equal to one third of the total capacity of the coil to ground. This latter quantity may be measured at low frequencies, or may be approximately determined by connecting one terminal of an identical coil to the top of the quartz pillar in such a fashion that it occupies the same relative position with respect to

ground as the coil to be used, and noting the change in tuning capacity necessary to restore resonance. Since the effective capacity is usually quite small it need not be determined to a high degree of accuracy.

Sources of Error

There are several sources of error in the determination of dielectric properties by this method which arise from the very nature of the sample condensers themselves. While a rectangular slab of material completely coated on two opposite faces with metal foil is probably the simplest arrangement which can be devised, there are two objections which can properly be raised. One is based upon the fact that the presence of air bubbles between the electrodes and the material may lead to serious error. At much lower frequencies mercury electrodes are frequently employed for the purpose of obtaining intimate contact with the dielectric. However, with the present method at very high frequencies the small size of the samples which must be employed in order to obtain good accuracy makes the use of mercury electrodes inadvisable on account of their bulk and large stray capacities. At 18 megacycles, for instance, samples having an area of about one square inch and capacities of the order of 5–10 micromicrofarads are usually employed. Furthermore, the optimum size of the sample to be employed in connection with a given tuned circuit depends upon the losses in the material, so that in general a standard electrode size is not feasible. Hence it is considered preferable to use electrodes of very thin foil and to exercise care in securing as intimate contact as possible. By using accurately formed samples and by rubbing the coated surfaces with a burnishing tool or other blunt instrument it is possible to secure a degree of contact which is satisfactory in view of other minor sources of error in the method of measurement. Since the error resulting from air bubbles depends upon the thickness of the air gap compared with the thickness of the sample, the use of very thin samples should be avoided.

The second source of error arises from the presence of stray capacities between the two electrodes. If these capacities are neglected the values obtained for both Q_e and K will be too high. In the case of thick samples of small area the fringing capacity between the electrodes may become a very considerable proportion of the total, so that a suitable correction should always be made.

It has been found that the magnitude of the stray capacity of a rectangular sample can be calculated with sufficient accuracy by means of a formula given by Coursey.[1] This formula states that the total

[1] Coursey, "Electric Condensers," Pitman, London, p. 138, (1927).

capacity between two very thin parallel metallic plates of length l, breadth b, and separated in air by a distance d (centimeters) is given by the expression

$$C_0 = 0.0282l\left\{\frac{\pi b + d}{d} + \log_e\left[\frac{\pi b + d}{d} + \log_e\frac{\pi b + d}{d}\right]\right\}\mu\mu f \quad (6)$$

when b is much greater than d.

If $b > 30d$,

$$C_0 = 0.0295l\left[\frac{\pi b + 4.62d}{d}\right]\mu\mu f. \quad (7)$$

This expresses the total capacity between the electrodes in air. The portion of this capacity due to a uniform field between the two plates is given by the expression

$$C_1 = 0.0885\frac{bl}{d}\mu\mu f. \quad (8)$$

Then the fringing and stray capacities, C', will be the difference between (7) and (8), so that

$$C' = C_0 - C_1. \quad (9)$$

With the dielectric slab between the electrodes, C_1 will be increased by a factor K, the dielectric constant of the material. Assuming that C' is the same as before, the total measured capacity will be

$$C = C' + KC_1 \quad (10)$$

from which K may be readily calculated.

$$K = \frac{C - C'}{C_1}. \quad (11)$$

The applicability of Coursey's formula to the present problem has been investigated experimentally. An air condenser was constructed from two brass plates 3 inches × 5 inches supported by means of a large hard rubber frame in the form of the letter C. The amount of hard rubber used was kept at a minimum, and it was well removed from the field of the condenser. The capacity of this condenser was measured at 1000 cycles and the results compared with the calculated values. The following results were obtained:

Spacing	Measured C_0	Calc. C_0 by (6)	Calc. C_1 by (8)	C'
0.25 inch	15.3 $\mu\mu f$	15.20 $\mu\mu f$	13.45 $\mu\mu f$	1.75 $\mu\mu f$
0.38 inch	10.6	10.43	8.74	1.69

C' is seen to be far from negligible, amounting to 11.5 and 16.2 per cent of the total in the two cases.

A second test was made by making a sample condenser from a sheet of material the dielectric constant of which had been previously determined at 1000 cycles by a highly refined method employing mercury electrodes and a guard ring. The dimensions of the sample were 2.0 inches $\times$ 0.98 inch $\times$ 0.052 inch, and it was coated with tin foil in the usual fashion. Calculation of K on the basis of a 1000-cycle measurement on this sample gave a value of 3.35 while the more precise method had given a value of 3.36. The fringing correction amounted to 8.1 per cent of the total, so that if no correction had been made a value of 3.43 would have been obtained.

Thus it appears that Coursey's formula is sufficiently accurate to justify its use, particularly since considerable error can be tolerated in the determination of a correction which does not usually amount to more than 10 to 15 per cent.

An additional source of error, which can become very appreciable when the losses in the dielectric sample under consideration are very low, can arise from the existence of sizeable metallic losses in the plates of the variable tuning condenser. If all of the losses in the tuning condenser are in its dielectric support, the portion of the series resistance of the circuit due to this loss will not be altered when the sample is connected since the total tuning capacity remains the same. However, at very high frequencies the losses in a good variable condenser are largely metallic and of a value which depends upon the distribution of current in the plates. Hence, when the capacity of the tuning condenser is decreased to compensate for the added capacity of the sample its series resistance will change, and the apparent loss in the sample will be in error.

The existence of an appreciable amount of metallic loss in the tuning condenser may be readily detected by attempting to measure the losses in a sample of some such material as fused quartz which is known to have exceedingly low losses at lower frequencies. In case the metallic loss in the tuning condenser is appreciable the resistance of the circuit may actually decrease when the sample condenser is added since only a part of the total current will now flow through the tuning condenser, and as a result the equivalent resistance of the sample will appear to be negative.

It has been found that the metallic losses in a variable condenser having brass plates with soldered joints could be reduced to a figure which apparently did not introduce appreciable error in most cases by plating the entire metallic structure with copper or silver followed by

an extremely thin coating of lacquer to prevent subsequent tarnishing. Dielectric loss may be kept very low by using fused quartz insulation.

As an example of the reduction which may be effected by plating, a small brass plate condenser of the "Midget" type which has been reinsulated with a strip of fused quartz was found to have sufficient metallic resistance so that apparent negative losses were observed in samples of very low loss materials, such as fused quartz, at 18 megacycles. The condenser was then thoroughly copper-plated with the result that the resistance of the circuit in which it was used was reduced from 0.52 to 0.41 ohms, the total tuning capacity being 40 micromicrofarads, and in addition the results obtained with such materials were positive.

While it must be admitted that even with these precautions the metallic losses in the tuning condensers are not entirely reduced to zero, and that in the case of such substances as fused quartz the results, depending as they do upon the observation of a very small increase in circuit resistance, may be subject to considerable error, still in the case of most substances the loss is sufficiently great so that this residual source of error can be safely neglected.

It will be realized that the accuracy of any measurement of this kind will be dependent upon several factors the relative importance of which depends upon the size of the sample condenser, its losses, and the loss in the tuned circuit. In general the sample capacity should be of such size that it effects a reasonably large increase in the resistance of the circuit without necessitating too great a change in the setting of the tuning condenser. For this reason the resistance of the circuit alone should be made as low as possible. Materials which have moderately high dielectric loss present no great difficulty, but in case of very excellent substances the results become more questionable the lower the losses.

Some Results Obtained By This Method

In the remaining sections of this paper there will be given a few of the results which have been obtained by the method which has just been described.

The dielectric constant and power factor of a number of commonly used materials have been measured at a frequency of 18 megacycles. Comparison with published data obtained at frequencies of the order of one megacycle has indicated that no great change in these factors takes place over the range of about one to eighteen megacycles. In general there is a tendency toward increasing power factor and decreasing dielectric constant which is not very marked. Thus as a first

approximation the dielectric properties of a material at the higher frequencies can be predicted from data obtained at much lower frequencies.[2]

The accompanying table gives a few representative results which have been obtained by this method. All data were taken under average laboratory conditions of temperature and humidity. It must be realized that in the case of many substances considerable variation will be found among samples taken from different lots of the same material, and furthermore that some materials are capable of absorbing considerable moisture which has a marked effect upon their dielectric properties. In all cases the figures which have been given are believed to be representative under conditions which are ordinarily encountered in practice.

An interesting application of this method has been made in the study of the grid-filament impedance of vacuum tube voltmeters at high frequencies. A knowledge of this impedance is essential to the study of coil losses by the resistance variation method. Measurement has shown that the loss in the input circuit of a tube voltmeter which is not drawing grid current consists of two parts; namely, the normal dielectric loss which takes place in the base and glass supports within the tube when no space current flows, and an additional loss which appears when the tube becomes active. This latter quantity will be designated the "active grid loss" in the absence of a better term. Simultaneous with the appearance of the active grid loss there takes place a small increase in grid-filament capacity, a fact which has long been recognized. It was at first thought that this loss might be due to the presence of a small impedance in the plate circuit due to an inadequate by-pass condenser between plate and filament, but it was found that the addition of a number of extra condensers had no effect whatever. In addition, careful tests were made to insure that the grid was not taking even a minute amount of current.

Examination showed that there is a wide variation in active grid loss among different types of tubes. Considerable variation was also noted among different tubes of the same type. Furthermore, in certain tubes having a small glass bulb, the loss could often be very materially reduced by coating the outside of the bulb with tin foil which was grounded. Tubes in which the proximity of the bulb to the elements was less were not affected by the presence of the foil. These facts indicate

[2] Certain substances which exhibit the phenomenon of ionic polarization undergo considerable change in power factor in the very low-frequency range, so that estimates should not be based upon data obtained at frequencies much below 50 kilocycles.

that the phenomenon can be influenced by the presence of a charge on the glass envelope.

It was further shown that the active grid loss was a function of frequency, and that it could be approximately represented by a high resistance shunt which varied inversely with frequency. Thus it follows closely the law of ordinary dielectric loss and can therefore be combined with the dielectric leakage in the tube supports for evaluating the total grid-filament impedance of the tube.

The mechanism of the active loss in the grid circuit of a vacuum tube is of considerable complexity. The existence of a loss of this type

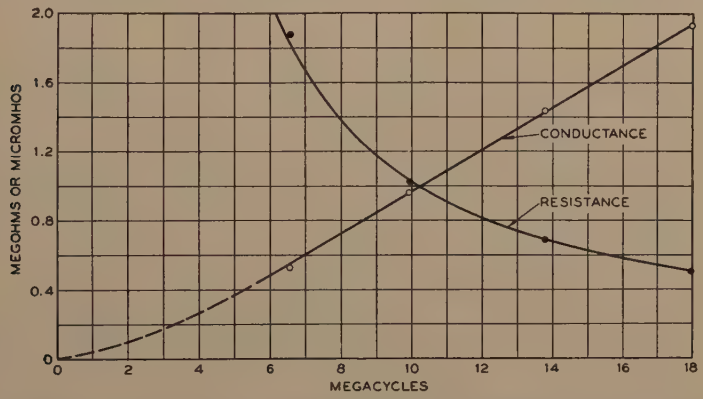

Fig. 3—Active grid loss vs. frequency in Western Electric No. 239A vacuum tube. Loss is expressed as the equivalent grid-filament resistance or conductance exclusive of dielectric leakage in tube supports.
$E_B = 67^v$. $E_C = -9^v$. $I_A = 0.25^a$

which increases with frequency has been demonstrated theoretically by Llewellyn in a recent paper[3] to which the reader is referred.

Measurement of the active grid loss in a number of receiving type tubes at 18 megacycles has yielded values which ranged between 48,000 and 500,000 ohms. In all of these cases the normal dielectric loss in the cold tube with the base removed was representable by a resistance of between one and three megohms. Thus the active loss is seen to be by far the greater of the two.

It is interesting to note that in the case of a screen-grid tube the grid resistance at 18 megacycles was about 200,000 ohms, which is less than the plate resistance.

The manner in which the active grid loss varies with frequency is shown by Fig. 3. Over the range of frequencies shown it is approxi-

[3] F. B. Llewellyn, "Vacuum tube electronics at ultra-high frequencies," Proc. I.R.E., vol. 20, p. 1532; November, (1933).

mately representable by a resistance between grid and filament which varies inversely as the frequency. This is similar to the behavior of dielectric leakage with frequency as is shown by Fig. 4, which gives data which were obtained in a similar fashion on a sample of vulcanized rubber. Though neither phenomenon follows precisely this simple law, it is convenient to lump the two effects in obtaining the grid filament resistance of a vacuum tube voltmeter.

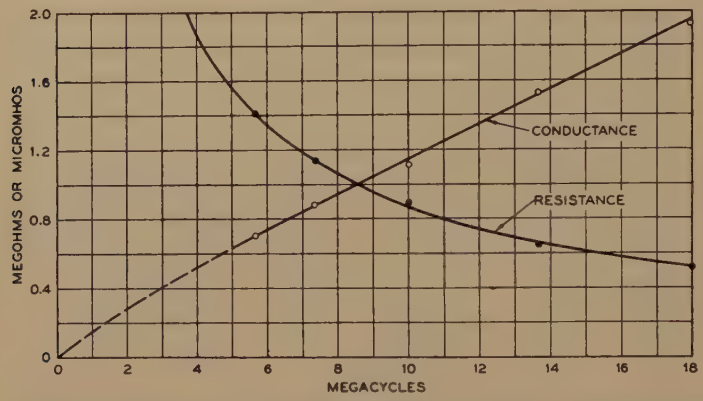

Fig. 4—Dielectric leakage and conductivity of a sample of vulcanized rubber vs. frequency. Compare with Fig. 3.

In view of the magnitude of the active grid loss (and the fact that it increases with frequency) it is probable that this phenomenon has an important bearing upon the operation of oscillators at ultra-high frequencies.

PROPERTIES OF CERTAIN DIELECTRICS AT 18 MEGACYCLES

Material	Dielectric constant K	Power Factor, %	$K \times$ Power Factor
Phenol fiber sample			
Black	4.7	6.0	28.
Natural brown	4.4	5.6	24.
Hard rubber sample	2.9	0.76	2.2
Glass (borosilicate)	5.1	0.59	3.0
Dry whitewood	1.7	2.3	3.9
Fused quartz	3.4*	<0.05	<0.17
Vulcanized rubber sample	3.9	2.9	11.
Dry baked soapstone-various grades	4.1–4.8	1.2–9.48**	4.9–2.3

* Air bubbles in sample probably account for low value.
** Increasing rapidly with absorbed moisture.

Proceedings of the Institute of Radio Engineers
Volume 22, Number 8 *August, 1934*

ELECTRON OSCILLATIONS WITHOUT TUNED CIRCUITS*

By

W. H. Moore

(The Canadian Marconi Company, Ltd., Montreal, Que., Canada)

Summary—*In some earlier investigations[1] on electron oscillations of the Barkhausen-Kurz type it was found by the author that oscillations could be produced in a positive grid valve with the usual grid-plate Lecher wire system omitted. The experimental fact that oscillations may be produced without this external Lecher wire circuit has been noted by many investigators, but few have studied the peculiarities of this particular case. The present paper describes some of the characteristics of this type of oscillator.*

I. Introduction

ELECTROMAGNETIC oscillations of wavelengths of the order of 150 centimeters and less may be produced with certain triode valves of symmetrical cylindrical structure by applying high positive potentials tc the grid and zero or slightly negative potentials to the plate, in a circuit having a Lecher wire system connected between grid and plate. This is the usual type of Barkhausen-Kurz oscillator, and has been studied by numerous investigators since its original discovery by Barkhausen and Kurz.[2] The oscillations are produced by a cloud of electrons vibrating back and forth in the interelectrode spaces of the valve. The wavelength is independent of the adjustment of the external Lecher wire system, being controlled by the potentials applied. It was later found by Gill and Morrell[3] and others that under some conditions the external circuit did control the wavelength produced. When the external circuit did not control the wavelength, it was found that it did affect the power output, the output being a maximum when the external circuit was tuned to the frequency of the electron oscillations.

In some earlier investigations on electron oscillations of the Barkhausen-Kurz type it was found by the author[1] that oscillations could be produced in a positive grid valve with the usual grid-plate Lecher wire system omitted. This type of oscillation is now investigated, the particular objective being the determination of how closely existing theories and wavelength relationships could be applied to this case. The experimental fact that the external Lecher wire circuit is not es-

* Decimal classification: R133. Original manuscript received by the Institute, January 4, 1934.

[1] W. H. Moore, *Can. Jour. of Research*, vol. 4, pp. 505–516, (1931).

[2] H. Barkhausen and K. Kurz, *Phys. Zeit.*, vol. 21, p. 1, (1920).

[3] E. W. Gill and J. H. Morrell, *Phil. Mag.*, vol. 44, pp. 161–178, (1922); vol. 49, pp. 369–379, (1925).

sential for the production of oscillations has been noted by numerous research workers, but not much work has been done in determining the peculiarities, if any, of this particular case.[4] This paper describes the results of some investigations on a Barkhausen-Kurz oscillator having no tuned circuit connected to it.

II. Calculation of Oscillation Frequency

Several theories have been developed to account for the production of oscillations under the conditions obtaining in the Barkhausen-Kurz oscillator. These theories have provided the basis for the derivation of a number of formulas expressing the relationship between the wavelength produced and the various circuit parameters. Barkhausen and Kurz derived a formula giving the oscillation wavelength for the simplified case of plane electrodes. This is as follows:

$$\lambda = \frac{2000}{\sqrt{E_g}} \cdot \frac{r_a \cdot E_g - r_g \cdot E_a}{E_g - E_a} \tag{1}$$

where λ is the wavelength in centimeters, E_g and E_a the grid and anode voltages, with respect to the filament, and r_a and r_g are the anode and grid distances in centimeters from the filament. When the plate is connected directly to the filament, $E_a = 0$, and the formula becomes

$$\lambda = \frac{2000 \cdot r_a}{\sqrt{E_g}}. \tag{2}$$

When this relationship is applied to the case of valves with cylindrical elements, it is sometimes written

$$\lambda = \frac{1000 \cdot d_a}{\sqrt{E_g}} \tag{3}$$

where d_a = anode diameter, since $d_a = 2r_a$.

These formulas do not give accurate results when applied to the case of valves having cylindrical electrodes. Since this is the only type of valve which can be made to produce Barkhausen-Kurz oscillations satisfactorily, it was desirable to obtain the wavelength relationship for the somewhat more complicated case of valves of cylindrical construction. A formula for this case was developed by Scheibe,[5] and is as follows:

$$\lambda = \frac{4cr_1}{\sqrt{2 \cdot \frac{e}{m} \cdot E_{fg} \cdot 10^8}} \left\{ f\left(\sqrt{\log_e \frac{r_1}{r_0}} \right) + g\left(\sqrt{\frac{E_{fg}}{E_{fg} - E_{fp}} \log_e \frac{r_2}{r_1}} \right) \right\} \text{ cm.} \tag{4}$$

The various quantities in this formula are defined as follows: λ is the wavelength in centimeters; $c=3\times10^{10}$ cm/sec.; $e/m=1.765\times10^{7}$ e.m.u./gm.; r_0 is the filament radius, r_1 the grid radius, and r_2 the plate radius, all in centimeters; E_{fg} is the grid potential and E_{fp} the plate potential in volts, with respect to the filament. The $f(\ )$ and $g(\ )$ functions may be evaluated from the following:

$$f(x) = x\cdot e^{-x^2}\int_0^x e^{u^2}\cdot du.$$

$$g(x) = x\cdot e^{x^2}\int_0^x e^{-u^2}\cdot du.$$

where,

$$x = \sqrt{\log_e\cdot\frac{r_1}{r_0}} = 1.52\sqrt{\log_{10}\cdot\frac{r_1}{r_0}},\ \text{in } f(x),$$

and,

$$x = \sqrt{\frac{V_{fg}}{V_{fg}-V_{fp}}\cdot\log_e\cdot\frac{r_2}{r_1}} = 1.52\sqrt{\frac{V_{fg}}{V_{fg}-V_{fp}}\cdot\log_{10}\cdot\frac{r_2}{r_1}},\ \text{in } g(x).$$

In the case where $E_{fp}=0$, the latter value of x simplifies to $1.52\sqrt{\log_{10}\cdot r_2/r_1}$. A table of numerical values of $f(x)$ and $g(x)$ is given in the Appendix. When r_0, r_1, and r_2 are of the usual order of magnitude it is not necessary to know r_0 very accurately, as the form of the function is such that large variations in r_0 will produce but very slight changes in the result.

A wavelength formula developed by Hollmann[6] for the case of plane electrodes with grid equidistant from plate and filament is as follows:

$$\lambda = \frac{4000\sqrt{E_g - E_0}}{E_g - \dfrac{4\cdot E_0}{\pi^2}}\cdot d \text{ cm} \qquad (5)$$

where E_g is the direct grid voltage, upon which is superimposed an alternating potential E_0 which may sometimes be produced at the grid by the alternating field, while d is the grid-anode distance in centimeters. When $E_0=0$, this formula drops into the same form as the Barkhausen-Kurz relationship (3), since $d=d_a/4$.

[4] G. Breit, *Jour. Frank. Inst.*, vol. 197, pp. 355–358, (1924).
[5] A. Scheibe, *Ann. der Phys.*, vol. 73, no. 4, pp. 54–88, (1924).
[6] H. E. Hollmann, *Ann. Phys.*, vol. 86, pp. 129–187, (1928).

Another wavelength relationship was developed by Jonescu[7] for the case of valves containing an appreciable amount of gas. This formula is

$$\lambda = \frac{c}{\frac{2}{\pi}\sqrt{\frac{e}{m}\cdot\frac{k}{9\pi}\cdot\frac{E_g}{r^2}}} \tag{6}$$

where r is the grid radius, e/m and c have their usual significance, and k is a constant whose value is determined by the gas content of the valves. Substituting

$$k' = \frac{c}{\frac{2}{\pi}\sqrt{\frac{e}{m}\cdot\frac{k}{9\pi}}}$$

in (6), we see that this equation now becomes

$$\lambda = \frac{k'r}{\sqrt{E_g}},$$

which again is of the same form as the Barkhausen-Kurz relationship.

Working from a somewhat different viewpoint Rostagni[8] has developed a wavelength relationship which involves the volume included in the grid-plate space, and the total number of electrons in this space. It is thus applicable to the case of cylindrical electrodes and is a function not only of their distance apart but also of their length. Rostagni's formula is as follows:

$$\lambda = \frac{K}{\sqrt{N}} = \sqrt{\frac{\pi m v}{e^2 N}} = \frac{3.35\cdot 10^6\sqrt{v}}{\sqrt{N}} \text{ cm} \tag{7}$$

where v is the volume enclosed by the grid and plate elements and N the number of electrons within this volume. It may be written in the form

$$\lambda = \frac{3.35\cdot 10^6}{\sqrt{\frac{N}{v}}} = \frac{\text{constant}}{\sqrt{\text{electron density}}}.$$

Written in this form it becomes evident that this formula does not actually represent the wavelength as varying with the length of the

[7] T. V. Jonescu, *Comptes Rendus*, vol. 193, pp. 575–577; October 12, (1931).
[8] A. Rostagni, *Comptes Rendus*, vol. 193, pp. 1073–1075; November 30, (1931).

electrodes, if the electron density remains constant. Doubling the length of the grid and plate elements, for example, will not alter the wavelength provided that the filament length is also doubled. This formula is similar in form to that of Barkhausen and Kurz, except that electron density replaces the grid potential.

III. Experimental Investigations

The circuit shown in Fig. 1 was used. It was desired to investigate pure electron oscillations only, hence in order to inhibit the production of Gill-Morrell oscillations, the grid-plate Lecher wire system was omitted. Radio-frequency choke coils were inserted in the grid, plate, and filament leads, but were found to have no effect on the wave-

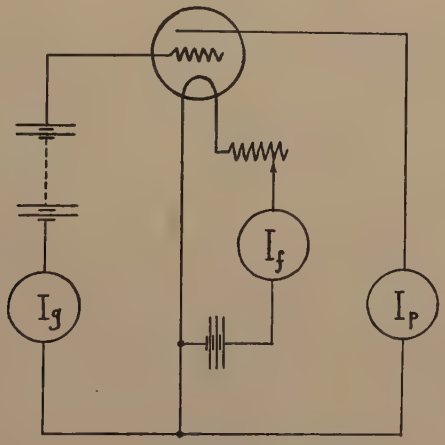

Fig. 1—Circuit for the production of electron oscillations.

length. They were therefore omitted in later experiments. The leads were also moved about to determine if the external connections were providing a resonant circuit. This did not affect the wavelength, it was found.

A number of valves were connected in the Barkhausen-Kurz oscillator of Fig. 1 and measurements carried out on each valve. The graphs of Figs. 2 to 14 are self-explanatory as regards the variations in the voltages applied. The positive side of the grid battery was connected directly to the grid, and the negative side directly to the negative end of the filament. The plate was also connected directly to the negative side of the filament. Filament current was held constant at 0.7 ampere, the rated value, except where otherwise noted.

The grid potential was varied from 0 to 200 volts positive, and the values of grid and plate currents recorded over this range. The wavelength was also measured whenever oscillations appeared. The curves indicate how the wavelength, plate current, and grid current—λ, I_p, and I_g, respectively—varied as the grid potential was altered. These curves do not extend beyond 200 volts, as it was found that in no case did further oscillations appear when the grid voltage was increased beyond this value. Also at higher voltages there was danger of damage to the valves due to excessive heating. The application of negative potentials to the plate decreased the plate current in every case, reducing the amplitude of oscillations, hence the curves were taken at zero plate potential.

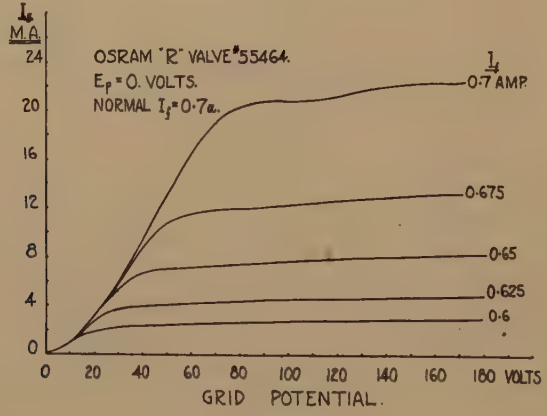

Fig. 2

A set of grid current vs. grid potential curves was also obtained for one of the valves for several values of filament current other than normal. These are shown in Fig. 2. Oscillations do not occur at low values of filament current, but their presence when I_f is sufficiently high is indicated on the 0.7-ampere curve by the distinct depression at grid potentials in the neighborhood of 110 volts.

It was found that of the eleven "*R*" valves investigated, nine produced oscillations when certain values of grid potential were applied. The remaining two valves, although supposedly similar to the others, could not be made to oscillate under any conditions. The curves for the two latter valves are given in Figs. 12 and 13. Their characteristics are discussed later. Of those valves which did produce oscillations, the one feature common to all of them is the region of oscillations which was found to occur at grid potentials in the neighborhood of 100 volts,

the wavelength being around 80 centimeters in every case. In some cases one, and occasionally two, additional regions of oscillation were found, the corresponding wavelengths being in the neighborhood of 130 centimeters, and 50 centimeters, in the two regions. At the critical values of grid potential at which the wavelength jumped from one

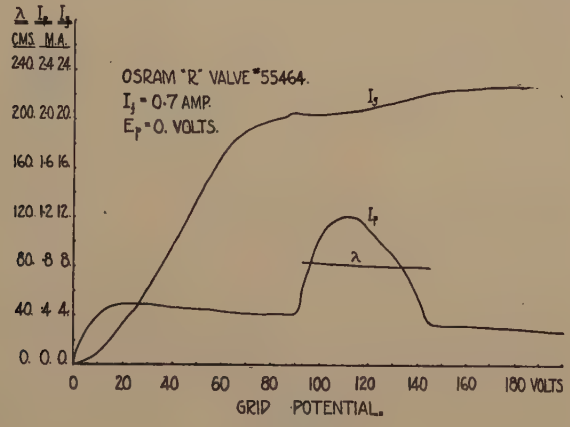

Fig. 3

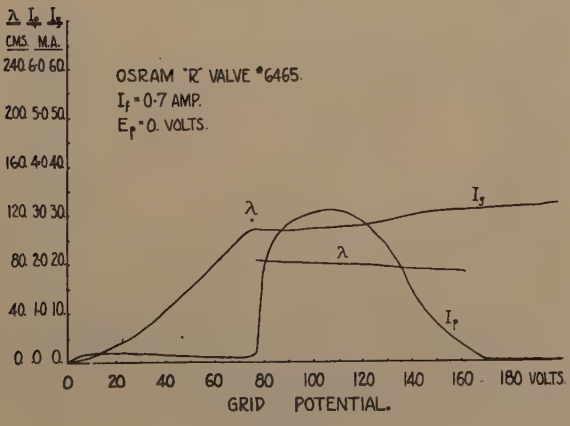

Fig. 4

region to another, conditions were unstable. The wavelength tended to jump back and forth erratically between the two possible values with no oscillations occurring at intermediate values.

Wavelengths produced with the various valves over the range of potentials investigated are grouped together in the set of curves given in Fig. 14. Curves showing the values of wavelengths calculated from

the Barkhausen-Kurz and Scheibe formulas are also included in this figure. Wavelength measurements were made by means of absorption type wavemeters,[9] the indication being obtained from a deflection of the plate-current meter.

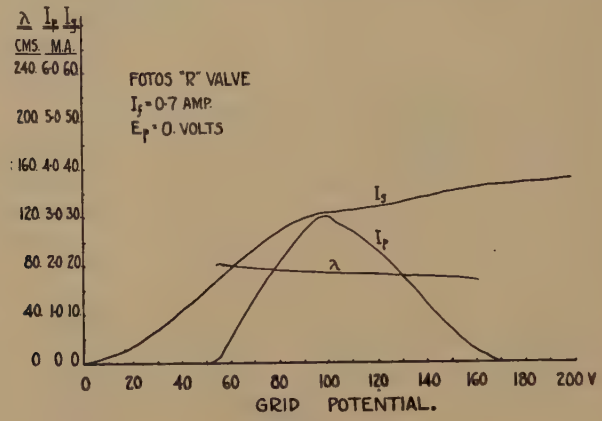

Fig. 5

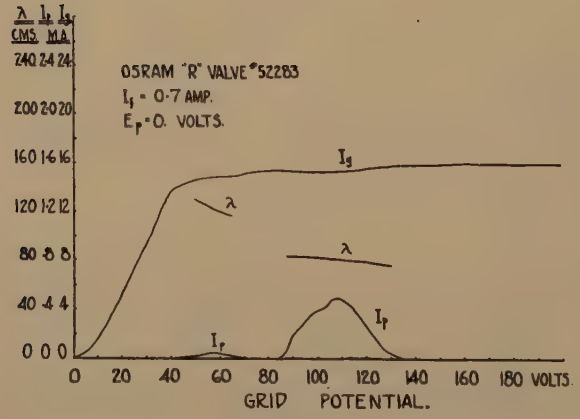

Fig. 6

IV. Discussion of Results Obtained

It is generally considered that this type of oscillation does not commence until the space current in the valve has reached its saturation value. This is borne out by all of the valves examined and which produced oscillations, except one. The Fotos valve (Fig. 5) exhibits but

[9] W. H. Moore, "Simple ultra-short-wave wavemeters," *Electronics*, p. 311, November, (1933).

one region of oscillations, and this commences well below the knee of the grid-current curve, which is the point where saturation is reached. The fact that the oscillations belonged to the type whose wavelength is about 80 centimeters indicates that oscillations sometimes occur more readily in this region than in the other two regions, since the

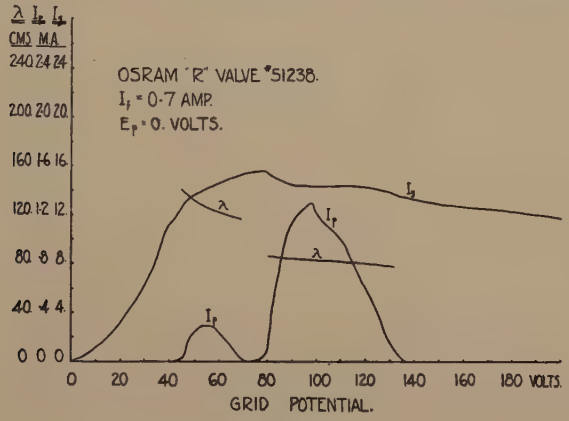

Fig. 7

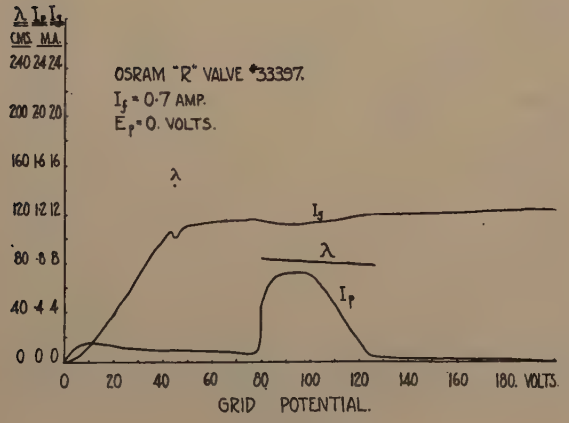

Fig. 8

others were not present in this case. The first oscillations to appear were usually of one of the other two types. It is also found that every valve which produced oscillations had this 80-centimeter region, whether either or both of the other regions were present or not. The significance of these observations is discussed below.

It was desired to determine to what extent the existing theory was

adequate to interpret the results obtained, as indicated by agreement, or lack of it, between calculated and experimental values of wavelength obtained at various grid potentials. The wavelength relationship given by Barkhausen and Kurz (equation 3) gives the smooth curve denoted as "Calculated Filament-Plate Wavelengths

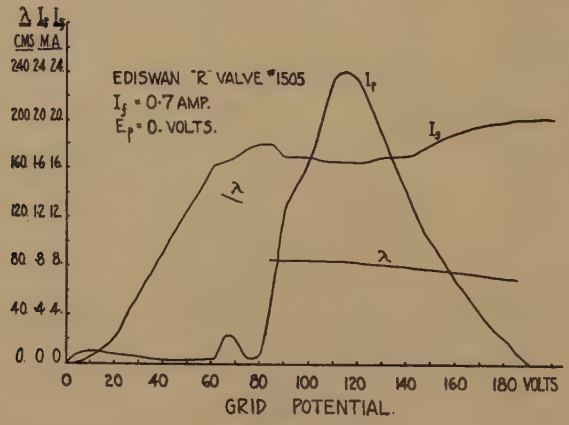

Fig. 9

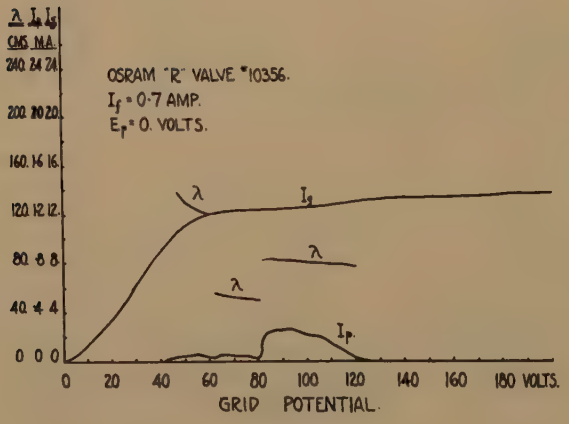

Fig. 10

from B-K" on Fig. 14. It is seen that the only experimental curves which at all approximate the calculated curve are those of the first region of oscillations; i.e., the region whose wavelengths lie in the neighborhood of 130 centimeters. The wavelength curve calculated from Scheibe's formula (4) agrees much more closely with the experimental first region curves. This is what would be expected, since this

formula is developed from assumptions more closely agreeing with the actual conditions than the assumptions made in developing the Barkhausen-Kurz formula.

There remain the other two distinct regions of oscillation which do not coincide with the calculated curves even approximately.

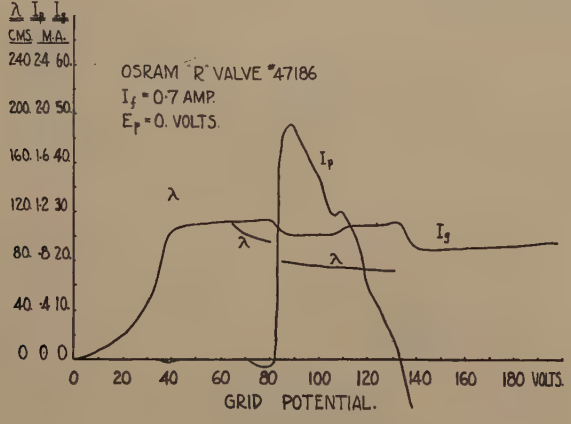

Fig. 11

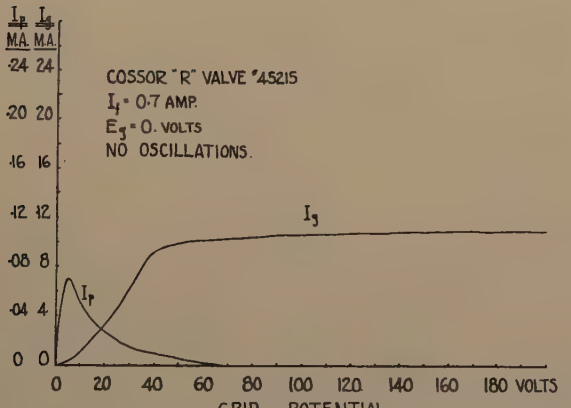

Fig. 12

The several regions of oscillation which occur as the grid potential is varied with fixed filament current, do not appear to be amenable to explanation from the simple Barkhausen theory. The Barkhausen-Kurz formula indicates a single continuous wavelength curve as shown in Fig. 14. The curves obtained experimentally are each divided into several discrete sections, and these do not coincide with the Barkhausen-Kurz curve. The explanation does not lie in the presence of

Gill-Morrell oscillations, with an external tuned circuit resonant at several frequencies, since there is no external tuned circuit.

Nevertheless it will be seen from the following that the existing theory is adequate to explain the experimental results observed, the complete explanation being a combination of the various proposed theories.

The first region of oscillations, commencing at grid potentials in the neighborhood of 45 volts, is a region of pure electronic (i.e., Barkhausen-Kurz) oscillations, and takes place in the filament-plate space. It follows the Barkhausen-Kurz wavelength relationship reasonably well, as can be seen from an inspection of the curves in this region in

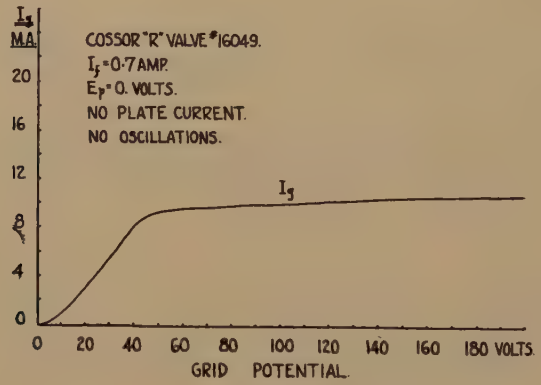

Fig. 13

Fig. 14. The curves do not coincide, however, the experimental wavelengths being about 8 per cent shorter than those calculated from the Barkhausen-Kurz formula. This is explained by the fact that the space charge about the filament reduces the length of traverse of the oscillating electron cloud by a small amount, so that the quantity d_a in the Barkhausen-Kurz formula, which is equal to twice the filament-plate distance, should be reduced by this small amount. Also the actual plate diameter measurements used in the calculations could not be made with a high degree of precision, unless each valve had been destroyed by removing the glass envelope. It was necessary to make the measurements from outside the glass, thus introducing a possible error of several per cent. If we apply a constant correction factor to the formula to take account of the above factors, we find that the experimental and calculated wavelengths agree quite well. This constant is later found to be of the same numerical value as that derived by Scheibe.

The second region of oscillations consists of pure electronic oscillations taking place in the filament-plate space at approximately double the frequency. By substituting half the plate diameter in the Barkhausen-Kurz formula we find that calculated wavelengths agree with experimental as well as can be expected, considering the accuracy of the measurements. Experimental values are again slightly shorter than those calculated, for the same reason. Although wavelengths in this region are not exactly half the value of any wavelength in the first region they can, nevertheless, be considered second harmonics of the first region oscillations. No higher order harmonics were observed.

These two regions of Barkhausen-Kurz oscillations are very similar to what Potapenko[10] calls normal waves and dwarf waves of the

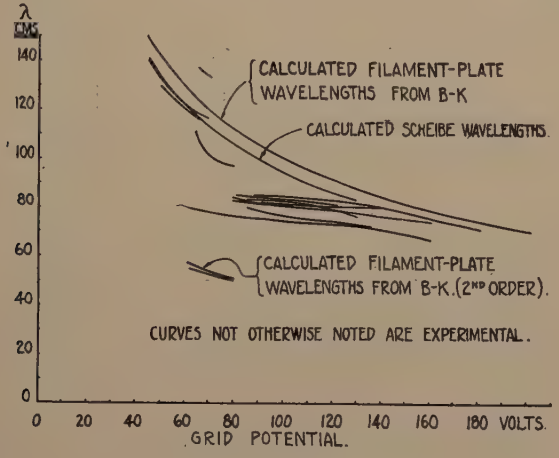

Fig. 14

first order. He speaks of Gill-Morrell oscillations, since he used an external tuned circuit of the Lecher wire type connected to plate and grid. In his case the tuning of the grid-plate circuit was altered as well as the grid potential, to shift from the normal region to that of the dwarf waves, whereas in the Barkhausen-Kurz cases described here only the grid potential was varied to shift from one region to the other.

The third region of oscillations consists of Gill-Morrell oscillations, with the grid and plate electrodes forming the tuned circuit. This is why the wavelength in this region is so nearly constant, merely dropping a little as the grid potential is increased (see Fig. 14) instead of following the Barkhausen-Kurz curve. It was at first thought that the

[10] G. Potapenko, *Zeit. für tech. Phys.*, vol. 10, pp. 542–548, (1929); *Phys. Rev.*, vol. 39, pp. 625–637, 638–665, (1932); *Phil. Mag.*, vol. 14, no. 7, pp. 1126–1142; December, (1932).

resonant circuit might consist of the parallel wire leads between the electrodes and the valve pins, but a calculation of the inductance of these leads gave a value of 0.09 microhenry. This in combination with the measured grid-plate capacity gives a wavelength about 60 per cent higher than that observed. Hence the "external" tuned circuit does not include the leads, but consists only of the grid and plate elements themselves.

Several isolated wavelength values will be noted in Fig. 14. These were instances of oscillations occurring at single critical values of grid potential. Oscillations in these cases were not stable and tended to die away. At the values of grid potential at which oscillations changed

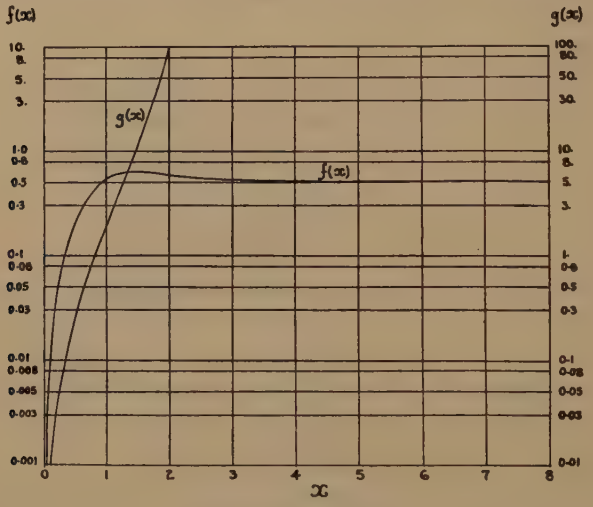

Fig. 15—See Table.

from one region to another conditions were also unstable, the wavelength tending to jump from one region to the other.

Wavelengths calculated from Scheibe's formula lie along a curve similar in form to that of Barkhausen-Kurz, but are in closer agreement with experimental values than the latter (see Fig. 14). This is to be expected since the Barkhausen-Kurz formula was developed for the simplified case of a valve with plane electrodes, whereas the Scheibe formula was developed for cylindrical electrodes, which is the type of electrode structure in the *R* valves investigated.

The Rostagni wavelength formula (7) is difficult to apply since the quantity N, the number of electrons in the grid-plate space, cannot be evaluated accurately. If N is considered to be directly proportional to I_g, then the wavelength calculated from this formula would vary

very little with E_g, since I_g increases but slightly beyond the saturation value. On this account it was thought that this formula might be applicable to the oscillations of the third region, but this proved not to be the case.

Jonescu's formula (6) could not be applied to the cases investigated here since nothing was known of the gas content of the valves. If K, the gas constant, is determined experimentally to make the formula fit an experimental value, this formula then becomes identical with that of Barkhausen and Kurz.

Wavelengths found experimentally for the gassy valve (No. 47186) did not agree with the formulas, as can be seen from Fig. 14. The third region wavelengths were similar to those of the other valves, however, thus providing additional evidence to verify that wavelengths in this region are controlled by a tuned circuit. The ionized gas renders the electron oscillations quite erratic, but does not affect the frequency of the resonant grid-plate circuit, since the interelectrode capacity is not appreciably altered. The erratic results in the first two regions indicate that the wavelengths of oscillations in valves containing an appreciable amount of gas cannot be represented completely by a formula as simple as that of Jonescu.

Since there was no method of measuring any alternating potential E_0 which may have been produced at the grid, Hollmann's variation of the Barkhausen-Kurz formula (5) was not used. The insertion of appropriate values of E_0 in Hollmann's formula would allow theoretical curves to be obtained which would more closely agree with each individual experimental curve. The presence of this alternating potential at the grid is another cause of variation in the experimental curves of the pure Barkhausen-Kurz regions.

V. Summary

Several of the proposed wavelength formulas for Barkhausen-Kurz oscillations have been compared with the author's experimental results, and reasonable agreement found with some of them. An explanation is given of the several types of oscillations obtained with a series of valves connected in a circuit with positive grid and no external tuned circuit, in terms of theories already developed for the explanation of the more usual type of Barkhausen-Kurz oscillations.

In a recently published paper[11] on ultra-short-wave oscillations, some of those who contributed to the discussion commented on the fact that no oscillations had been produced with positive grid valves

[11] E. C. S. Megaw, *Jour. I. E. E.* (London), vol. 72, part 436, pp. 348–352; April, (1933).

without external tuned circuits. The present paper describes investigations on the production of oscillations of this type by the author.

Appendix

Table of Values of $f(x)$ and $g(x)$ in A. Scheibe's Wavelength Formula (4). (See Fig. 15.)

x	$f(x)$	$g(x)$
0.0	0.	0.
0.1	0.00993	0.010
0.5	0.21228	0.289
0.8	0.42568	0.998
1.0	0.53808	2.030
1.2	0.60872	4.088
1.5	0.64237	12.190
1.8	0.62419	40.360
2.0	0.60268	98.010
3.0	0.534	—
4.0	0.516	—
5.0	0.510	—
7.0	0.504	—
∞	0.500	—

Proceedings of the Institute of Radio Engineers
Volume 22, Number 8 *August, 1934*

A NOTE ON MAGNETRON THEORY*

By

F. T. McNamara
(Yale University, New Haven, Connecticut)

A difference of opinion exists as to the paths pursued by the electrons in a magnetron tube when the controlling magnetic field is greater than the critical value. In the original paper on the magnetron[1] by A. W. Hull it was deduced that these paths were quasi cardioids as shown in Fig. 1. In a later paper[2] by the same author it was stated that "for magnetic fields stronger than the critical value . . . all the electrons move in concentric circles around the cathode." Data on ionization phenomena were quoted to support this statement.

In a recent article[3] by E. C. S. Megaw, Hull's second interpretation is brought into question. Megaw derives an equation showing that the space-charge density is constant within some critical radius determined by the magnetic field intensity, and is zero beyond that radius.

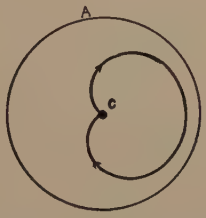

Fig. 1—Quasi-cardioid path of electrons in magnetron.

He continues, "This result is evidently the 'special solution' reported in abstract by Hull and interpreted by him as meaning that all electrons constituting the space charge travel in concentric circles around the cathode. This interpretation does not appear to be justifiable. The only sense in which we can deduce that i (current) $=0$ when $H>H_c$ (magnetic field strength greater than critical value) either from the foregoing theory or from experimental results is in the sense that the average charge crossing unit area in unit time is zero. . . . This condition is fulfilled when the electrons move in the quasi-cardioid paths deduced from Hull's original equations. It is probably impossible to decide which of the two paths actually exists by any measurements made out-

* Decimal classification: R139. Original manuscript received by the Institute, January 22, 1934.

[1] *Phys. Rev.*, vol. 18, p. 31, (1921).
[2] *Phys. Rev.*, vol. 23, p. 112, (1924).
[3] *Jour. I.E.E.* (London), vol. 72, p. 326, (1933).

side the valve, since the space charge at any point will be the same whether it is the individual or the average radial electron velocity which is zero."

In the cylindrical systems used as magnetrons practically all the voltage drop occurs in the near vicinity of the central electrode or cathode. Consequently, if a perforated third electrode, at anode potential, be inserted between the other two, in a region of low potential gradient, only a small change will be produced in the normal potential distribution of the system and electrons will be free to pass between

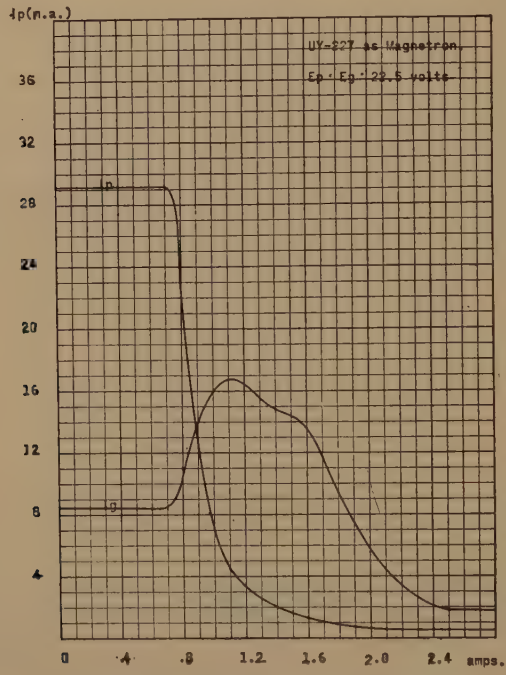

Fig. 2—Relation between electrode currents and magnetic field strength in UY-227 tubes.

cathode and anode as before the insertion of the third electrode. Since the magnetic field required to turn back electrons from a given electrode varies inversely as the diameter of the electrode, a weaker field will be required to stop current flow to the anode than to the third electrode. If, for magnetic fields greater than this critical value, the paths of the electrons are circular, no increase in current to the third electrode should be encountered; in fact the current to the third electrode should simultaneously drop to zero. If, on the other hand, the paths are quasi cardioids, it would be expected that as the electrons

were turned back from the anode, thus decreasing the anode current, some would strike the third electrode on the return trip and thus increase the current to that electrode.

This experiment was performed on a UY-227 tube which approximately fulfills the conditions of the problem. The control grid was used as the third electrode. Both the control grid and the anode were held at $22\frac{1}{2}$ volts positive with respect to the cathode. The results of the experiment are depicted in Fig. 2. It is evident that the critical field which reduces the anode current simultaneously increases the current to the third electrode. Moreover the essential character of the result is not changed if the potential of the third electrode is slightly below that of the anode. Consequently it is concluded that Megaw's interpretation, which agrees with Hull's original interpretation, is the correct one.

Proceedings of the Institute of Radio Engineers
Volume 22, Number 8 *August, 1934*

NOTE ON A CAUSE OF RESIDUAL HUM IN RECTIFIER-FILTER SYSTEMS*

By

Frederick Emmons Terman and Sidney B. Pickles
(Stanford University, California)

Summary—*The capacitance of the power transformer secondary to ground is shown to by-pass the filter system when the filter chokes are in the negative lead and the negative output is grounded. This results in a residual ripple voltage across the output that may be greater than the ripple voltage passed by a very good filter. The remedy is either to place the filter inductance in the positive lead or to ground the positive output terminal.*

WHILE making measurements on a rectifier-filter system arranged as shown in Fig. 1 with constants such as to produce excellent filtering, it was found that the hum voltage developed across the output was several times that which calculations would lead one to expect, and increasing the amount of filtering had no appreciable

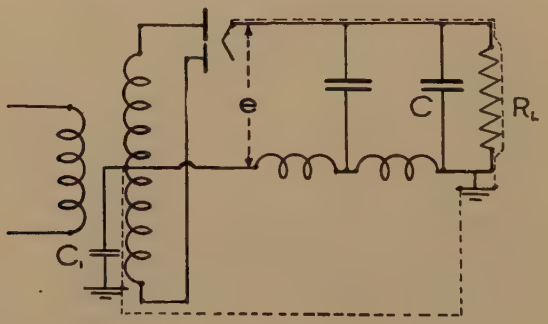

Fig. 1

effect upon this hum. In endeavoring to locate the cause of this behavior it was found that either grounding the positive lead, or placing the filter inductances in the positive line as shown in Fig. 2, brought the hum down to the predicted value.

Consideration of these factors lead to the conclusion that the residual hum must be the result of the capacitance between the secondary winding and ground. This capacitance obviously by-passes the entire filter system of Fig. 1 and causes a small ripple current to flow as shown by the dotted lines in Fig. 1. This produces a voltage across the load

* Decimal classification: R386. Original manuscript received by the Institute, February 14, 1934.

impedance, and also a voltage between the negative line and ground if the negative line is grounded through an impedance.

If e is the ripple voltage delivered by the rectifier output then the residual hum current flowing along the dotted path in Fig. 1 is very nearly

$$\text{hum current} = j\omega C_1 e. \tag{1}$$

This is because C_1 offers nearly all of the impedance present in the dotted path. Since the final filter condenser C always has a low re-

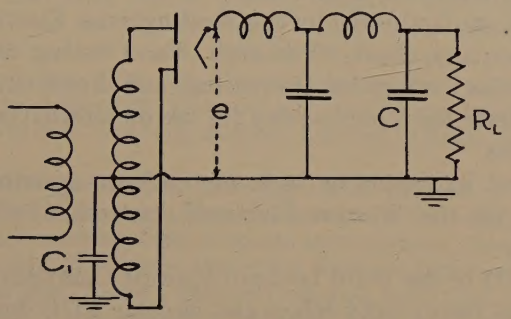

Fig. 2

actance compared with the load, the hum voltage developed across the load is approximately

$$\text{hum voltage across load} = e\frac{C_1}{C}. \tag{2}$$

In the case observed the capacitance C_1 as measured was 600 micro-microfarads. The 120-cycle component of the ripple delivered by the rectifier was 240 volts. Substitution of (1) shows that the expected residual 120-cycle ripple current would be 108 microamperes, which is to be compared with an actually measured value of 113 microamperes. With an 8-microfarad output condenser this current develops approximately 0.018 volt hum across the load, which is enough to cause trouble in many circumstances.

These considerations make it apparent that for low hum the filter reactors should be in the positive lead. In the case that other considerations make it necessary to place some chokes in the negative lead, then the last section of filtering must have its impedance in the positive line.

BOOKLETS, CATALOGS, AND PAMPHLETS RECEIVED

Copies of the publications listed on this page may be obtained gratis by addressing a request to the publisher or manufacturer.

"What's Behind the Dial?" describes the structure of measuring instruments manufacturered by the Westinghouse Electric and Manufacturing Company, East Pittsburgh, Pa. Catalog Section 41–340 describes auxiliary relays for alternating- and direct-current use. Section 43–950 describes a photo-relay for use on alternating- and direct-current circuits.

Power level indicators or "d.b. meters" are described in circular M-10 issued by the Weston Electrical Instrument Corporation of Newark, N.J.

Bulletin 131 of the Ward Leonard Electric Company, Mt. Vernon, N.Y. describes heavy duty relays and circular 507B describes protective magnetic relays for radio transmitters.

Police radio equipment for cities and states is described in Bulletin GET-627 issued by the General Electric Company, Schenectady, N.Y.

Portable instruments for direct- and alternating-current are de-described in Catalog 123 of the Roller-Smith Company, 233 Broadway, New York City.

RCA Radiotron Company of Harrison, N.J., has issued an errata notice on Application Note No. 35. Application Note No. 40 on high power output from type 45's is now available for distribution.

CONTRIBUTORS TO THIS ISSUE

Barrow, W. L.: See PROCEEDINGS for February, 1934.

Chaffee, J. G.: Born March 6, 1901, at Hackensack, New Jersey. Received S.B. degree, Massachusetts Institute of Technology, 1923. Engineering department, Western Electric Company, 1923–1925; Bell Telephone Laboratories, 1925 to date. Associate member, Institute of Radio Engineers, 1926.

Jackson, Willis: Born 1904 at Burnley, England. Received B.Sc. degree, Manchester University, 1925; M.Sc. degree, 1926. Lecturer in electrical engineering, Technical College, Bradford, 1926–1929. Metropolitan Vickers Electric Company, Manchester, 1929–1930. Lecturer in electrical engineering, Manchester University, 1930–1933. Demonstrator, engineering laboratory, Oxford University, 1933 to date. Associate member, Institute of Radio Engineers, 1928; Member, 1931.

Llewellyn, Frederick Britton: Born September 16, 1897, at New Orleans, Louisiana. Received M.E. degree, Stevens Institute of Technology, 1922; Ph.D. degree, Columbia University, 1928. Ship and shore operator, American Marconi Company, 1915–1916; U.S. Navy, 1917–1919. Vreeland Laboratory, 1922–1923; member technical staff, Western Electric Company, 1923–1925; Bell Telephone Laboratories, 1925 to date. Associate member, Institute of Radio Engineers, 1923.

McNamara, Francis T.: Born July 6, 1896, at Clinton, Massachusetts. Received Ph.B. degree, Yale University, 1921; E.E. degree, 1924. General Electric Test Course, 1922. Philadelphia Electric Company, 1923. Instructor, Yale University, 1923–1928; assistant professor of electrical engineering, 1928 to date. Associate member, Institute of Radio Engineers, 1931.

Moore, William Herbert: Born September 10, 1906, at Belfast, Ireland. Received B.Sc. degree, McGill University, Montreal, 1927; M. Eng. degree, 1932. Bell Telephone Company, Montreal, 1924; Northern Electric Company, Ltd., 1925. Royal Canadian Corps of Signals, 1926. Ultra-short-wave research, National Research Council of Canada, 1926–1927. Demonstrator, department of electrical engineering, McGill University, 1927–1928; demonstrator, physics department, 1929–1930. Ship radio operator, 1928; engineer, short-wave radio station CGP, 1928–1929; Canadian Marconi Company, Ltd., 1930 to date. Member, Sigma Xi. Associate member, Engineering Institute of Canada; Associate member, Institution of Electrical Engineers. Junior member, Institute of Radio Engineers, 1927; Associate member, 1928.

Pickles, Sidney B.: Born April 23, 1909, at Monterey, California. Received B.A. degree in physics, Stanford University, 1931; E.E. degree, 1933. International Business Machines Corporation, 1933 to date. Student member, Institute of Radio Engineers, 1932.

Strutt, M. J. O.: Born 1903 at Java, Dutch East Indies. Studied at University of Munich; Institute of Technology, Munich; Institute of Technology, Delft; graduated Munich, 1924, Delft, 1926. Assistant physics department, Delft, 1926–1927. Doctor Technical Science, Delft, 1927. Research Staff, Philips' Incandescent Lamp Works, Ltd., 1927 to date. Nonmember, Institute of Radio Engineers.

Terman, Frederick Emmons: See PROCEEDINGS for March, 1934.